



بِسْمِ اللَّهِ الرَّحْمَنِ الرَّحِيمِ



In The Name Of

GOD



دانشگاه علوم پزشکی
و خدمات بهداشتی درمانی تهران

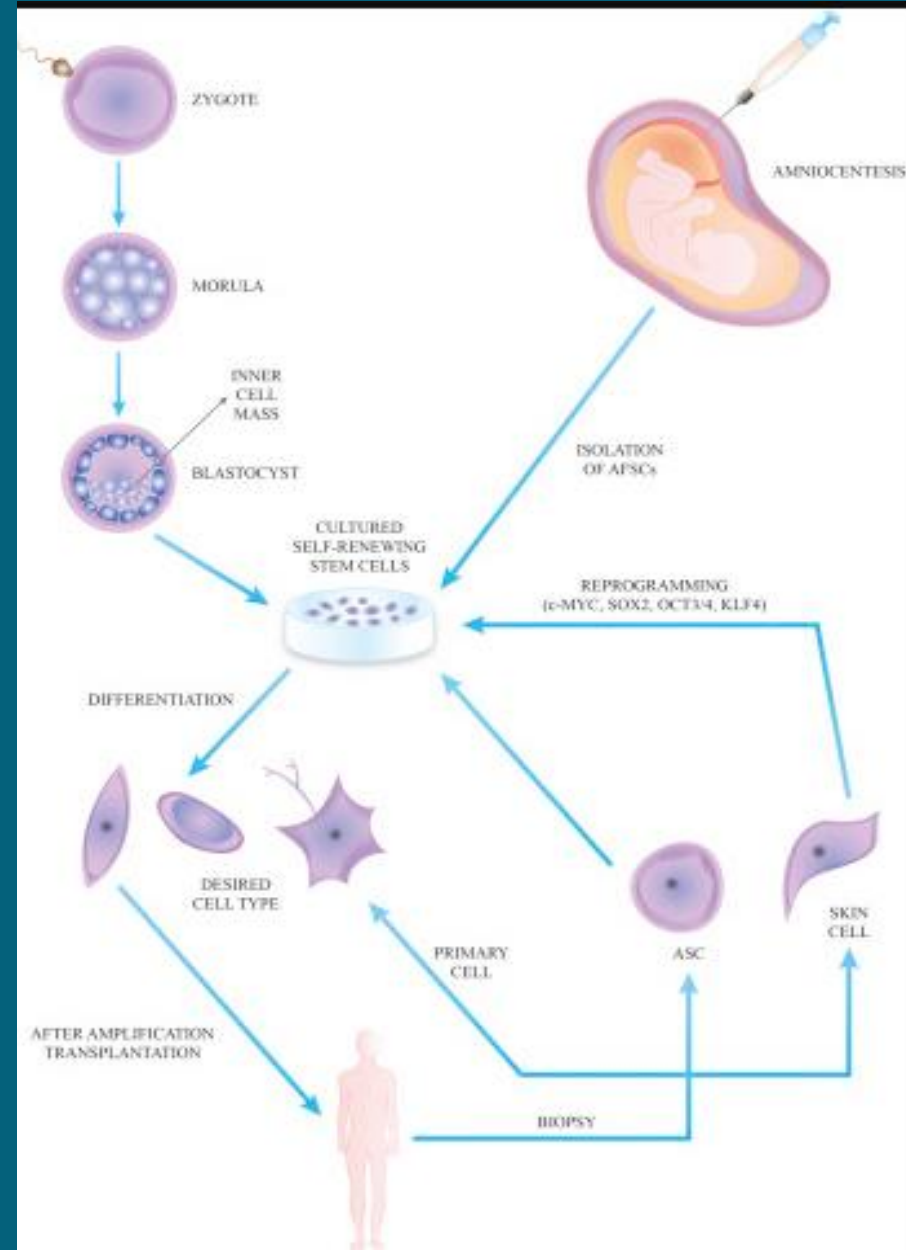
Tissue Engineering and Regenerative Medicine In Urology

History of Regenerative Medicine

- The first studies of cell regeneration was done by Thomas H. Morgan in 1901.
 - His study concluded that regeneration occurs in special circumstances in which cell growth and replacement take place with in the organism.
- In 1920, Hans Spemann studied earthworms. When he couldn't find out why earthworms could regenerate scientists started transplanting random organs and limbs from many different organisms. One day Robert Briggs and Thomas kings transplanted a frogs nuclei into a frog egg and the result was a clone which raised questions about the limits of what cells r capable of.
- In 1934, Thomas H. Morgan realized that there are 2 types of cell regeneration. In one type, the new cell develops by remodeling of the old cell. In the other the new cell is formed out of the material of the old cell.

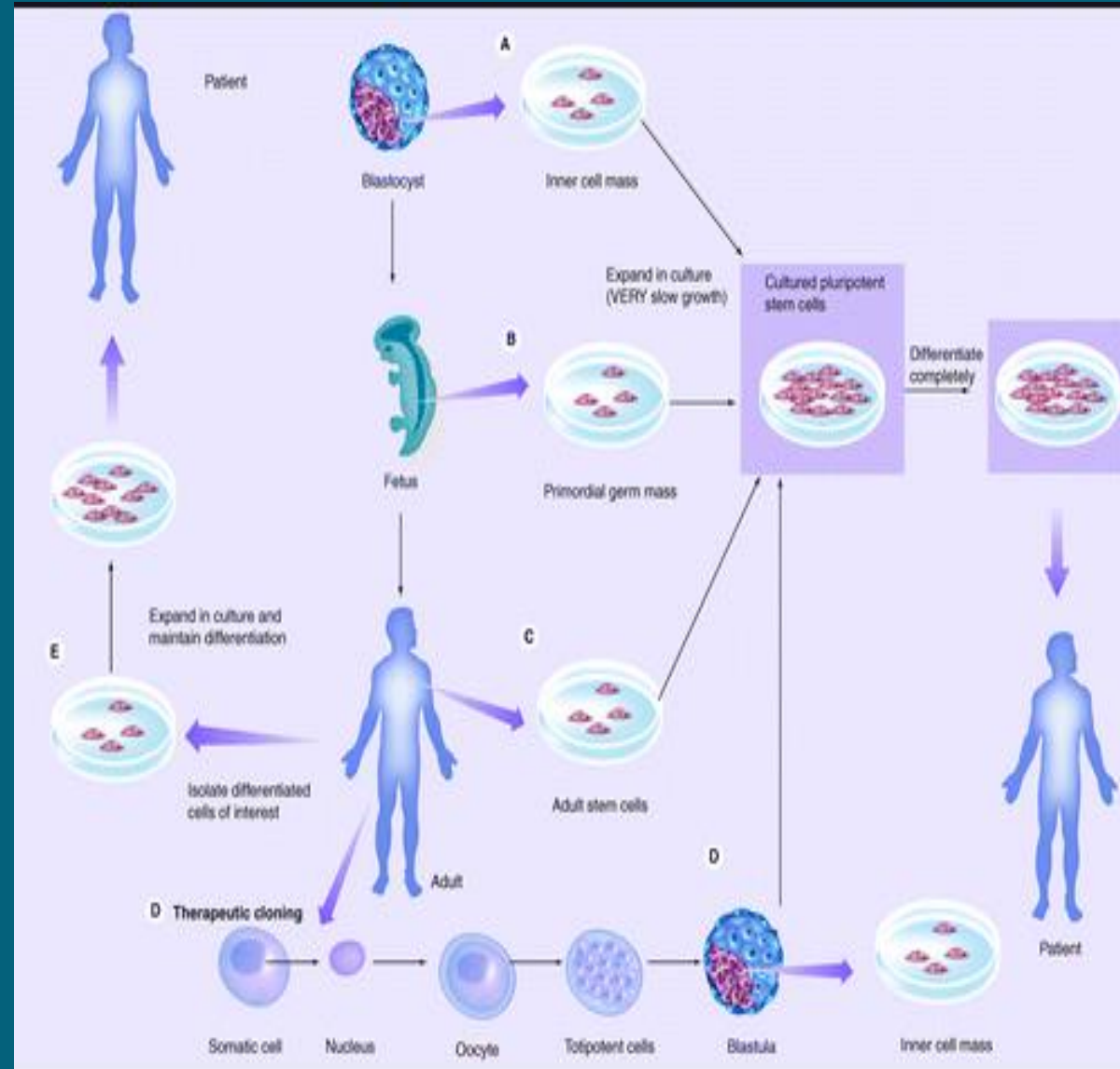
Historical background

- Regenerative medicine (RM) implies the replacement or regeneration of human cells, tissue or organs, to restore or establish normal function.
- The term “regenerative medicine” is widely considered to be coined by William Haseltine during a 1999 conference on Lake Como, in the attempt to describe an emerging field, which blent knowledge deriving from different subjects: tissue engineering (TE), cell transplantation, stem cell biology, biomechanics prosthetics, nanotechnology, biochemistry

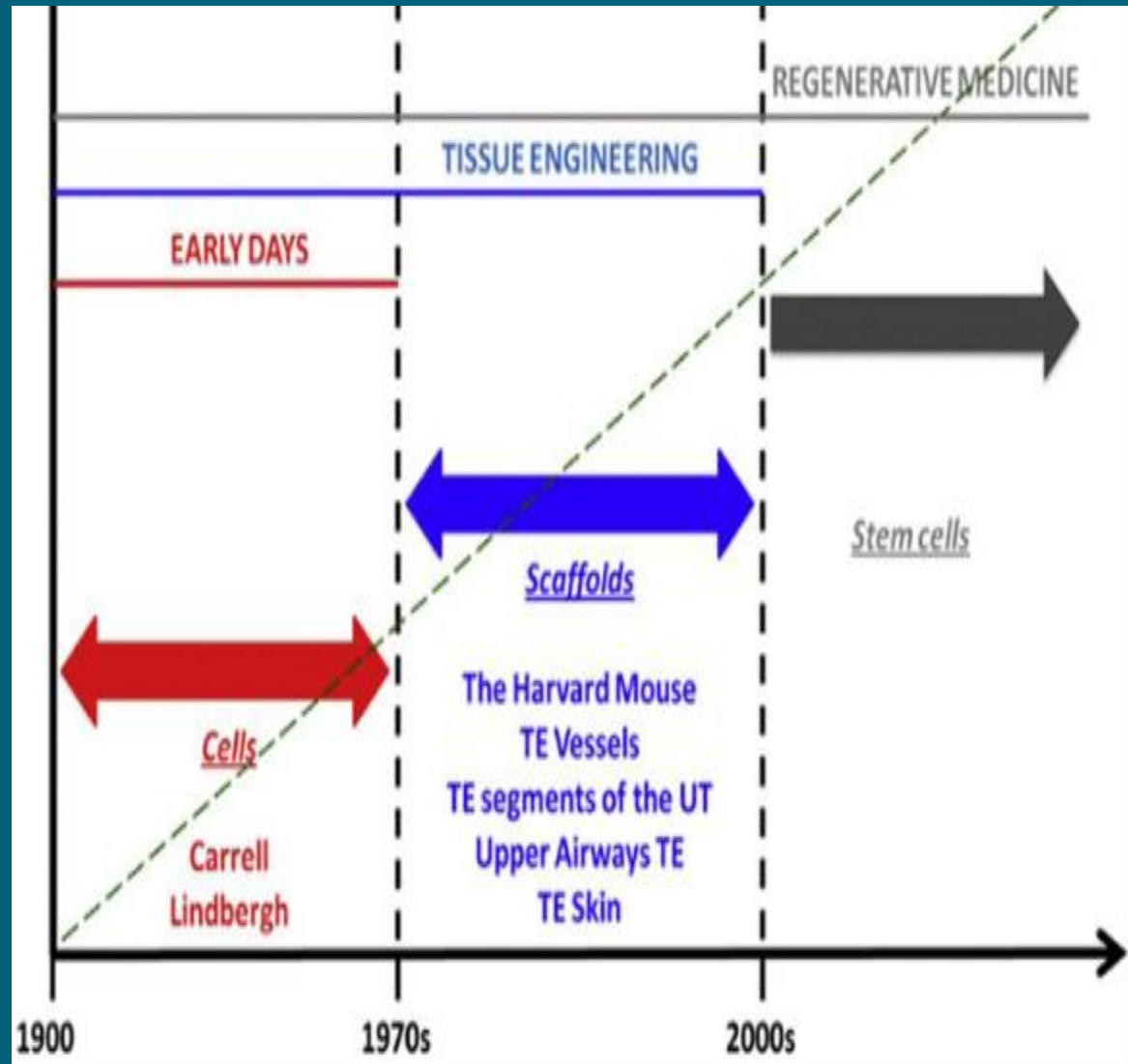


This term was found for the first time in a 1992 paper by Leland Kaiser, who listed the technologies which would impact the future of hospitals.

RM is considered a novel frontier of medical research, but the idea of creating artificial organs is not so recent. In 1938, a book, called “The culture of new organs”, was published and the authors were Alexis Carrell, a Nobel Prize winner for his study on vascular anastomosis, and Charles Lindbergh, the first aviator to fly across the Atlantic alone.



- Wondering why his sister-in-law's fatal heart condition could not be repaired surgically, Lindbergh, despite not being a professional, ended up working together with Carrell at Rockefeller Institute for Medical Research during the 1930s, where they created an artificial perfusion pump allowing the perfusion of the organs outside the body during surgery: their work was the basis for the development of the artificial heart



History:

- As for organ replacements, in 1954, the kidney was the first organ to be substituted in a human, but between identical twins so that rejection did not arise.
- Later, also cell transplantation was achieved: an immunodeficient patient received his sibling's bone marrow .
- At first, transplants were relegated to research because of the adverse immunological responses, but the advent of cyclosporine in the 1980s transformed transplantations into life-saving treatments, as the risk of rejection could be drastically reduced.

History:

- Nowadays, lifelong immunosuppression carries many side effects, representing one of the two big problems related to transplantations.
- The other one is the shortage of donors, not being able to meet the ever increasing demand of organs.
- Due to the progressively aging population, transplantations will be increasingly needed to replace end-stage diseased organs injured by age-related diseases.

THE HISTORY OF STEM CELLS & REGENERATIVE MEDICINE

Since 1961, when the existence of Stem Cells was proven accidentally, regenerative medicine has bloomed, shrunk, contracted, been hated and misunderstood all at once.

Existence of stem cells proven

1961

1974

The U.S. Congress implements a ban on nearly all federally funded fetal tissue

President George H.W. Bush vetoes bill attempting to override the moratorium on stem cell research.

1990

1998

James Thomson from the University of Wisconsin isolates human embryonic stem cells.

2003

First genome sequenced

The ease of sequencing and gene editing today is having a profound effect on the field of regenerative medicine. We can understand in greater detail the biomarkers and pathways that we seek to silence or replicate, to allow us to further discern the specific genes that need to be expressed when editing sourced material in cell and stem cell therapies. This can also enable commercialization of the most bare-bones type of genomic medicine possible: gene therapy.

President Obama eases restrictions on embryonic stem cell research

2008

2007

Shinya Yamanaka of Kyoto University and James Thomson independently discover induced pluripotent stem cells in humans (iPS).

2010

NIH established the "Roadmap Epigenomics Project"-still ongoing

Genomics has brought great success to an industry that has been nascent for years. Just when we thought we had a grasp on how we could move forward, science throws us another monkey wrench. Even with perfectly genetically modified cells, sometimes the efficiency still isn't as high as it is desired.

Now, science is pointing at epigenetics – modifications at the DNA level – as a possible opportunity to disrupt the industry yet again.

2012

uniQure gets approval for Glybera in EU, first gene therapy approval in western world

WELCOME TO THE REGENERATIVE RENAISSANCE

Geron's Stem Cell
assets purchased by
Biotime, helmed by
Michael West.

2013

2014

EU approves Holoclar,
first stem cell-based
therapy; ViaCyte gains
FDA approval for a phase
I clinical trial for beta cells
derived from hESCs for
treating diabetes.

2015

**Novartis signs deals to
bring further CRISPR
gene editing tools into
its company, adding to
its newly created Cell
and Gene Therapy Unit**

> With commercial prospects seemingly non-existent and public opinion fickle as ever, the major players bowed out of the game. Sanofi sold their gene and cell therapy unit to Aastrom (now Vericel) and other companies opted to not get involved in the field at all.

Today, big pharma are returning to the field.

NOW TO THE FUTURE





TEHRAN UNIVERSITY
OF
MEDICAL SCIENCES



Pediatric Urology &
Regenerative Medicine
Research Center

Kidney Tissue Engineering in Preclinical Models of Renal Failure: Systematic Review and Meta-analysis

Supervisors:

Prof. Abdolmohamad
Kajbafzadeh



Dr. Zahra Hassannejad

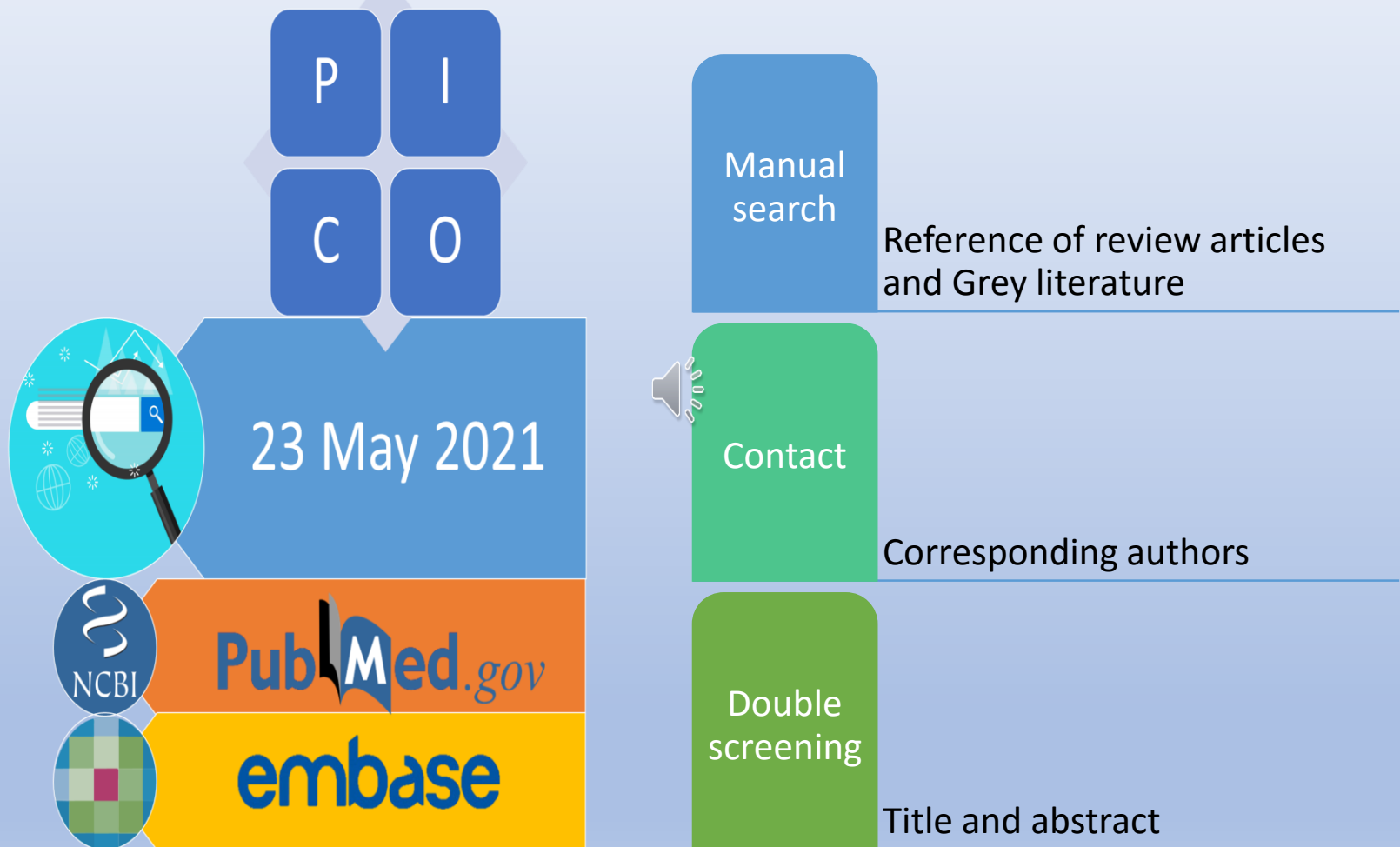
Advisor:

Dr. Hamid Arshadi

By:

Milad Mirmoghtadaei

Method: Search Strategy



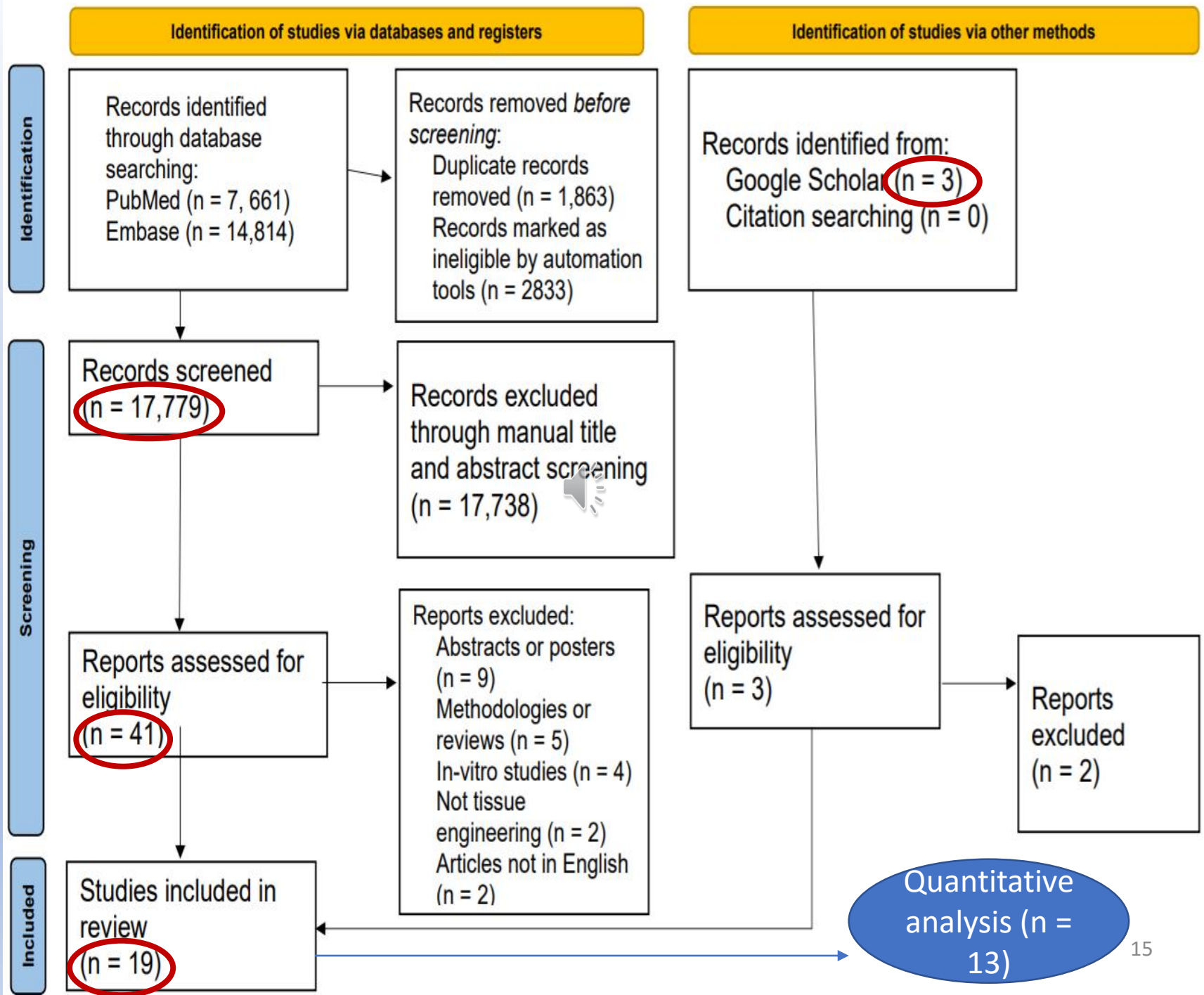
Outcome measures

Renal function

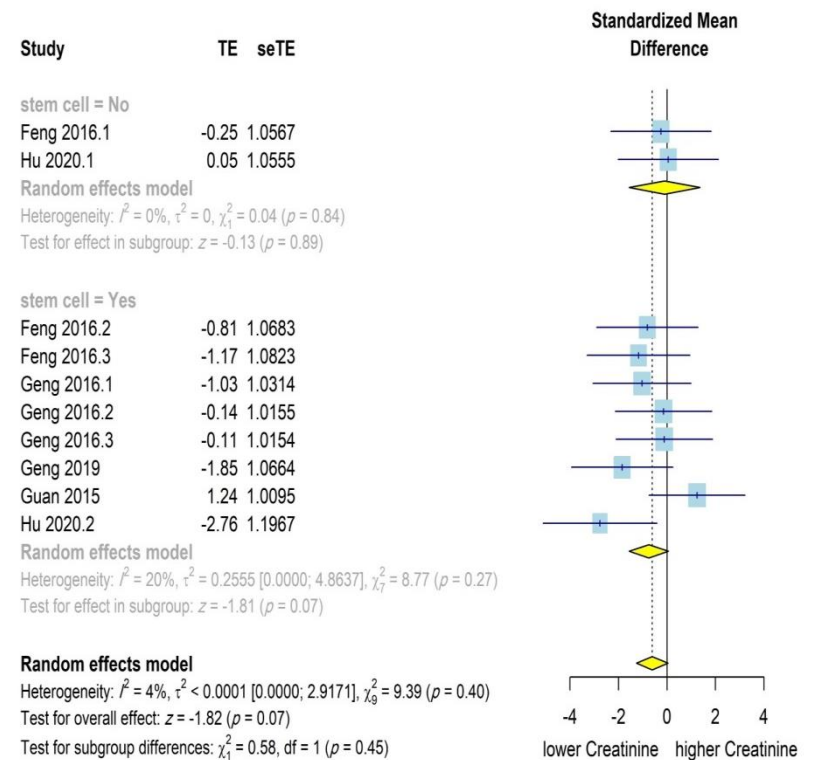
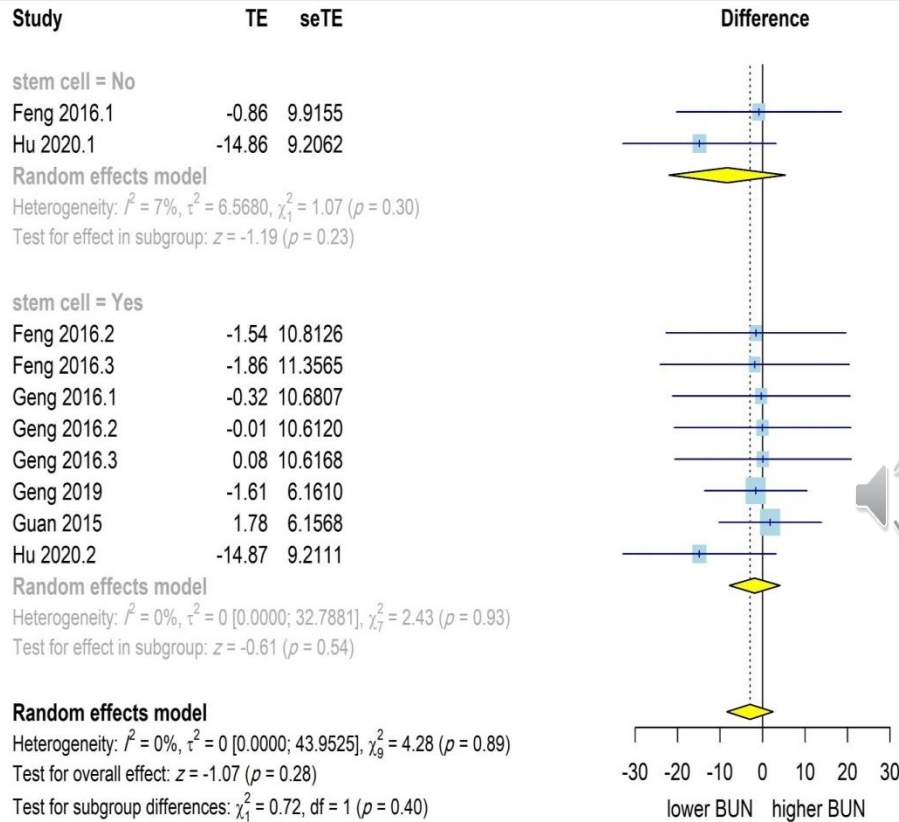
Regeneration

Fibrosis

Inflammation



BUN and Creatinine (Experimental vs. Active)



Gene Expressions

Cadherin

EMX2

KRT-10

Laminin



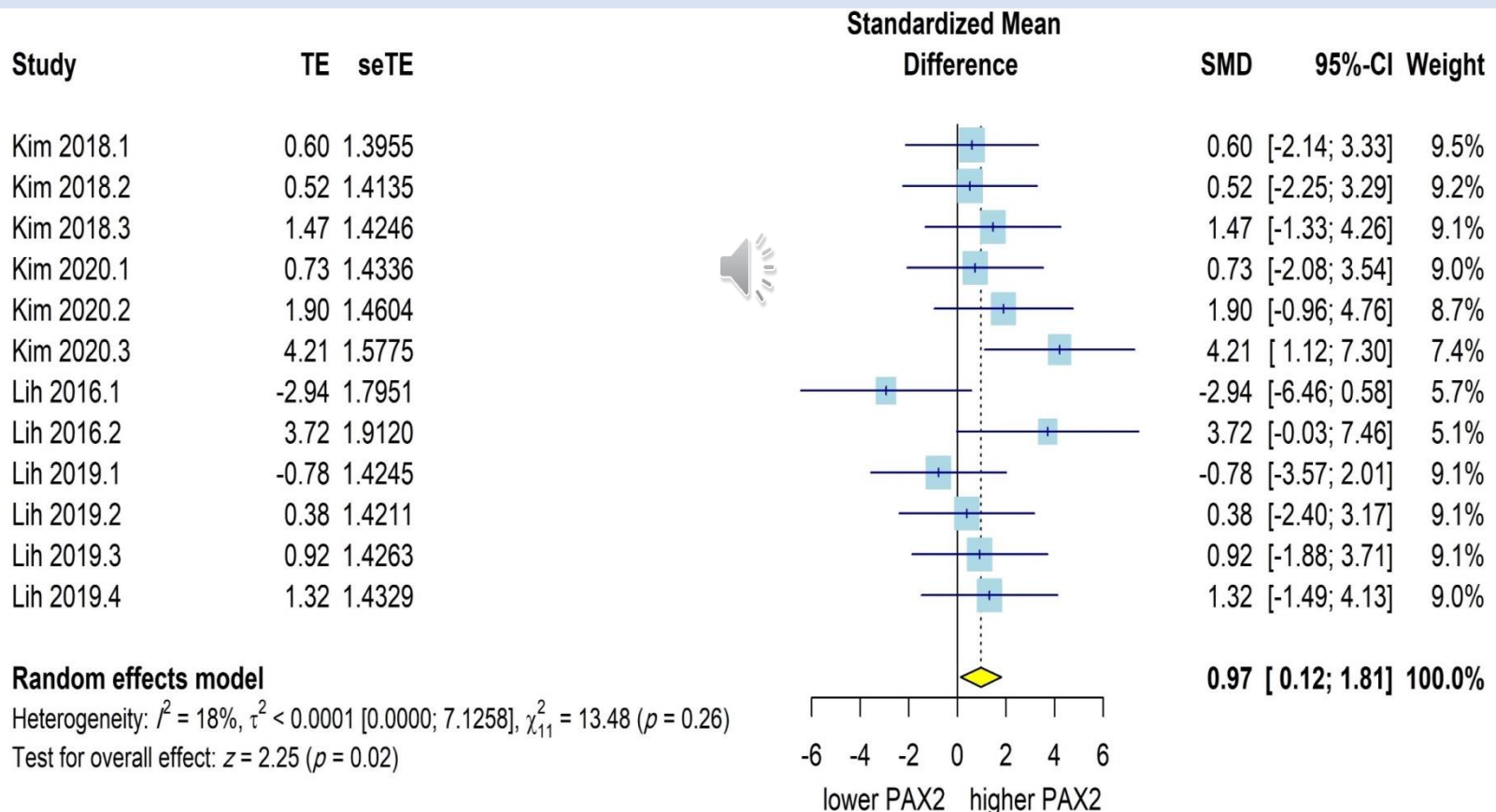
PAX-2

vWF

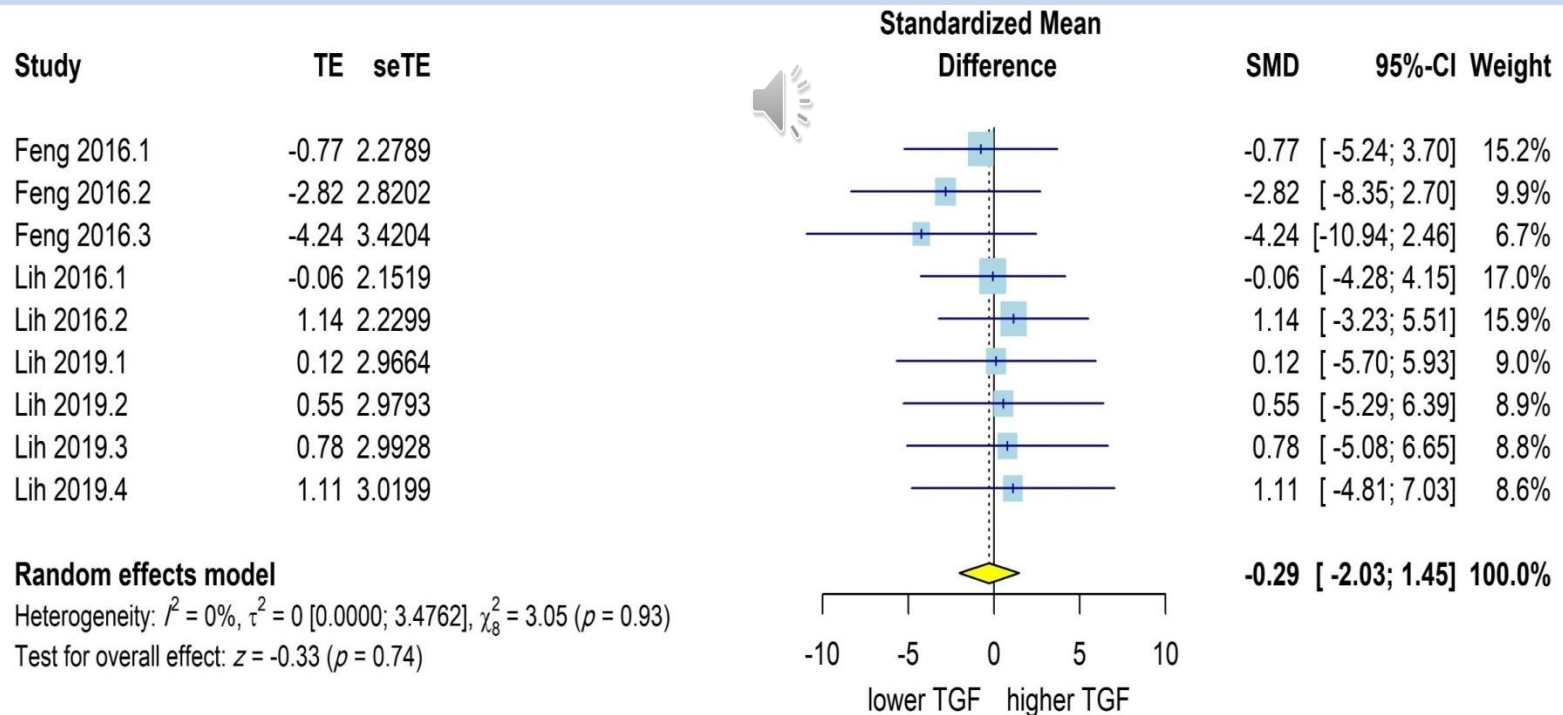
WNT

WT-1

PAX-2 gene expression (embryonic development)

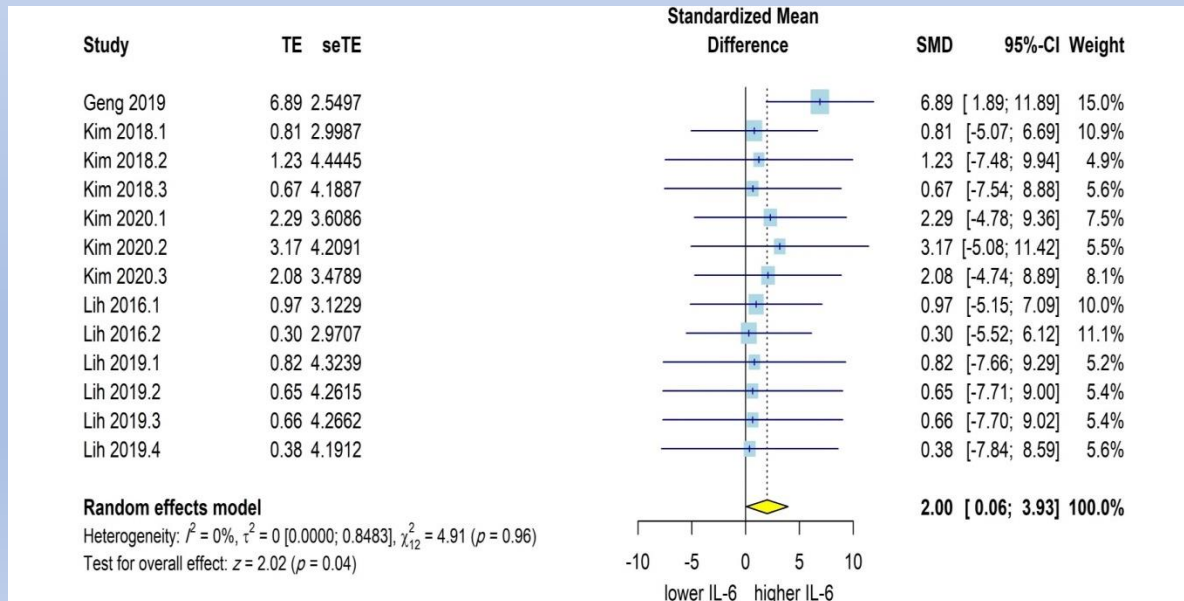
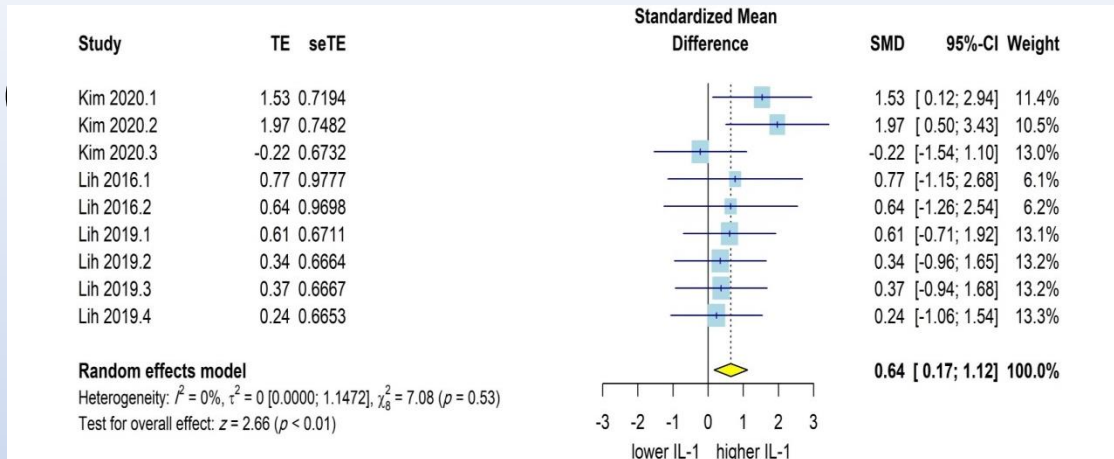


Transforming growth factor beta (TGF- β) gene expression




Int

ion



Conclusion

- More favorable outcomes with the use of **hybrid** composite scaffolds, with an element of PLGA combined with ECM, MH, or other bioactive materials.
-  **Cell** seeding tends to direct a more **accelerated** and closer to **normal** regeneration.
- **Growth factors** always helped.
- Our **quantitative** data did not support the authors' conclusions.



Journal

Biotechnic & Histochemistry >

Volume 90, 2015 - Issue 2

Enter keywords, authors, DOI etc.

This Journal



184

Views

0

CrossRef citations

0

Altmetric

Research article

Lung tissue engineering and preservation of alveolar microstructure using a novel casting method

A-m Kajbafzadeh ✉, N Sabetkish, S Sabetkish, Sm Tavangar, Rs Hossein Beigi, Ma Talebi, A Akbarzadeh & L Nikfarjam

Pages 111-123 | Accepted 12 May 2014, Published online: 30 Sep 2014

Download citation <http://dx.doi.org/10.3109/10520295.2014.957724> Crossmark

Full Article Figures & data References Supplemental Metrics Reprints & Permissions

[Get access](#)



Objectives:

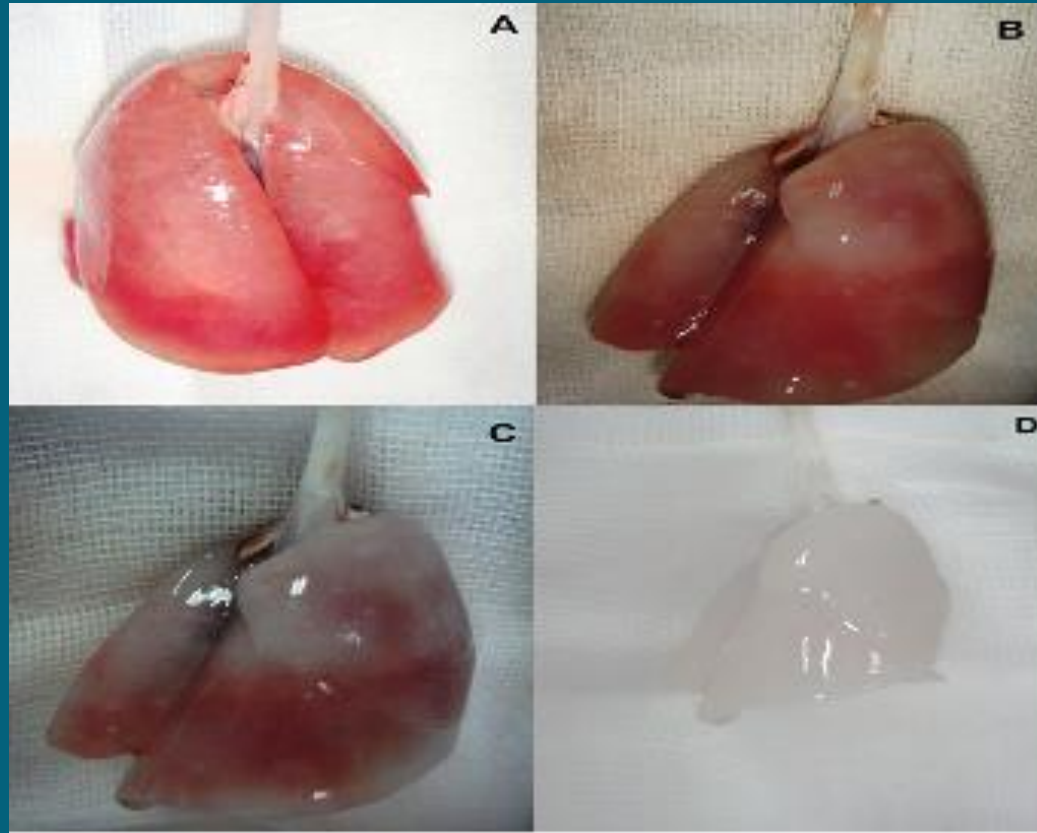
Decellularization and alveoli cell seeding on three-dimensional lung scaffold with preservation of alveoli micro-architecture was performed in rat model. We also tried to authenticate the preservation of terminal respiratory structure by SEM of the casts after decellularization process.

Material and Methods:

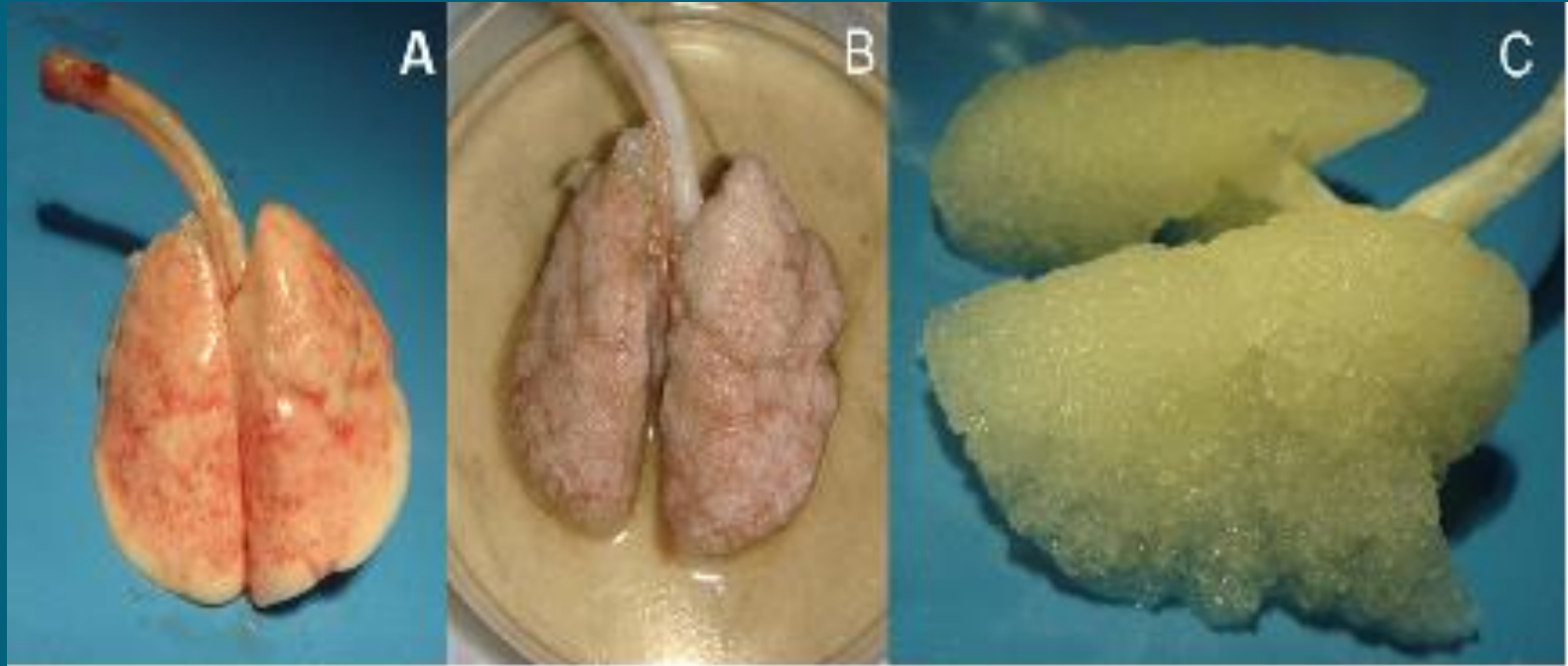
Whole lungs were obtained from 12 healthy Sprague Dawley rats, cannulated via the trachea under sterile condition, and decellularized with a detergent-based method. Casting of both natural and decellularized lungs was performed to authenticate the preservation of inner microstructure of scaffolds for further cell seeding. Alveolar cell seeding was performed with Green Fluorescent Protein (GFP) lung cells and non-GFP lung cells with a peristaltic pump in four lungs. Histological and immunohistochemical staining as well as enzymatic evaluation were conducted for assessment of cell seeding.

Results:

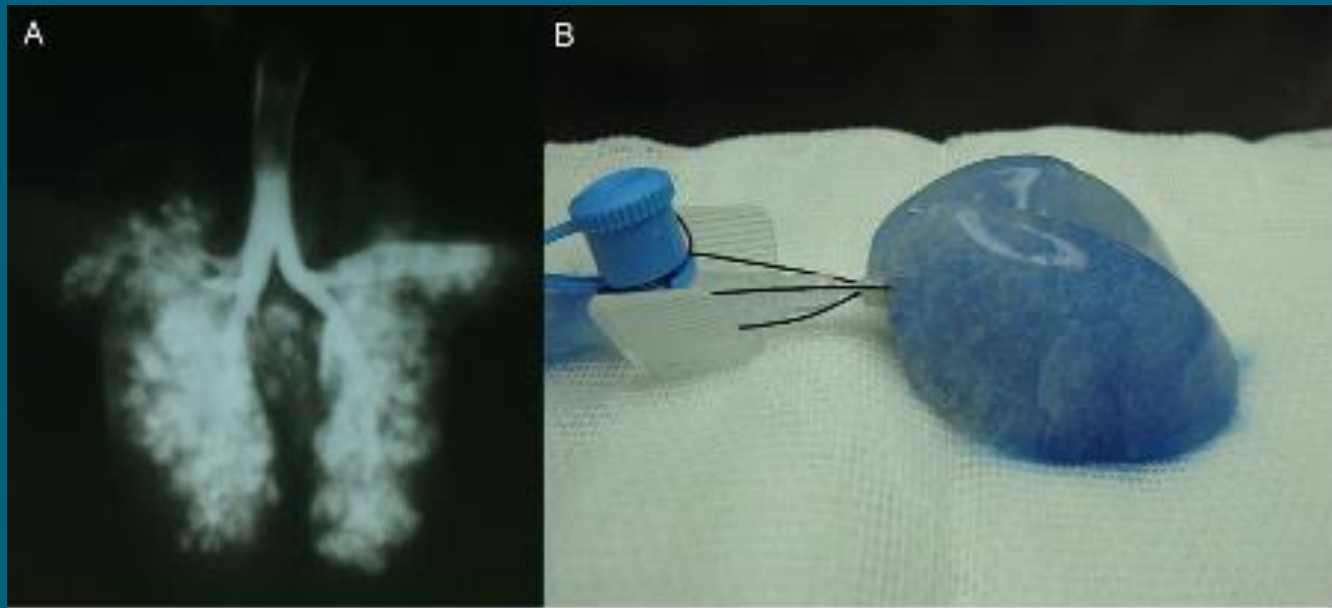
The results showed that all cellular and nuclear components were completely removed from the scaffolds. Histological staining and SEM of casts authenticated the preservation of tissue structure. Tensile test also revealed the conservation of biomechanical properties. The hydroxyproline content of decellularized organs was similar to native lung (0.19 $\mu\text{g}/\text{mg}$ vs 0.22 $\mu\text{g}/\text{mg}$). Histological and immunohistochemical evaluations revealed effective cell seeding on decellularized matrices. Enzymatic measurement suggested the potential functional properties of the regenerated lungs with satisfactory levels of trypsin and alpha 1 antitrypsin.



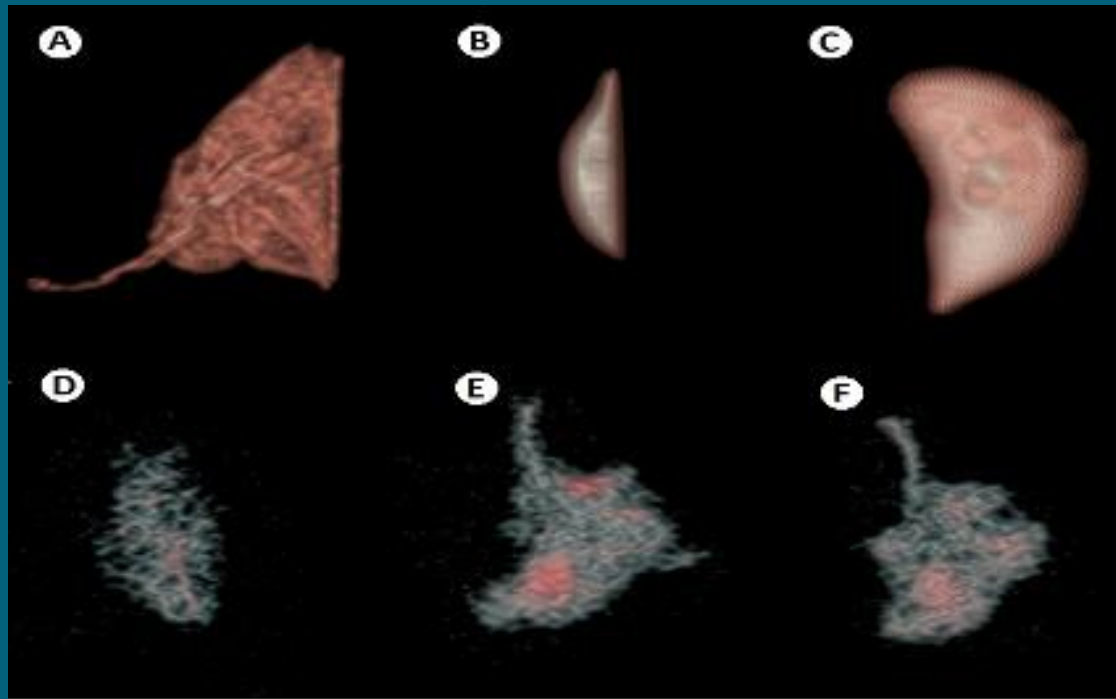
Decellularization steps of lung tissue: (A) Normal lung tissue just before the decellularization procedure (B) Lung tissue after washing with distilled water in the first cycle (C) The end of the first cycle (D) Decellularized lung after the second cycle.



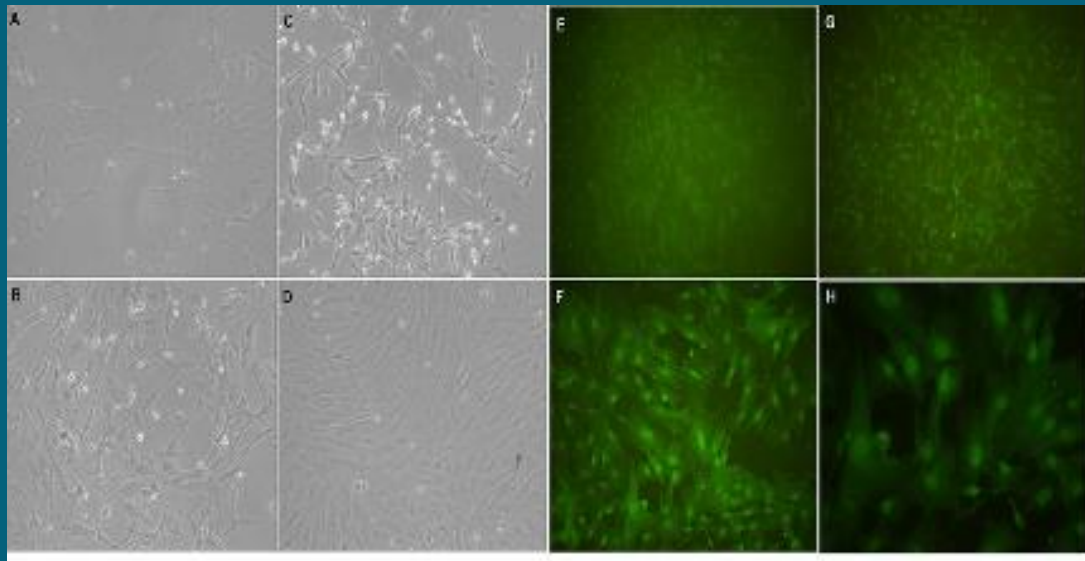
asting procedure: **(A)** Decellularized lung tissue after casting process, **(B)** The application of acetic acid for digestion of lung tissue, **(C)** Cast of decellularized lung scaffold after the application of digestive enzymes.



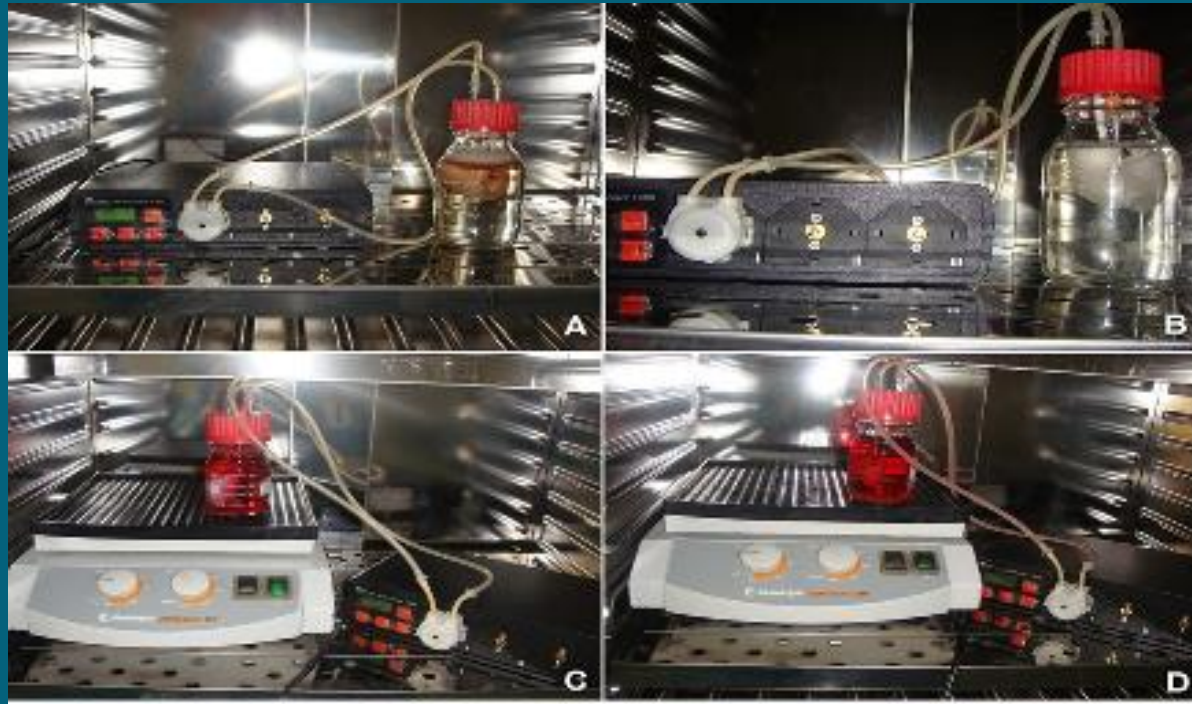
Evaluation of ECM preservation: (A) Radiography imaging depicted bronchial branches after decellularization protocol authenticating the efficacy of our procedure in terminal alveoli preservation, (B) Injection of methylene blue in the decellularized scaffold for demonstrating the preservation of bronchial branches and terminal alveoli without the leakage of the dye from the scaffold



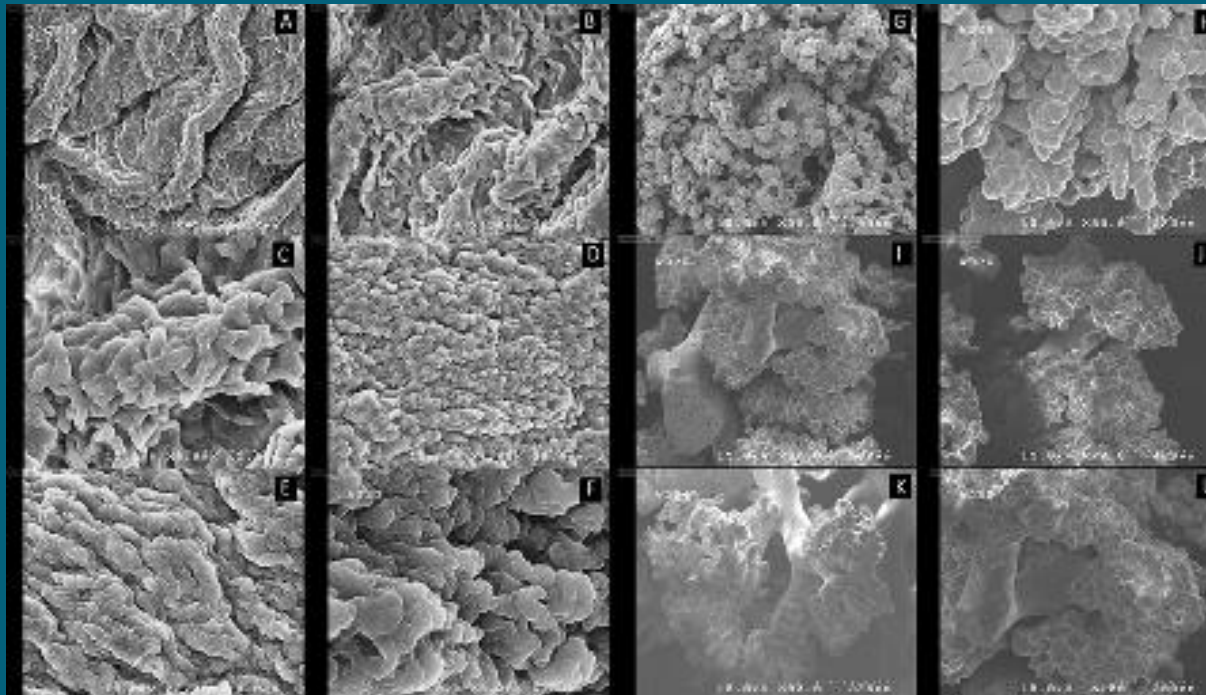
MRI and CT scan imaging: **(A-C)** Three-dimensional reconstruction of CT scan demonstrated cast, normal and decellularized lung scaffold, **(D-F)** Magnetic resonance imaging as a comparing test for cast, natural and decellularized lung tissue.



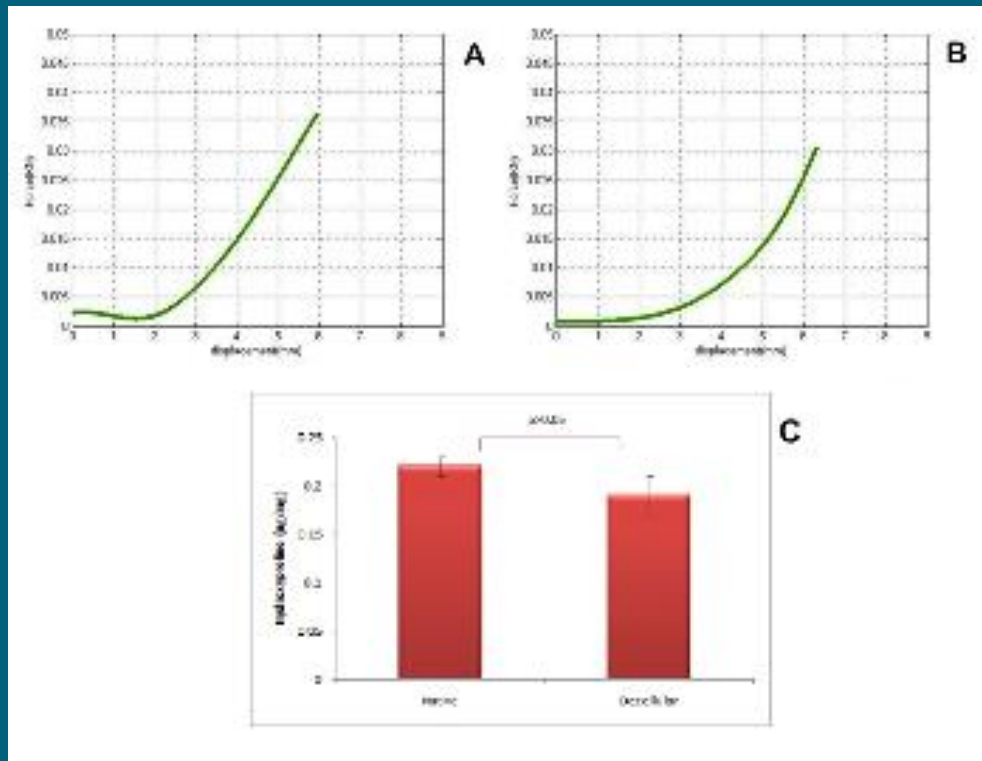
Lung cells in cell culture dish: (A-D) Non- GFP lung cells , (E-H) GFP positive lung cells



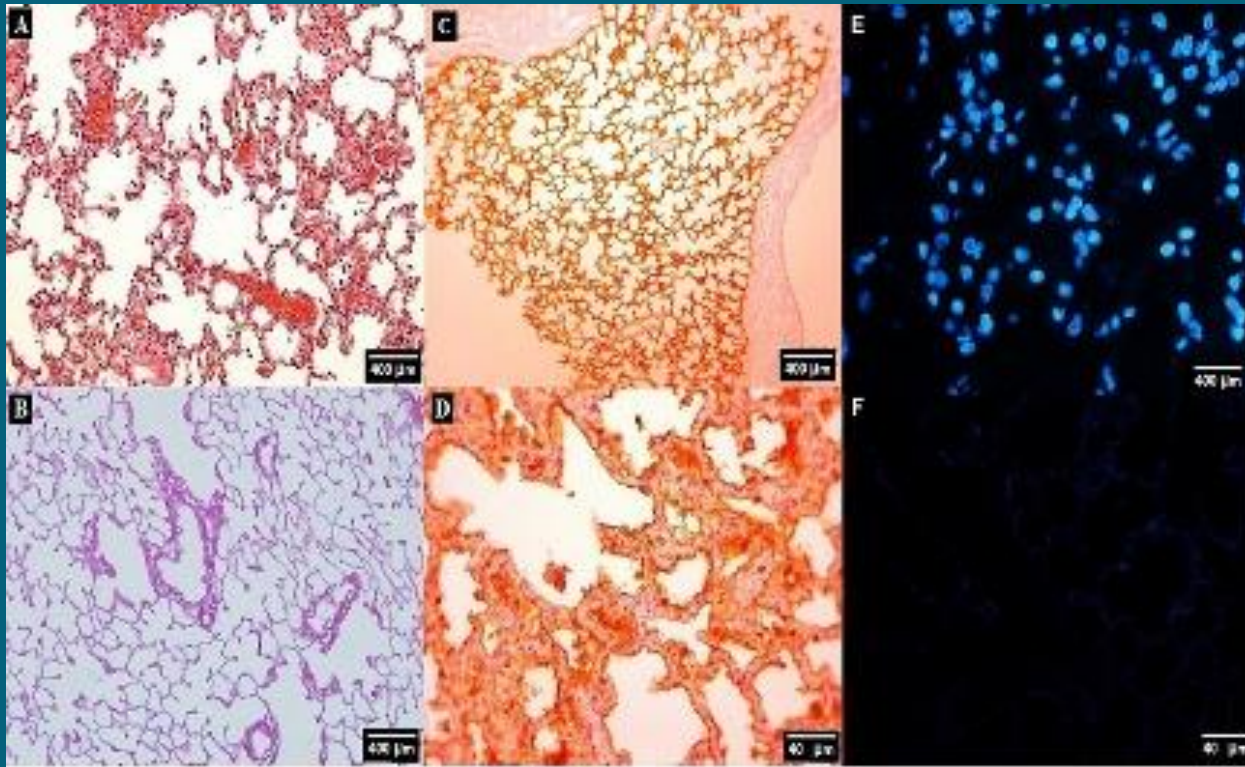
Recellularization steps: (A) Initial steps of lung decellularization in the bioreactor, (B) Decellularized scaffold that is washed with PBS and is ready for cell seeding, (C) Perfusion of medium and cells in the first day, (D) cell seeding process on the 8th day.



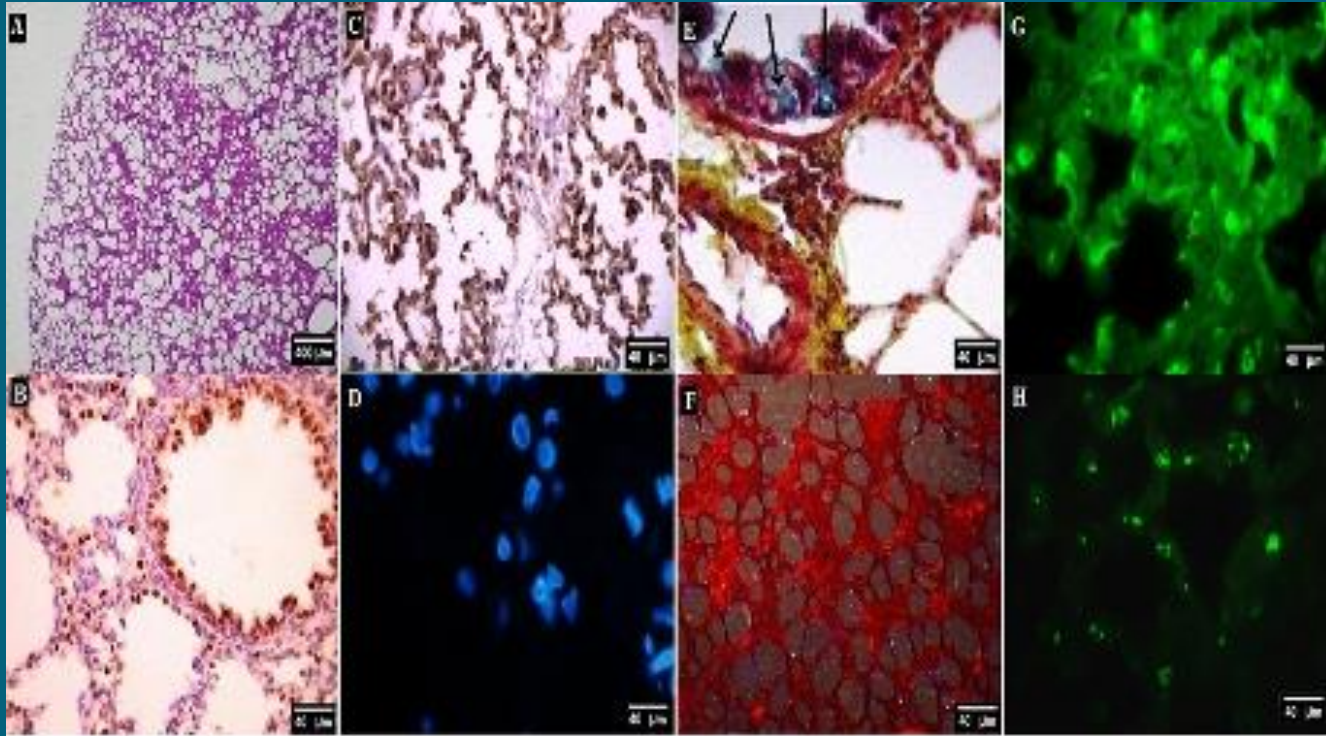
Scanning electron microscope: (A & B) Natural tissue, (C & D) Decellularized lung after the first cycle of decellularization procedure, (E & F) Complete lung scaffold after the second cycle of decellularization procedure, (G & H) SEM of natural lung tissue in cast, (I & J) Casts obtained from lungs after the first cycle of decellularization procedure, (K & L) Casts of complete decellularized lung scaffold after the second cycle of decellularization procedure.



Tensile test: Force/displacement curve comparing the maximum force tolerated by **(A)** natural and **(B)** decellularized lung scaffold, **(C)** Hydroxyproline contents of native and decellularized lung tissue. Data were not statistically different



Histological staining of natural lung and decellularized scaffold: H&E staining of (A) natural and (B) decellularized lung ,Determination of Laminin in (C) decellularized, and (D) intact lungs . DAPI staining of (E) natural and (F) decellularized lung scaffold.



Histological staining of recellularized scaffold: (A & B) H&E and IHC staining of non-GFP cell seeded scaffold with TTF1 antibody, (C) IHC staining of seeded scaffold with GFP positive cells by anti-GFP antibody, (D) DAPI staining, (E) Pentachrome staining of tissue-engineered lung. Mucin secretion in tissue-engineered lung (arrows), (F) Picrosirius red staining of tissue-engineered lung after recellularization. Red fibers depict type I collagens, (G&H) IF microscopy of natural GFP-positive lung and seeded scaffold, respectively.

Conclusion:

Casts produced by this method seems to have satisfactory geometrical properties for further cell seeding of lung scaffolds. Preservation of inner micro-architecture and terminal alveoli that was confirmed by SEM of lung casts appears to increase the probability of an effective cell seeding process.


[Surgery Today](#)

August 2015, Volume 45, [Issue 8](#), pp 1040–1048

In-vivo trachea regeneration: fabrication of a tissue-engineered trachea in nude mice using the body as a natural bioreactor

Authors

[Authors and affiliations](#)

Abdol-Mohammad Kajbafzadeh , Shabnam Sabetkish, Nastaran Sabetkish, Samad Muhammadnejad, Aram Akbarzadeh, Seyyed Mohammad Tavangar, Mohammad Javad Mohseni, Saeid Amanpour

Original Article

First Online: [26 July 2014](#)

DOI: [10.1007/s00595-014-0993-2](#)

Cite this article as:

Kajbafzadeh, A., Sabetkish, S., Sabetkish, N. et al. Surg Today (2015) 45: 1040.
doi:10.1007/s00595-014-0993-2

Objective:

To investigate the outcomes of implanting rat Decellularized Trachea Scaffold (DTS) between paravertebral muscles of **nude mice** by using the body as a bioreactor for total graft recellularization.

Material and Methods:

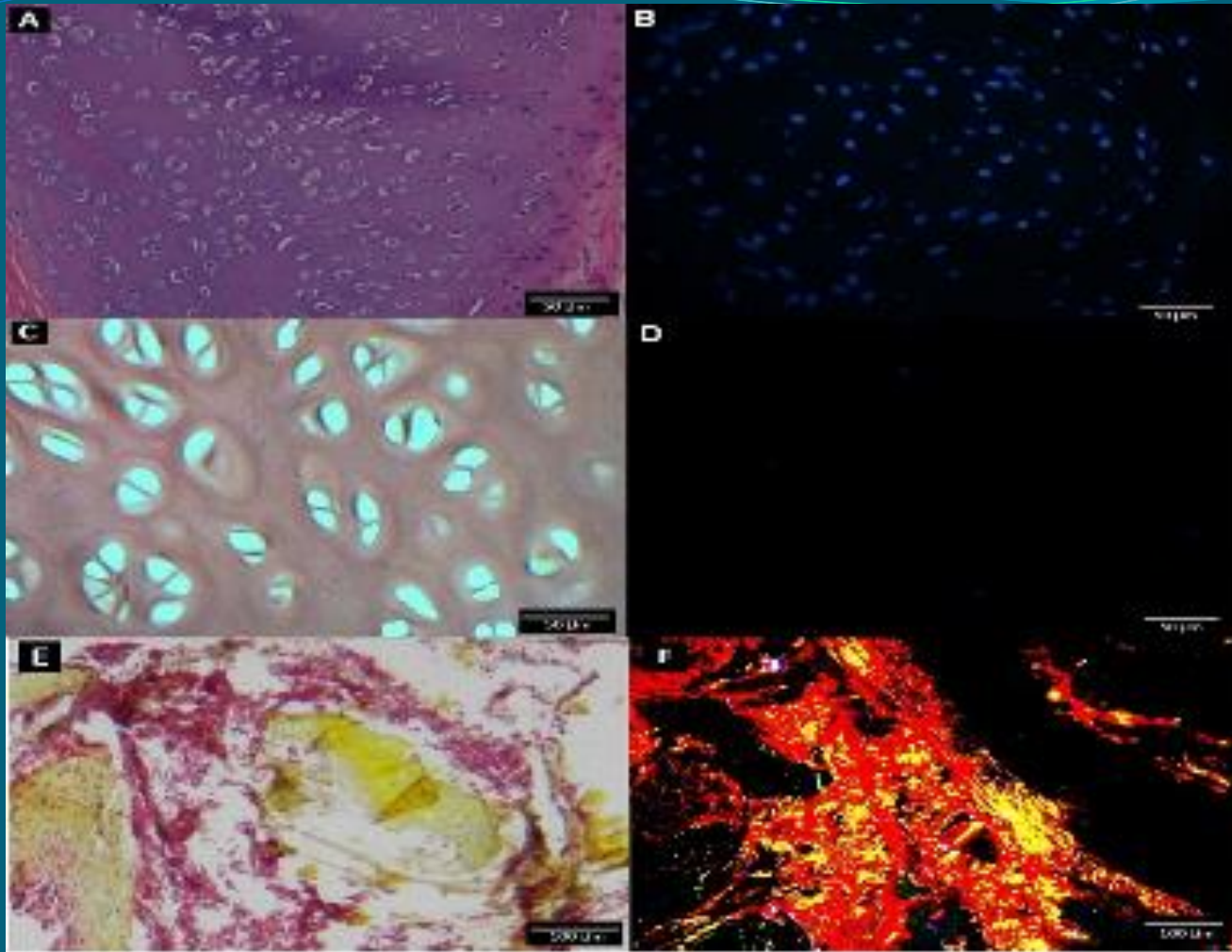
Tracheas of 4 rats were aseptically resected and decellularized. To assess the efficiency of decellularization procedure, all decellularized scaffolds and native control tissues were evaluated with scanning electron microscopy (SEM), DAPI staining, DNA quantification, biomechanical properties, and hydroxyproline measurement. They were then implanted between the paravertebral muscles of 4 nude mice. The grafts were preciously evaluated at 1, 3, 6, and 12 months postoperatively for tracheal cartilage and soft tissue recellularization by TTF1, CD34, S100, and Leukocyte Common Antibody (LCA) staining.

Results:

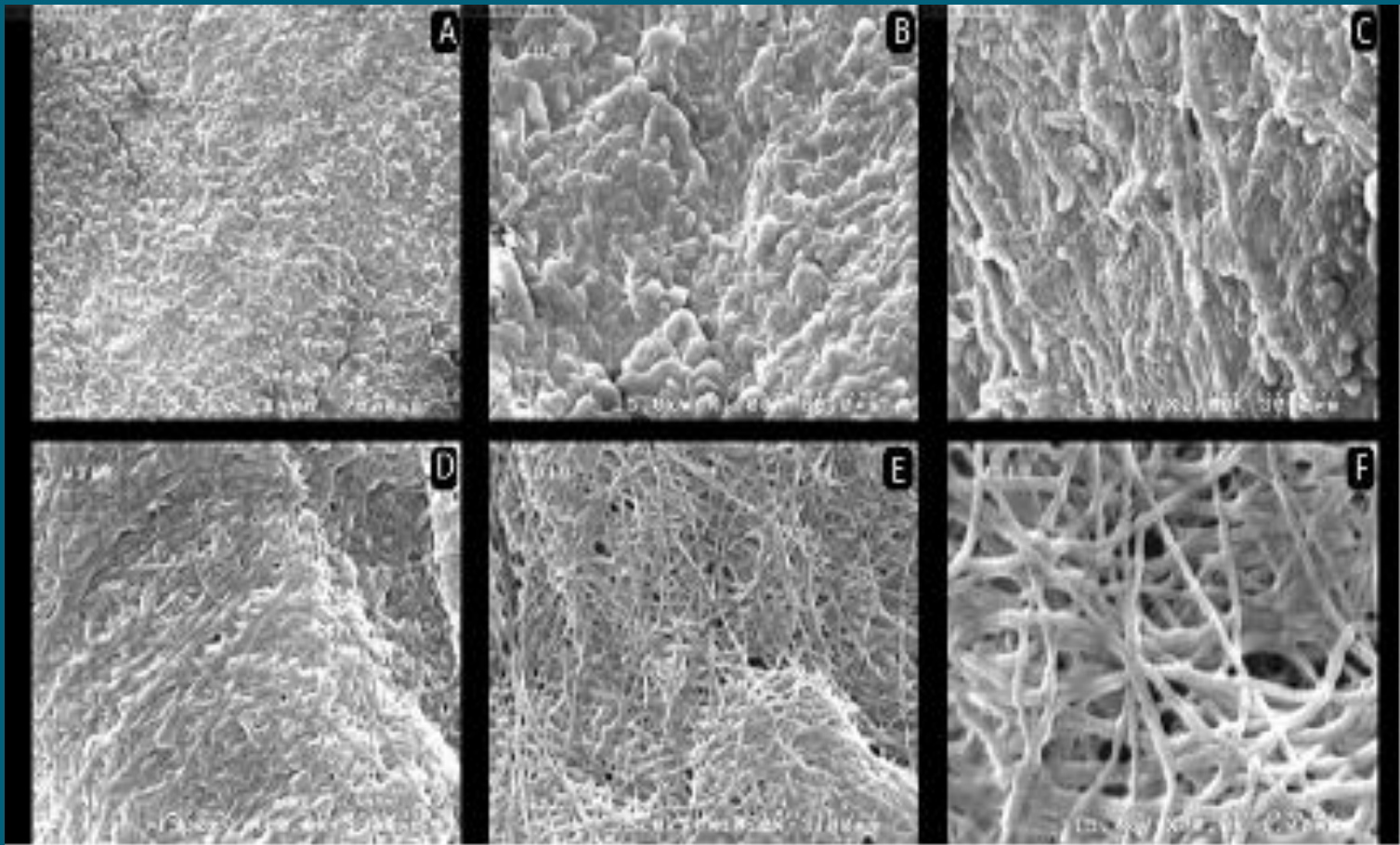
Hematoxylin and Eosin (H&E) staining, SEM, and tensile test confirmed the preservation of tissue structure, biophysical, and biochemical properties of DTS. The present study clearly demonstrated that the hydroxyproline content of DTS was similar to native tissue. On the other hand, in biopsies obtained after 12 months, histological evaluation showed superior organization and cell seeding in both cartilage and connective tissues.



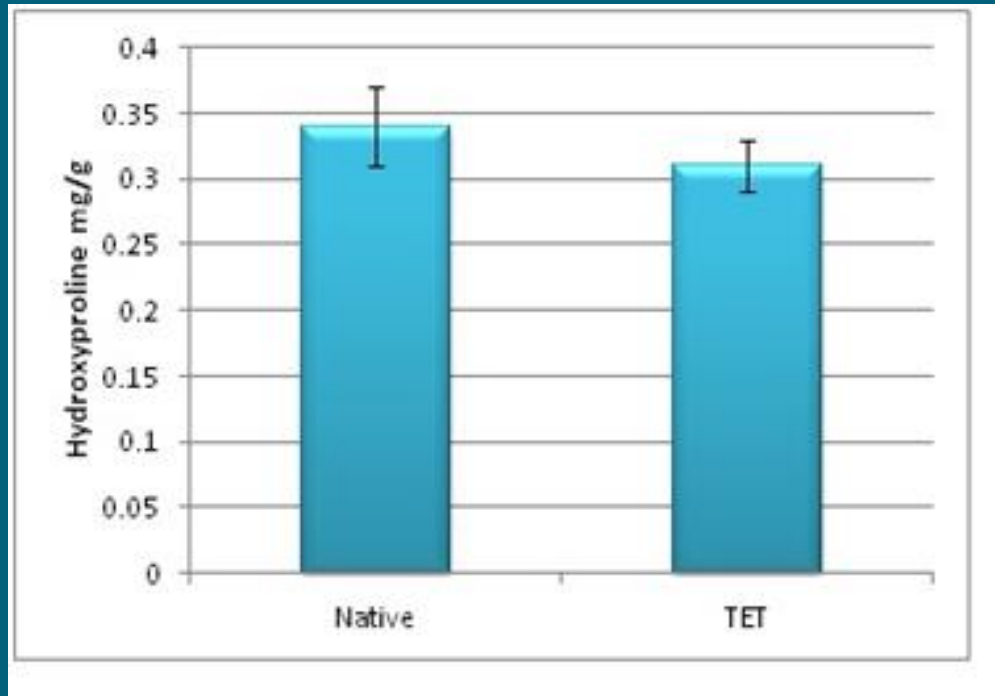
Surgical technique: (A) implanted DTS between the back muscles of nude mice (B) recellularized tracheas after 12 months of implantation



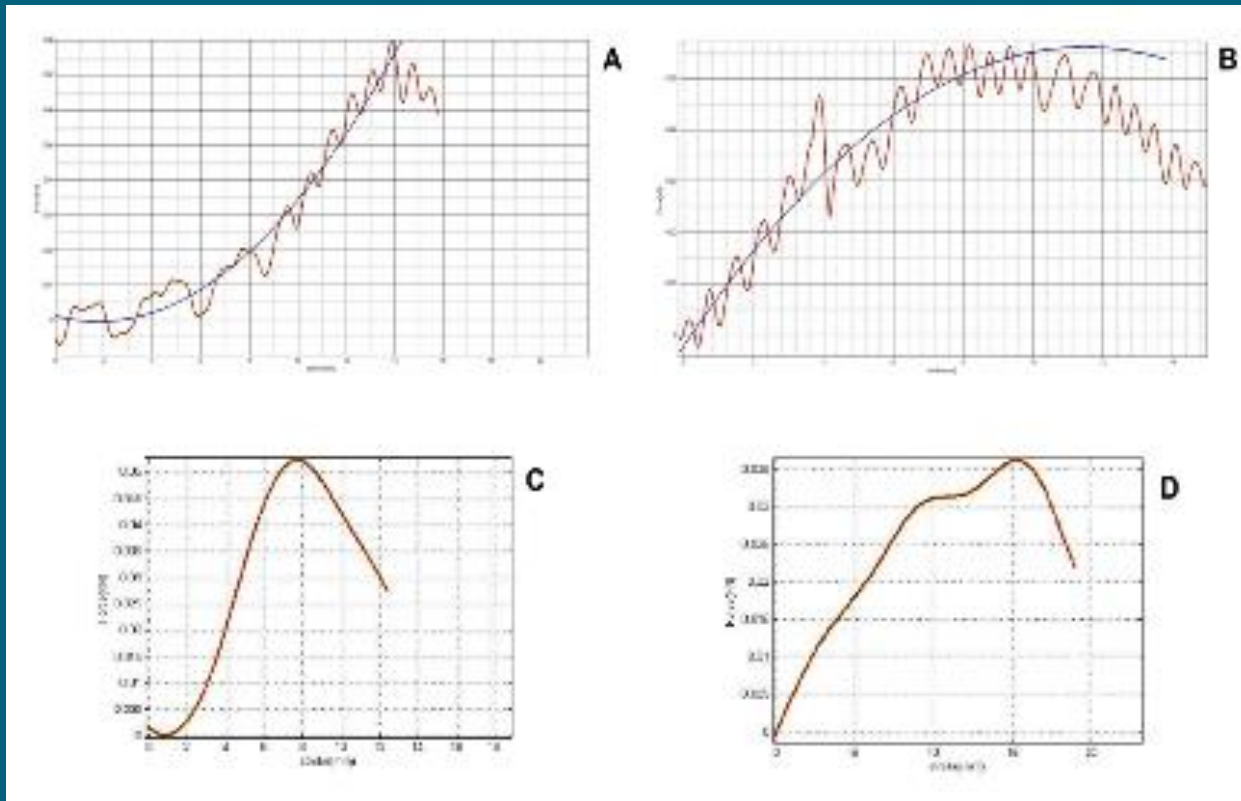
Histological examination: (A & B) H&E and DAPI staining of natural trachea before decellularization procedure (C & D) histological analysis and DAPI staining of DTS (E) Pentachrome and (F) Picro sirius red staining of DTS.



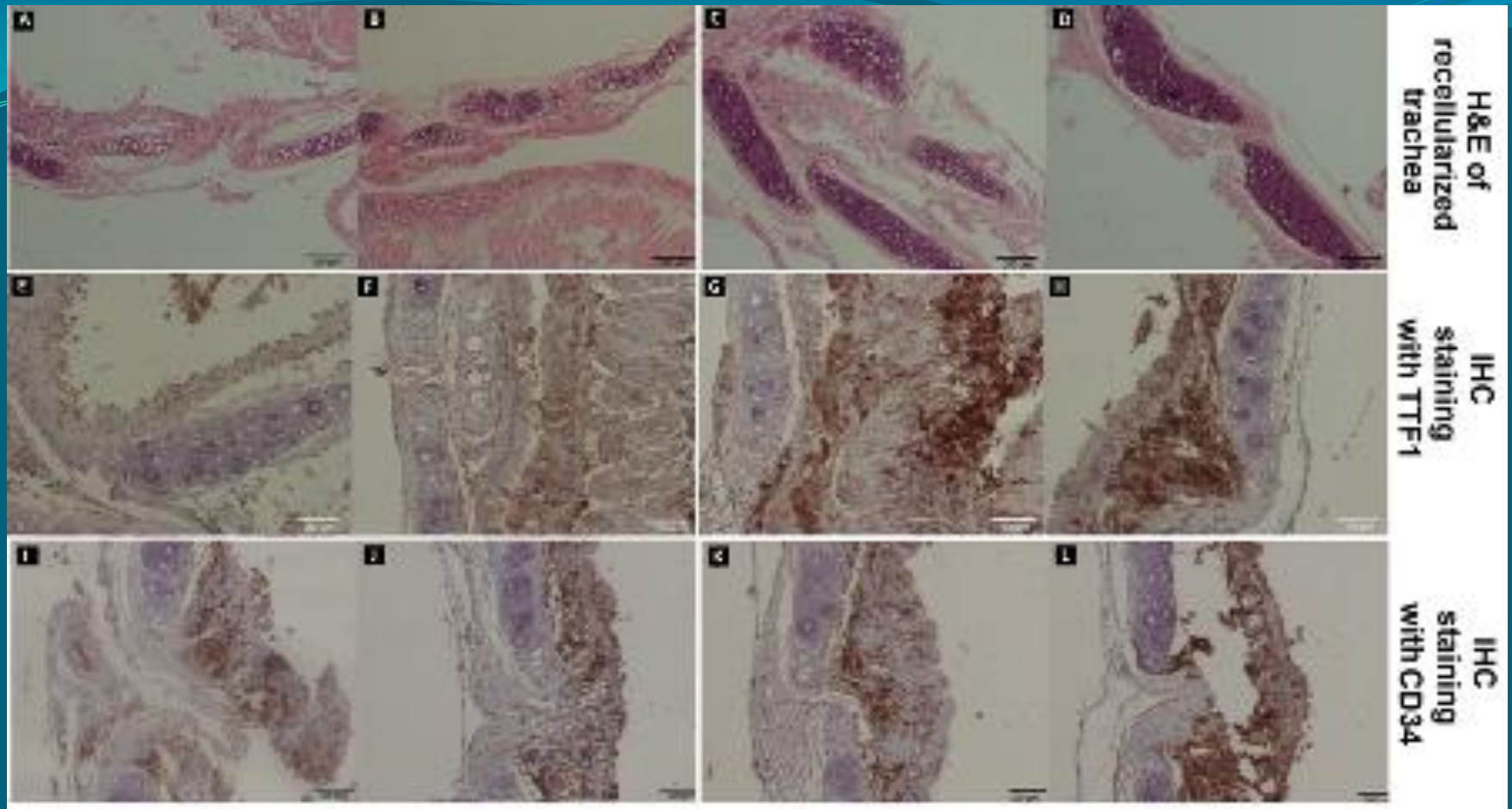
Scanning electron micrograph: (A-C) natural trachea (D-F) DTs



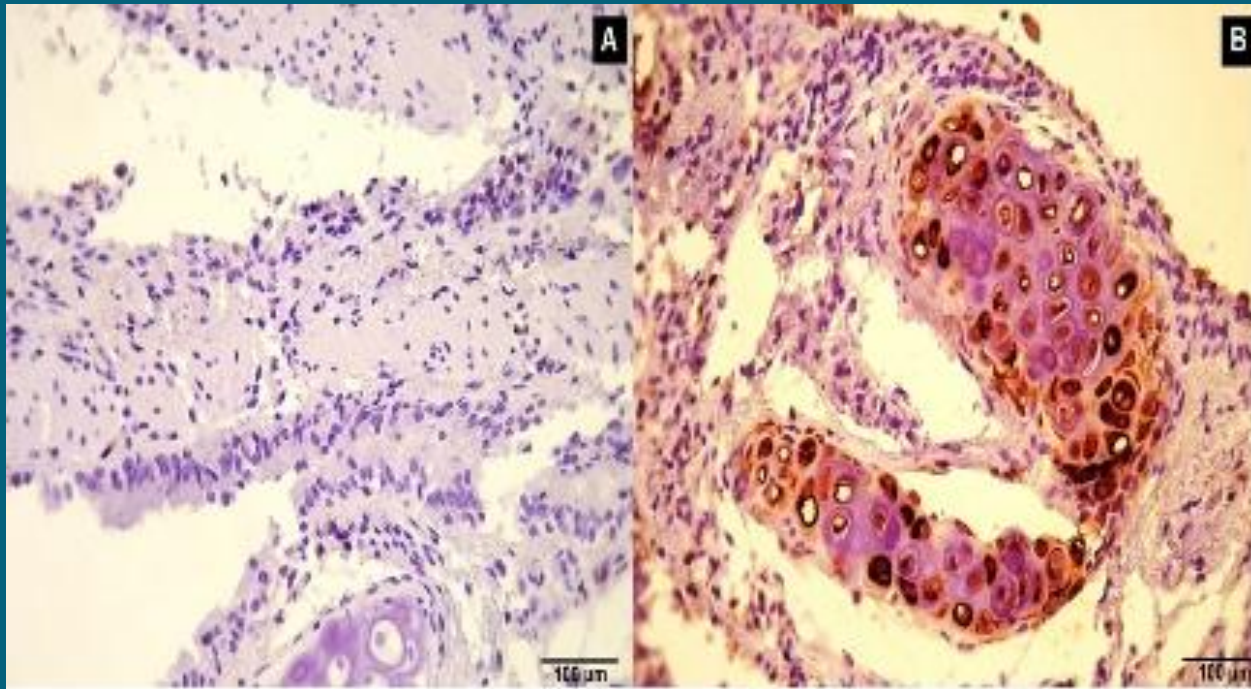
Comparison of hydroxyproline contents of native trachea and decellularized trachea.
Data were not statistically different



Tensile testing: (A & B) Hook test in which the cartilage component is evaluated in both fresh trachea and DTS, respectively (C & D) Tensional test for assessing connective tissue of DTS and natural trachea



Immunohistological Examination: (A) H&E staining of the grafted DTS, 1 month postoperatively (B) Histological evaluation of the graft with numerous cells seeded in the cartilage component without fibrosis or inflammation after 3 months of implantation (C) Histopathological analysis of the grafted DTS showed approximately natural trachea structure ,6 months postoperatively (D) Well-organized trachea structure in the grafts, 12 months postoperatively (E-H) IHC staining for TTF1 in 1, 3, 6, and 12 months of implantation (I-L) IHC staining for CD 34 in 1, 3, 6, and 12 months of implantation




Immunohistochemical evaluation: (A) IHC staining for LCA showed no staining, 12 months after implantation (B) Anti-S100 staining, 12 months after implantation

Conclusion:

This study demonstrated the feasibility of natural bioreactor in recellularizing DTS; which may have the potential to facilitate homologous transplantation for repair of segmental trachea defects.

[Go to old article view](#)

 [Get access](#)

 Text size  Share


**Journal of
Biomedical Materials Research** PART A



[Explore this journal >](#)

Original Article

Whole-organ tissue engineering: Decellularization and recellularization of three-dimensional matrix liver scaffolds

Shabnam Sabetkish, Abdol-Mohammad Kajbafzadeh, Nastaran Sabetkish, Reza Khorramirouz, Aram Akbarzadeh, Sanam Ladi Seyedian, Parvin Pasalar, Saghar Orangian, Reza Seyyed Hossein Beigi, Zahra Aryan, Hesam Akbari, Seyyed Mohammad Tavangar 

First published: 4 August 2014 [Full publication history](#)

DOI: 10.1002/jbm.a.35291 [View/save citation](#)

Cited by: 5 articles  [Citation tools](#)



None of the authors has direct or indirect commercial financial incentive associating with publishing the article and does not have any



[View issue TOC](#)
Volume 103, Issue 4
April 2015
Pages 1498–1508

Objectives:

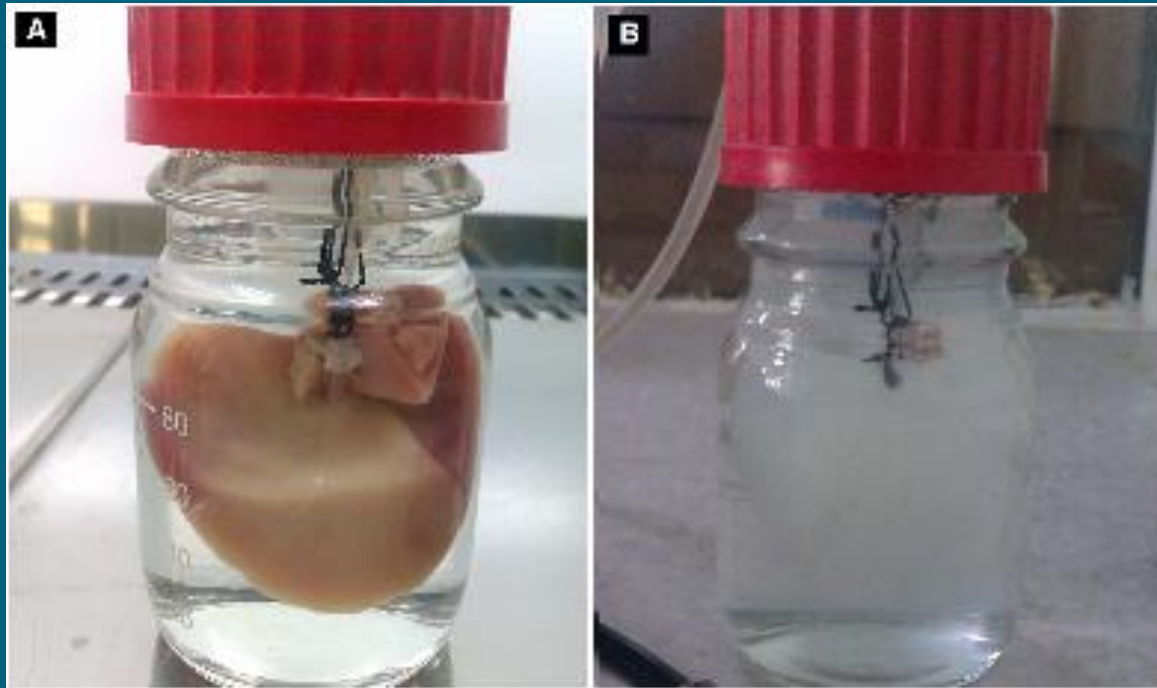
To report the results of whole rat liver decellularization, characterization of the extracellular matrix, and in-vitro whole liver recellularization with rats' neonatal green fluorescent protein (GFP)-positive hepatic cells by a designed bioreactor. To present the results of rat and sheep decellularized liver matrix (DLM) graft into the normal rat liver and compare natural cell seeding process in homo/xenograft of DLM by rat autologous circulating mesenchymal stem cells.

Materials and Methods:

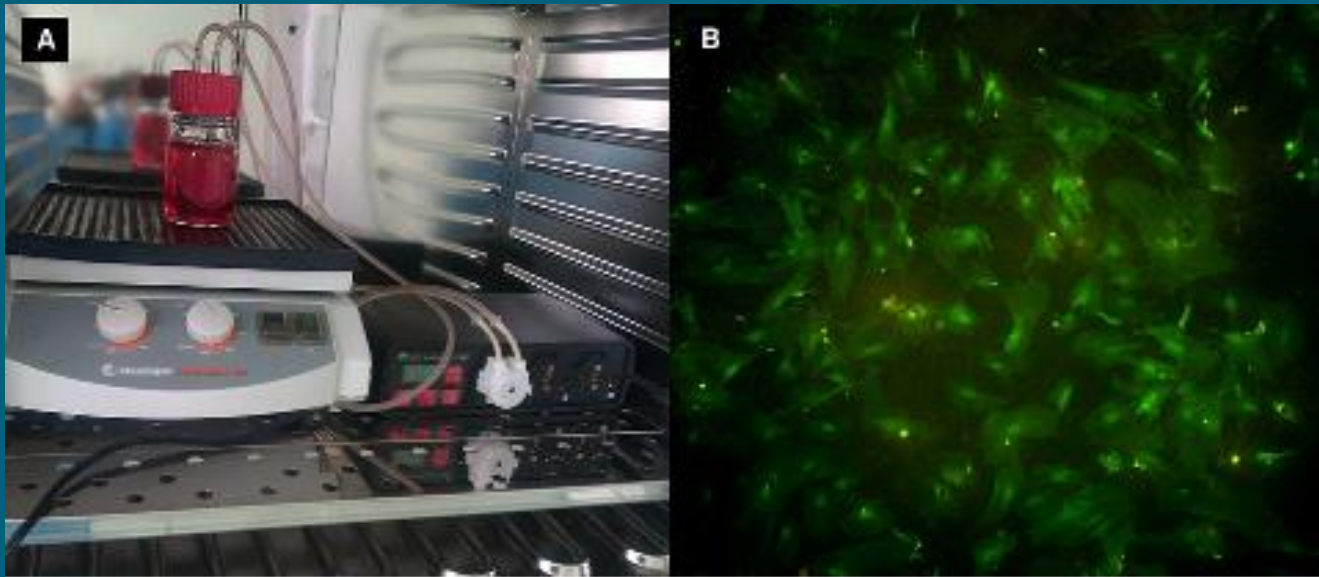
Whole liver of 8 Sprague Dawley rats and four sheep were resected and cannulated via the hepatic vein and perfused by pulsatile pump with two different protocols (*sodium dodecyl sulfate (SDS)* or Triton+ SDS). Several examinations were performed to evaluate and compare the efficacy of these two decellularization procedures and the micro vascular integrity structure. In-vivo recellularization was also performed following transplantation of multiple pieces of sheep and rat DLMs in the subhepatic area to compare the efficacy of different scaffolds in autologous cell seeding. Four rat's whole liver DLMs were recellularized in-vitro by perfusion of rat's fetal GFP-positive hepatic cells with pulsatile bioreactor. Histology, immunohistochemical staining, and enzymatic assay of recellularized livers were performed. Biopsies of both homograft and xenograft were assessed for liver recellularization 8 weeks post-operatively.

Results:

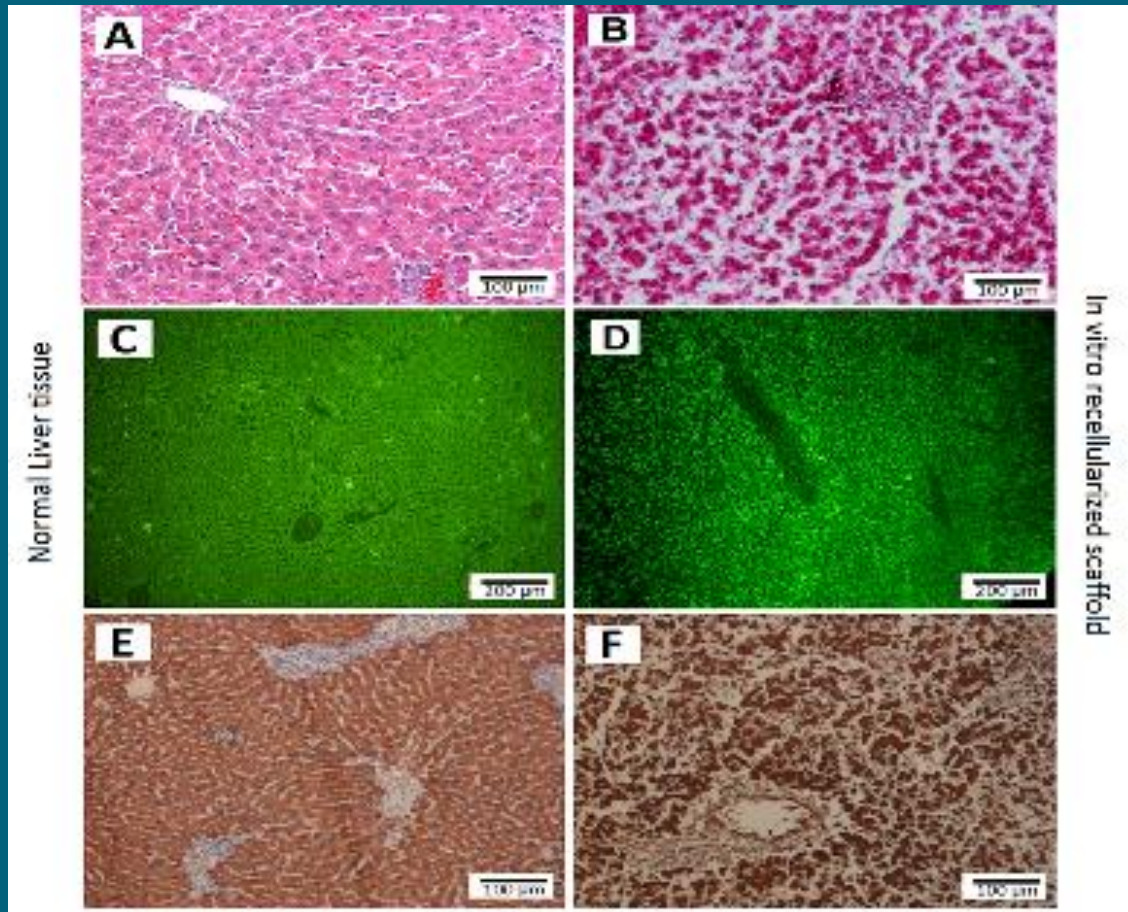
The preliminary results of this study demonstrated that the triton method is a promising decellularization approach for preserving the three-dimensional structure of liver to provide alternatives for whole organ decellularization. According to the biochemical assay and histopathological evaluations of the recellularized livers; in-vitro recellularized DLMs were more similar to natural ones compared with in-vivo recellularized livers. However, homografts showed better characteristics with more organized structure compared with xenografts.



Decellularization steps: (A) Normal cannulated Liver for decellularization process, (B) Second step of liver decellularization with triton and SDS

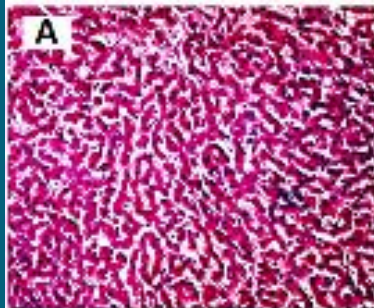


Recellularization steps: (A) Perfusion of medium and cells, (B) GFP-positive hepatic cells

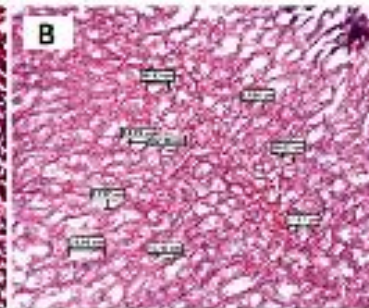


Comparison of normal and in vitro recellularized liver scaffold: (A&B) H&E, (C&D) immunofluorescent imaging, (E&F) IHC staining with anti-hepatocyte

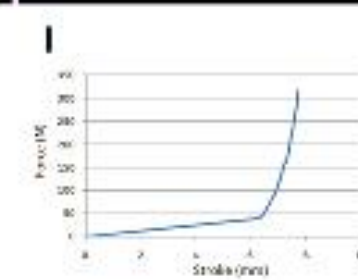
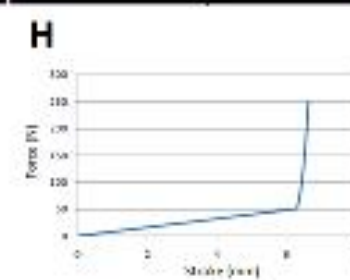
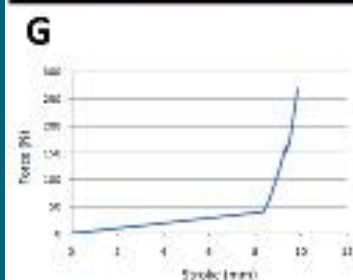
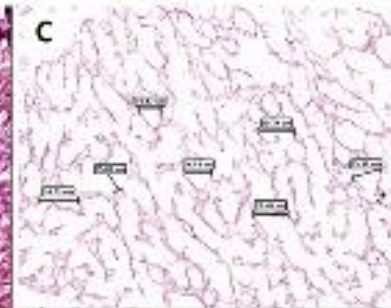
Natural Liver

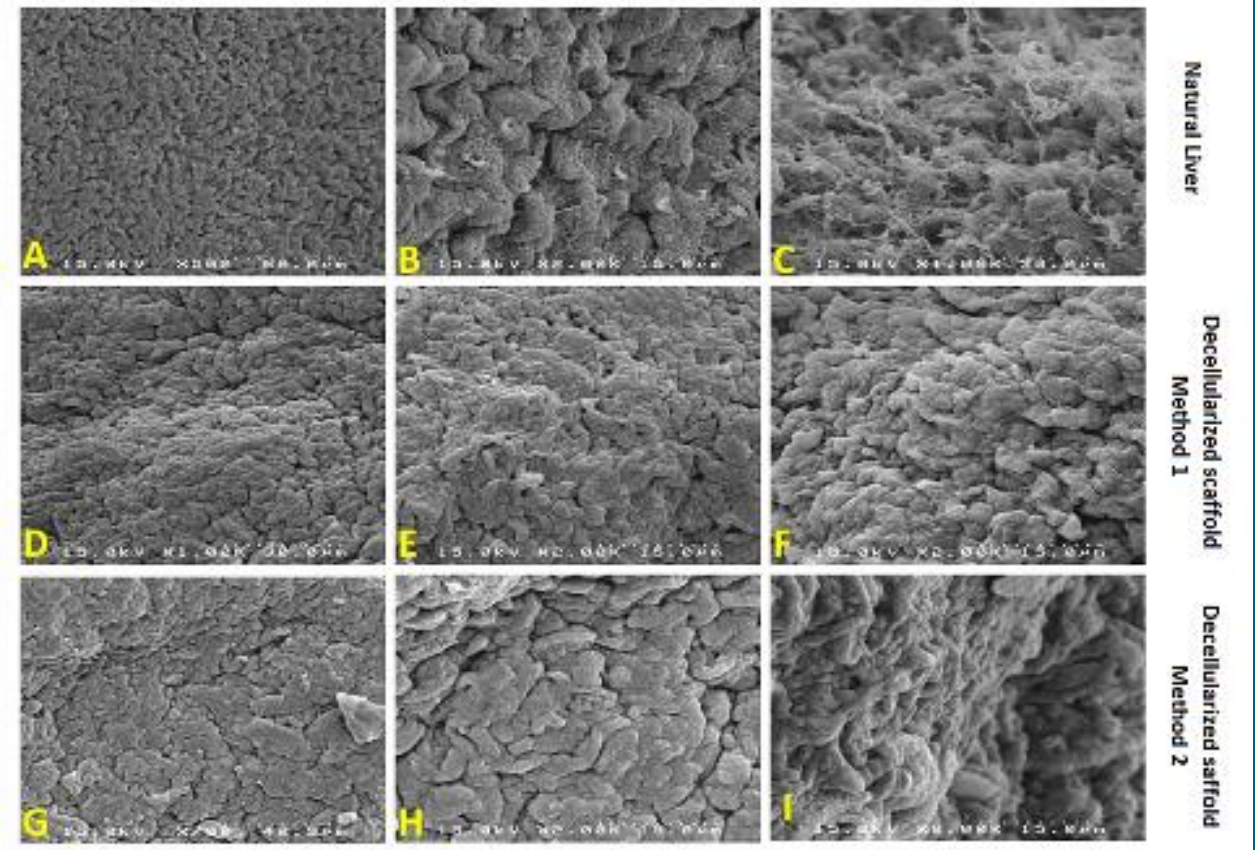


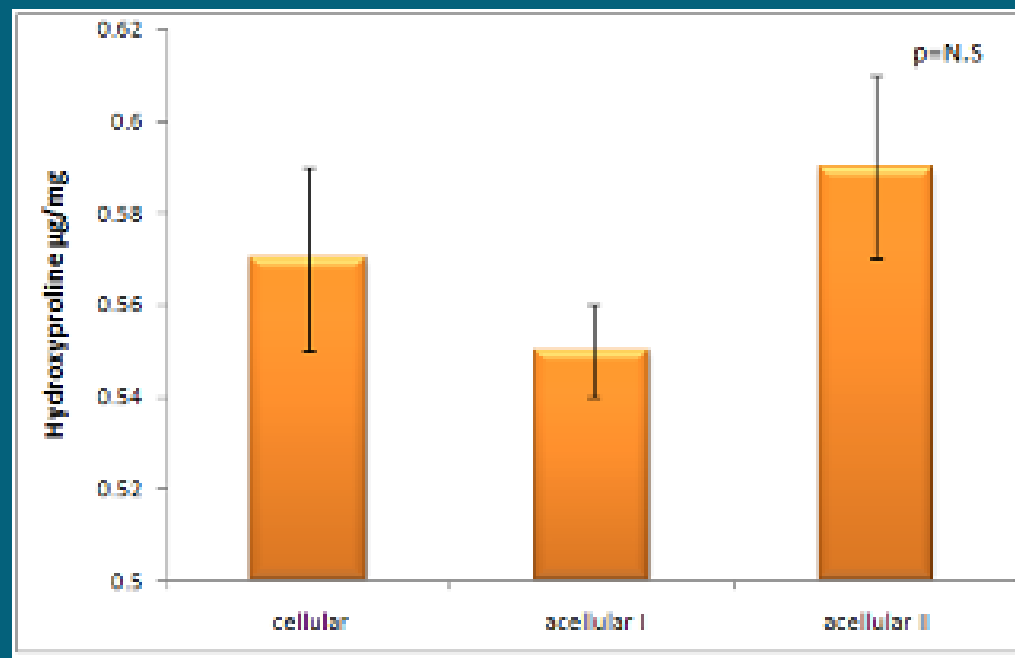
Decellularized scaffold
with method 1

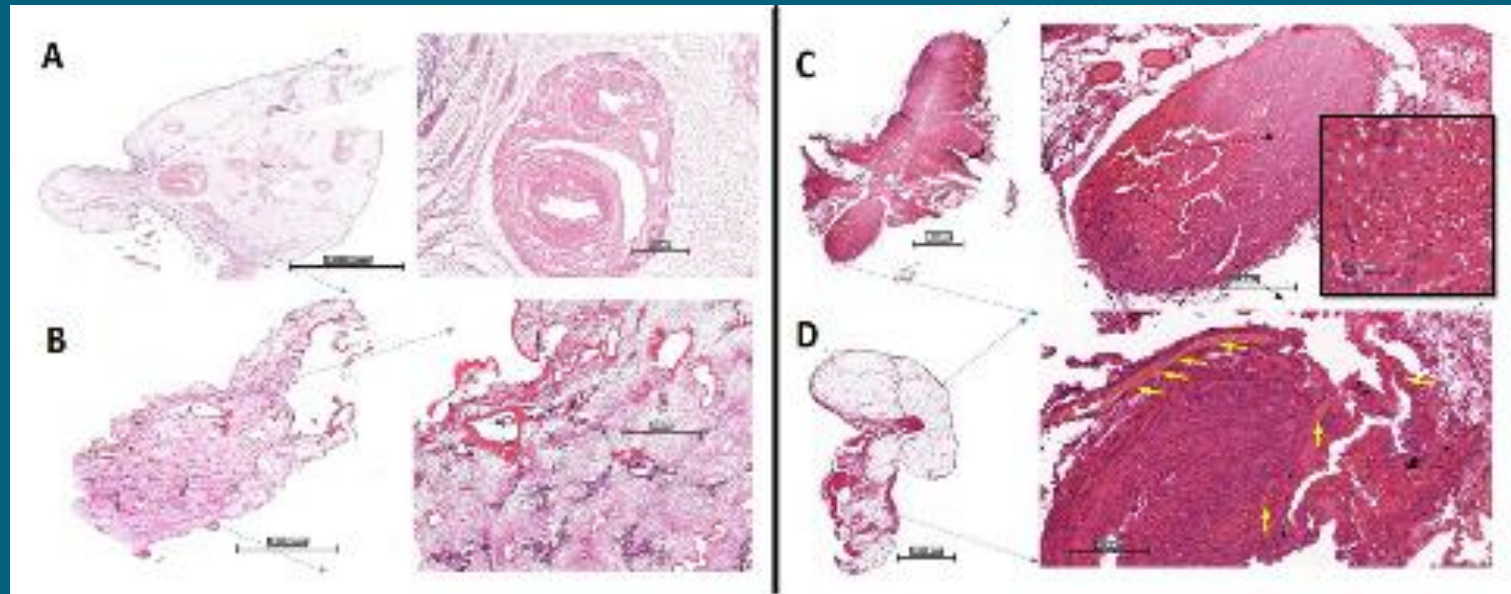


Decellularized scaffold
with method 2

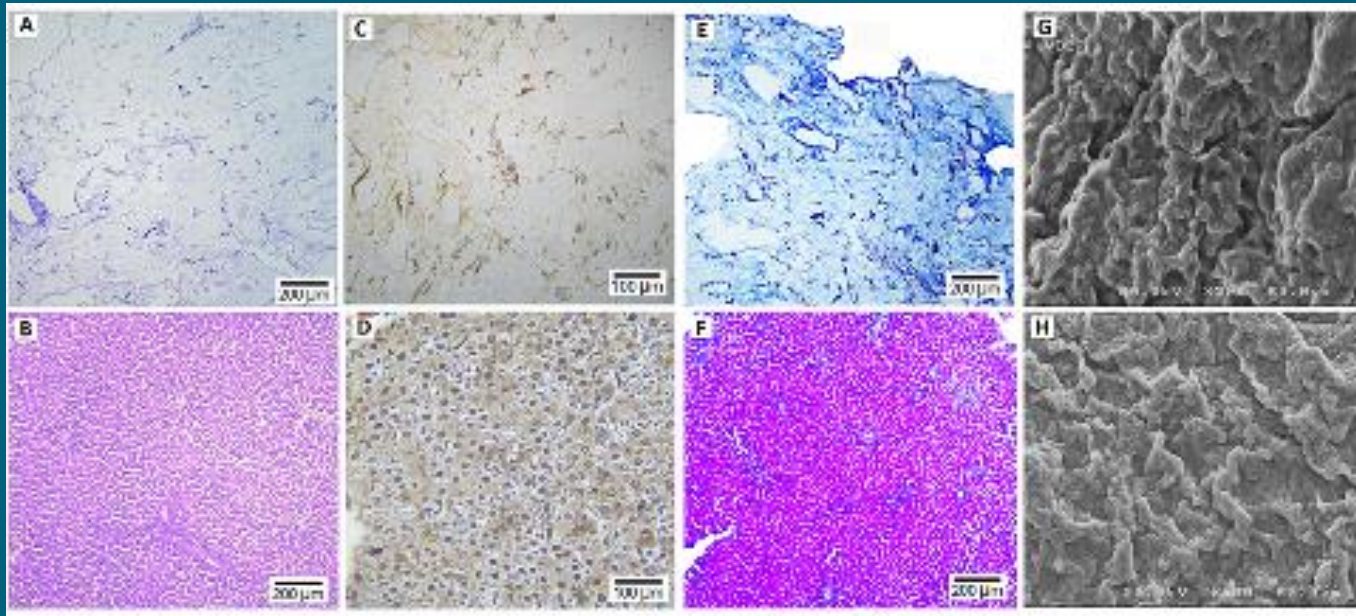




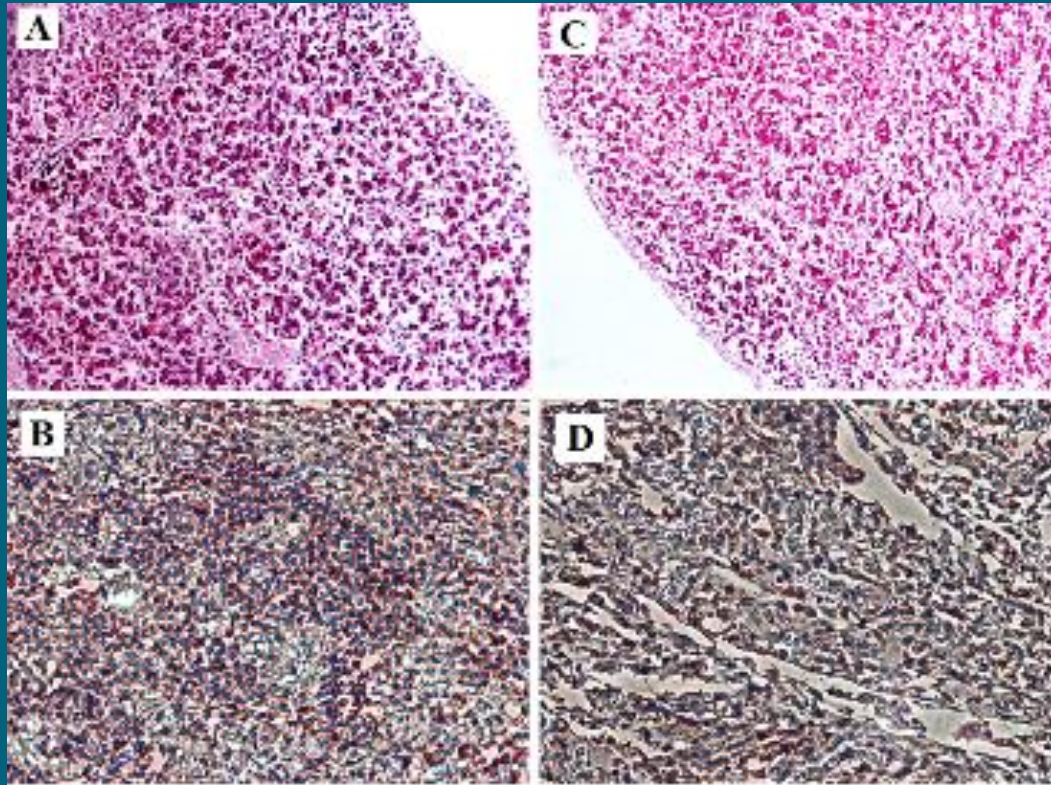




Histological examination of Sheep DLM before and after the transplantation: (A) Complete cell removal with preservation of basic structure frame was seen in the liver that was decellularized with method 1. The wall of the portal vein was thicker in method 1 with more connective tissue in the structure of portal vein wall, (B) More lysis reactions were found in method 2, (C&D) Xenogenic transplantation of DLMs with fibrotic changes in hepatocyte seeded scaffolds that were obtained from method 1 and 2



Evaluation of rat DLMs: (A-B) H&E staining of decellularized and normal scaffolds, (C-D) Reticulin staining of decellularized and natural livers, (E-F) Trichrome staining of processed and intact livers, (G-H) SEM analysis of decellularized and normal matrices



Histological evaluation of homotransplantation and xenotransplantation:
(A&B) H&E and hepatocyte staining of rat to rat transplantation
(C&D) H&E and hepatocyte staining of sheep to rat transplantation

Table 2: Hepatic enzymes level

	SGOT (IU/L)	SGPT (IU/L)	Alkaline phosphatase (U/L)	LDH (U/L)	Gamma GT (IU/L)
Normal liver	18962	1368	261	8694	407
In vitro recellularized liver	11394	924	194	5968	256
In vivo recellularized liver (sheep to rat)	402	33	11	45	59
In vivo recellularized liver (rat to rat)	1011	222	69	531	91

Conclusion:

Whole-organ tissue engineering in small scale is feasible. In-vitro recellularization of liver scaffolds with autologous cells represents an attractive prospective for regeneration of liver as one of the most compound organs. Small pieces of implanted DLMs into the liver tissue will be reseeded by autologous differentiated hepatocytes. This study theoretically may pave the road for in-situ liver regeneration probably by implantation of DLM into the diseased host liver.



[Pediatric Surgery International](#)

April 2014, Volume 30, [Issue 4](#), pp 371–380

Tissue-engineered cholecyst-derived extracellular matrix: a biomaterial for in vivo autologous bladder muscular wall regeneration

Authors

[Authors and affiliations](#)

Abdol-Mohammad Kajbafzadeh , Shabnam Sabetkish, Reza Heidari, Maryam Ebadi

Original Article

First Online: [28 January 2014](#)

DOI: [10.1007/s00383-014-3474-1](#)

Cite this article as:

Kajbafzadeh, A., Sabetkish, S., Heidari, R. et al. *Pediatr Surg Int* (2014) 30: 371.
doi:[10.1007/s00383-014-3474-1](#)

[7](#) Citations

[323](#) Views

Abstract

Purpose

We use cookies to improve your experience with our site. [More information](#)

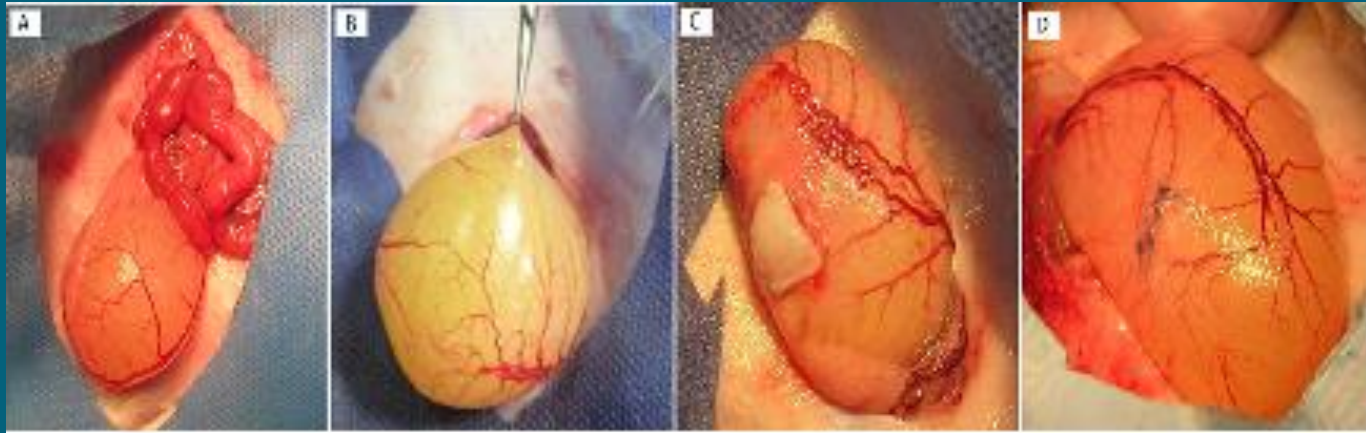
[Accept](#)

Objective:

To compare the biocompatibility and histological aspects of Cholecyst-Derived Extra Cellular Matrix (CDECM) graft, either alone or with application of Autologous Detrusor Muscles Small Fragments (ADMSF) on rabbit bladder mucosa for bladder augmentation.

Material and methods:

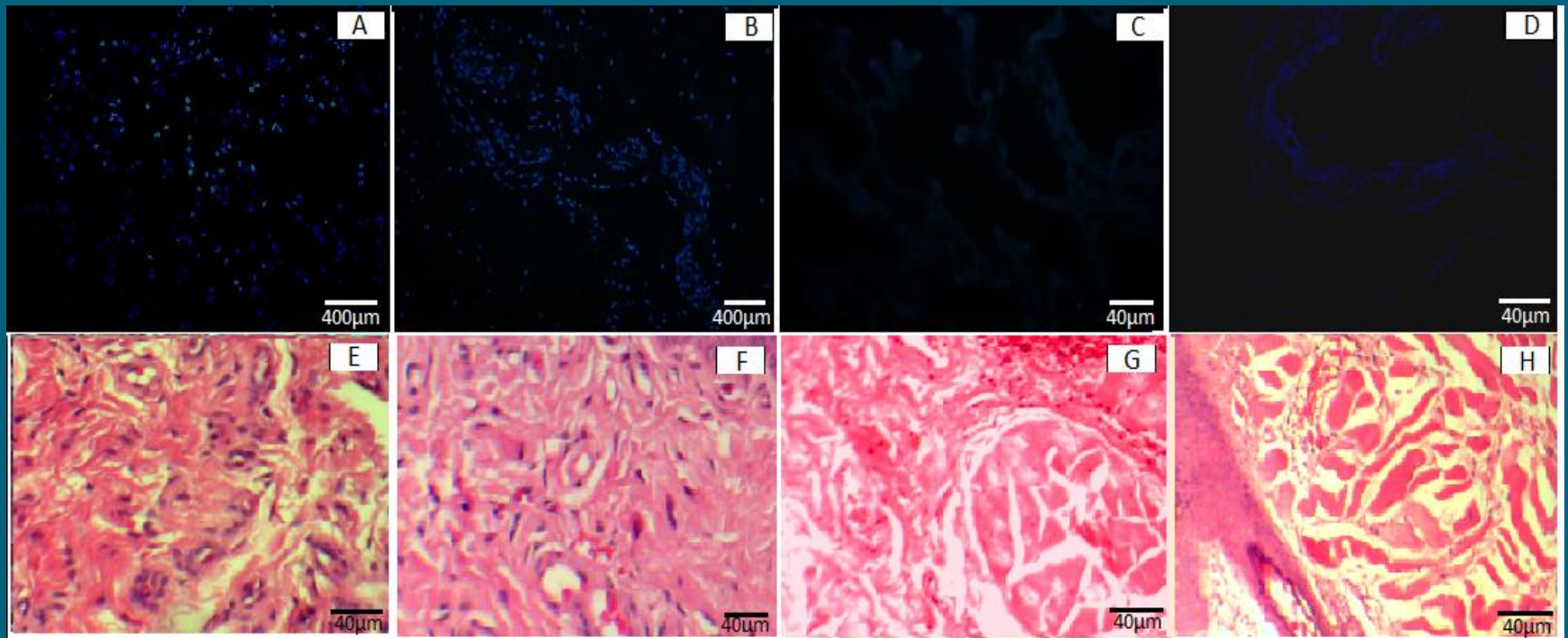
The gallbladders were acellularized and evaluated for preserved acellular matrix scaffold and biophysical properties. Thirty rabbits were divided into 5 groups. Rabbits in the control group underwent partial detrusorectomy followed by perivesical fat coverage. Groups I and II underwent the same procedure and bladder mucosa was covered either by Acellular Rabbit Gallbladder (ARG) (group I), or Acellular Sheep Gallbladder (ASG) (group II). Group III and IV underwent detrusorectomy and the bladder mucosal was seeded by ADMSF and covered by ARG (group III), or ASG (group IV). Biopsies were taken at 4, 12, and 24 weeks postoperatively.



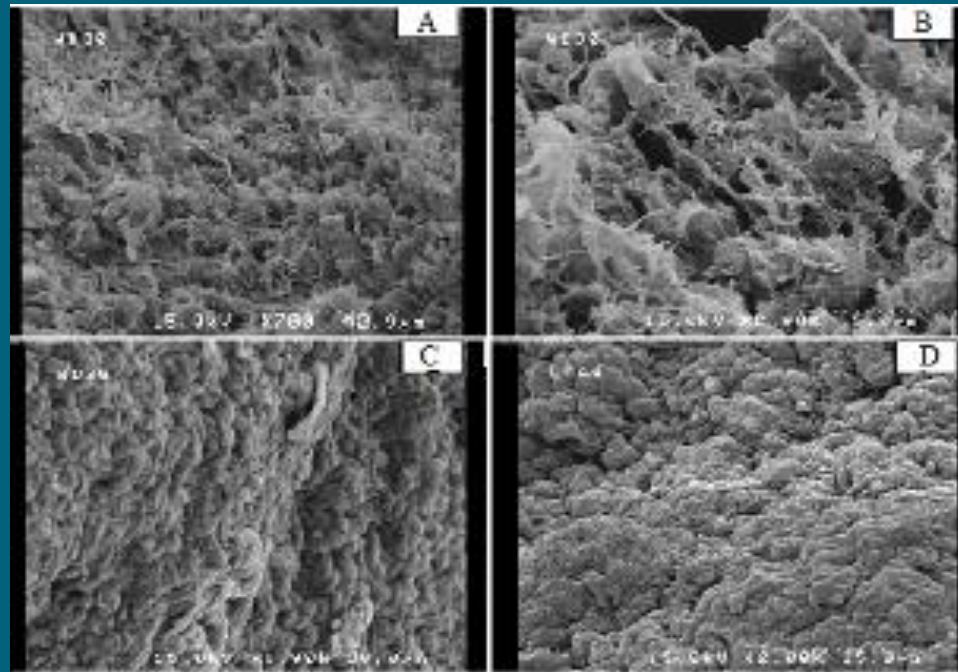
Surgical technique: (A) Bladder exposure, (B) Separation of bladder muscular and urothelium layers, (C) Acellular CDECM was inserted over the bladder mucosal layer, (D) The exposed bladder for explanting the transplanted scaffold after 24 weeks of bladder augmentation

Results:

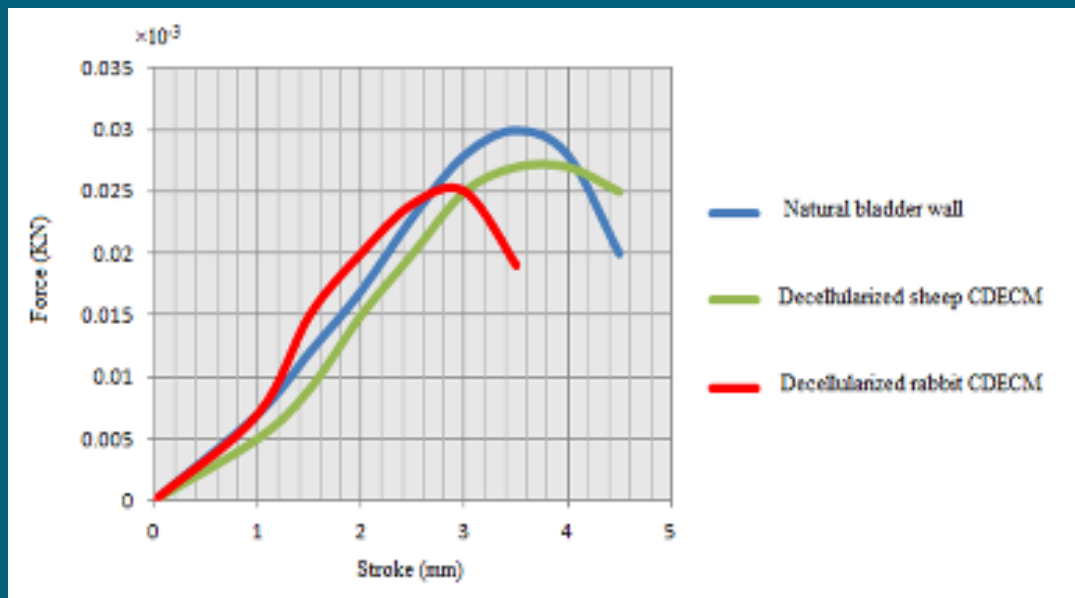
Higher expression of CD34 endothelial progenitor cells, CD31 microvessels, α -smooth muscle actin (α -SMA), S100, and cytokeratin with more organized muscular wall generation, were demonstrated in groups III & IV. Expression of IHC markers was higher in groups III & IV compared with groups I & II in all the time points.



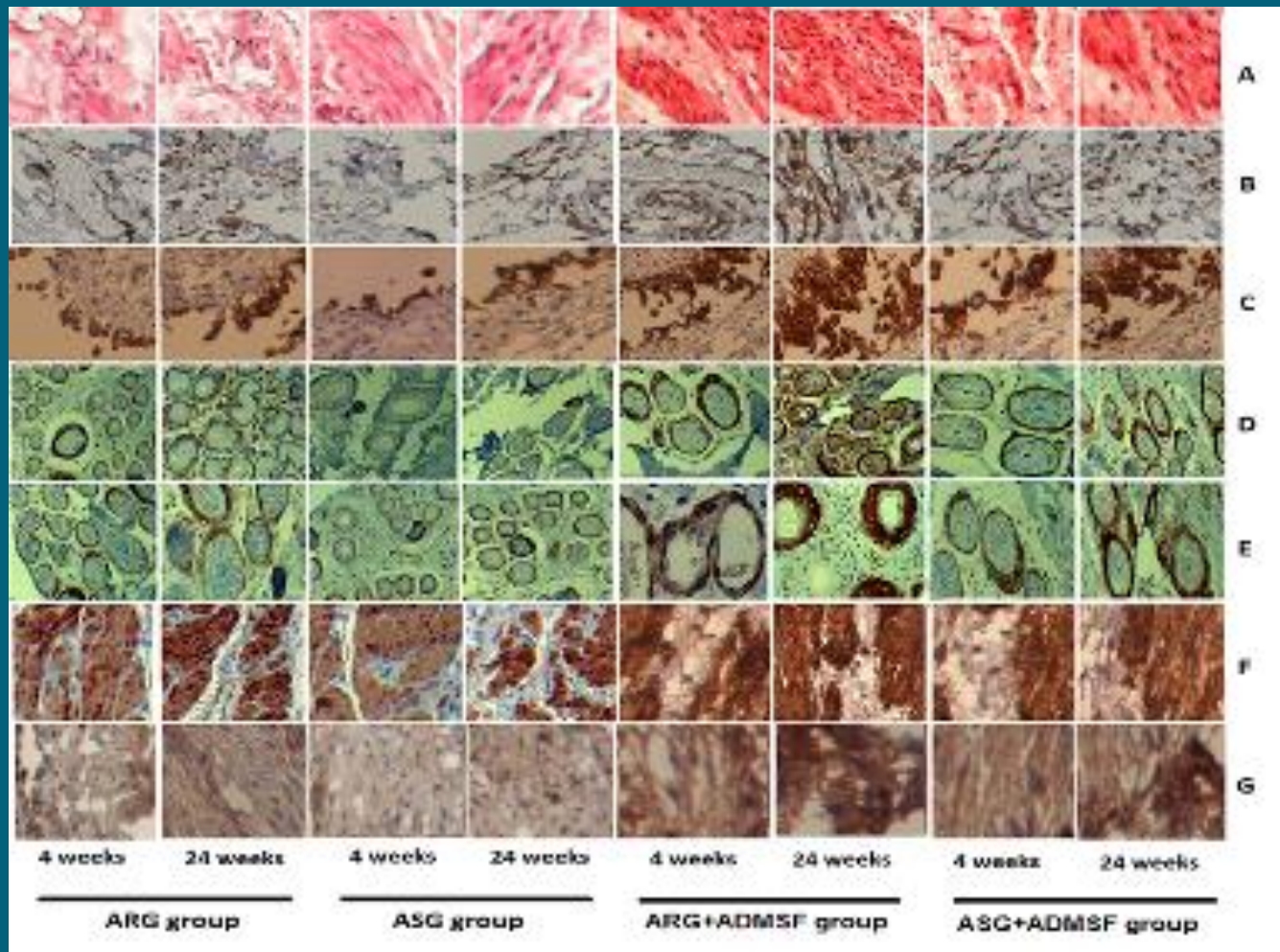
DAPI staining of **(A)** natural rabbit gallbladder **(B)** natural sheep gallbladder **(C)** ARG and **(D)** ASG. H&E staining of **(E)** natural rabbit gallbladder **(F)** natural sheep gallbladder **(G)** ARG and **(H)** ASG.



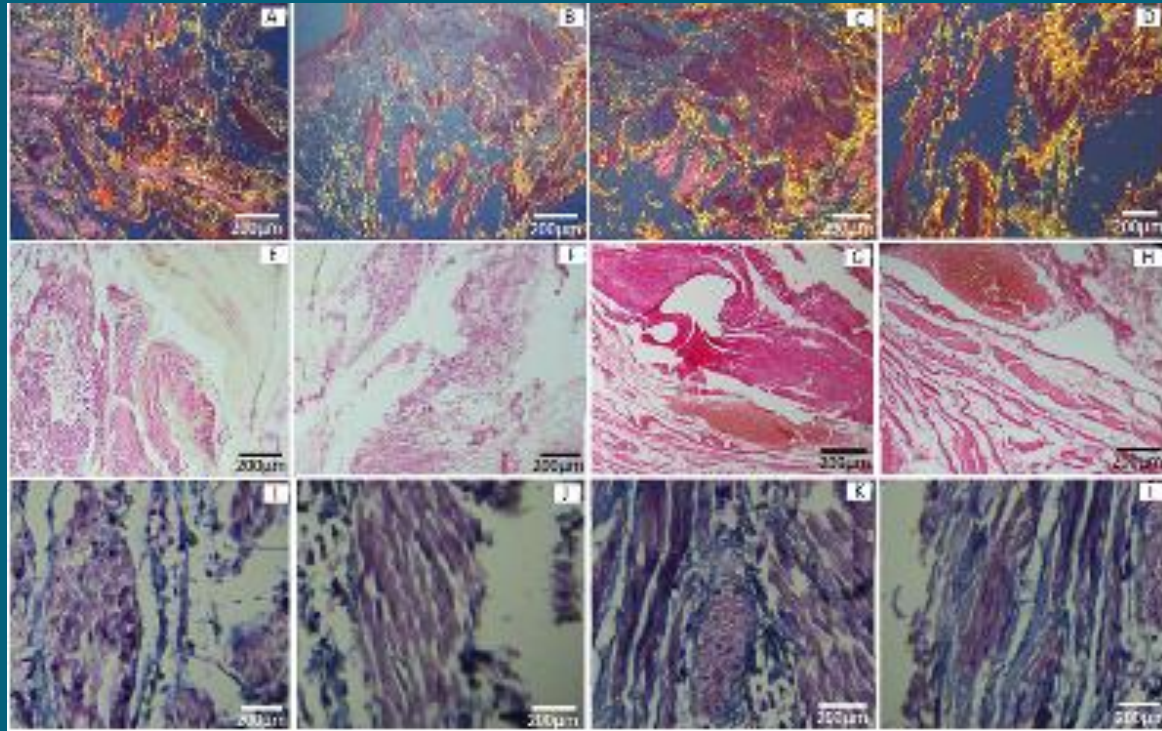
Scanning electron microscopy of (A) acellular rabbit gallbladder (B) acellular sheep gallbladder (C) natural rabbit gallbladder (D) natural sheep gallbladder.



Force/displacement (KN/mm) curve



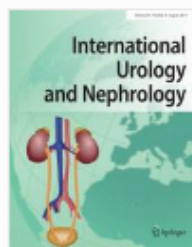
Histological evaluations : (A) H&E staining, (B) Vimentin Staining
 (C) Cytokeratin AE1/AE3 staining (D) CD34 staining (E) CD31
 staining (F) SMA staining (G) S100 staining.



Picrosirius red staining in (A) group I (B) group II (C) group III (D) group IV,.
 Pentachrome staining in (E) group I (F) group II (G) group III (H) group IV.
 Masson's trichrome staining in (I) group I (J) group II (K) group III (L) group IV

Conclusion:

The current study confirmed that autologous fragment-seeded CDECM can be considered as a reliable natural collagen scaffold for bladder augmentation.




[International Urology and Nephrology](#)

August 2014, Volume 46, [Issue 8](#), pp 1573–1580

The application of tissue-engineered preputial matrix and fibrin sealant for urethral reconstruction in rabbit model

Authors

[Authors and affiliations](#)

Abdol-Mohammad Kajbafzadeh , Shabnam Sabetkish, Ali Tourchi, Naser Amirizadeh, Kourosh Afshar, Hassan Abolghasemi, Azadeh Elmi, Saman Shafaat Talab, Peyman Eshghi, Mohammad Javad Mohseni

Urology - Original Paper

First Online: [12 March 2014](#)

DOI: [10.1007/s11255-014-0684-3](#)

Cite this article as:

Kajbafzadeh, A., Sabetkish, S., Tourchi, A. et al. Int Urol Nephrol (2014) 46: 1573. doi:10.1007/s11255-014-0684-3



Citations



Views

Abstract

We use cookies to improve your experience with our site. [More information](#)

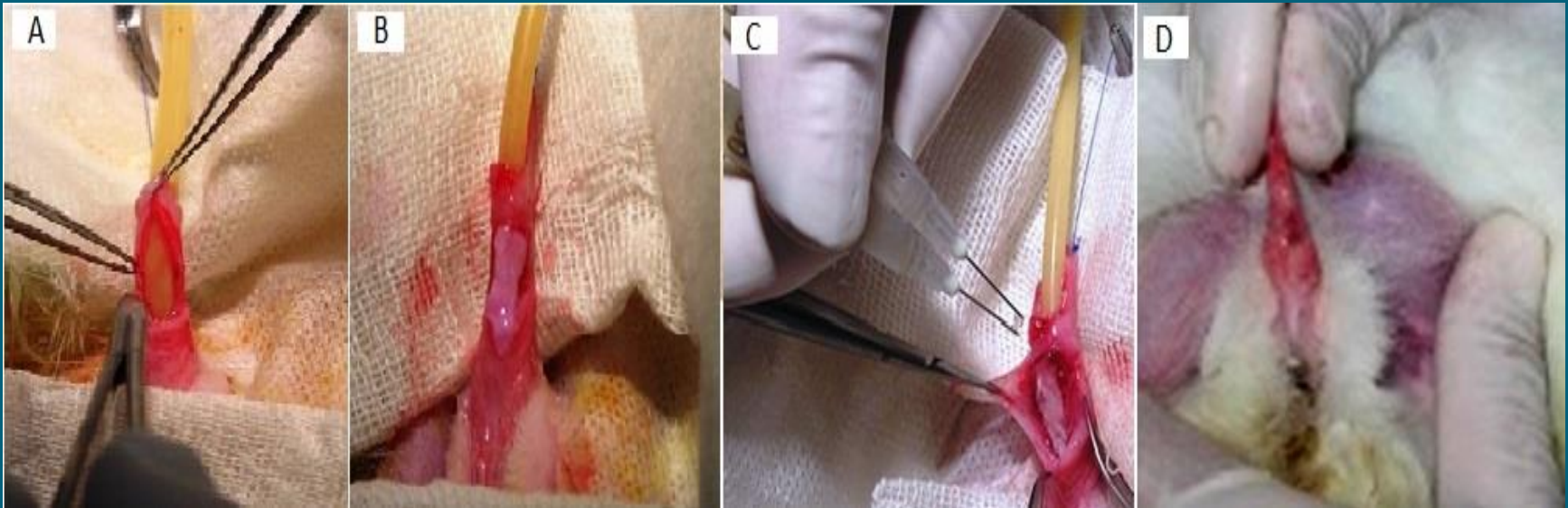
[Accept](#)

Objective:

To introduce the role of fibrin sealant and preputial acellular matrix (PAM) as a new source of inert collagen matrix for urethral reconstruction.

Material and Methods:

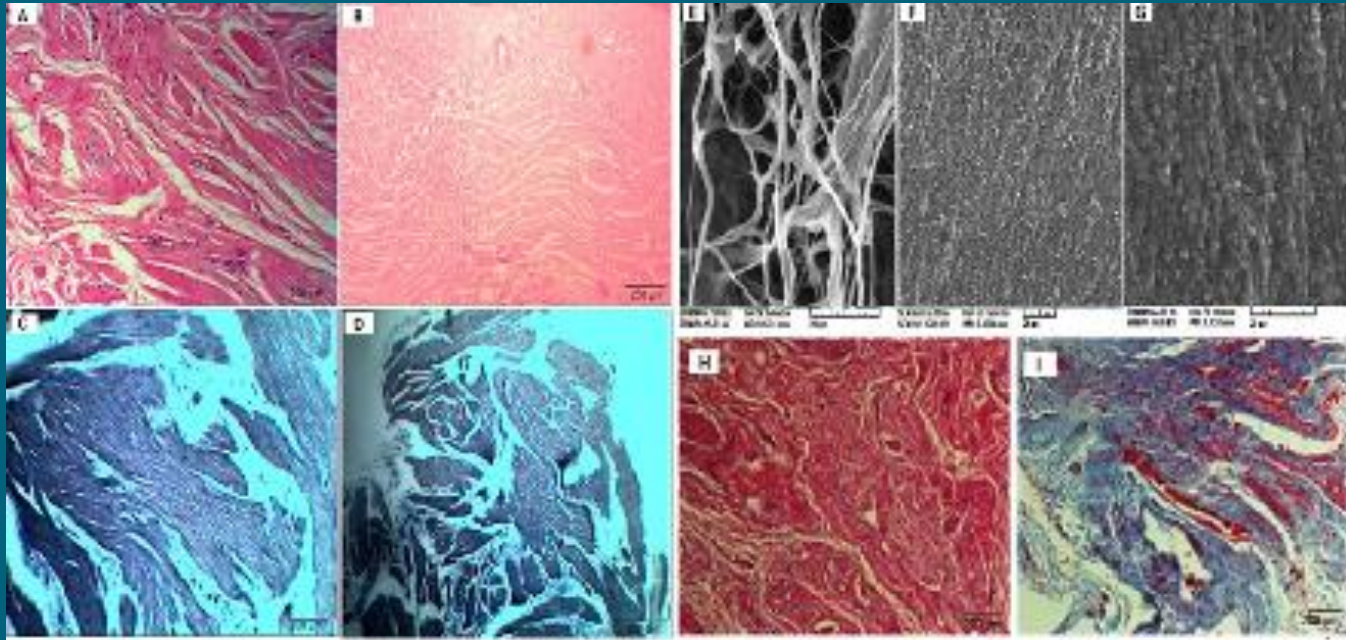
A dorsal urethral segmental defect was created in 24 rabbits divided into 4 groups. In group 1 (G1) urethrotomy was closed in layers. In group 2 (G2) closure was followed by applying fibrin sealant. In group 3 (G3) and 4 (G4) urethroplasty was performed with a patch graft of PAM, and in G4 fibrin sealant was also applied. Serial urethrography was performed before and after the operation. Then, the urethra was excised 1, 3, and 9 months postoperatively for further examinations.



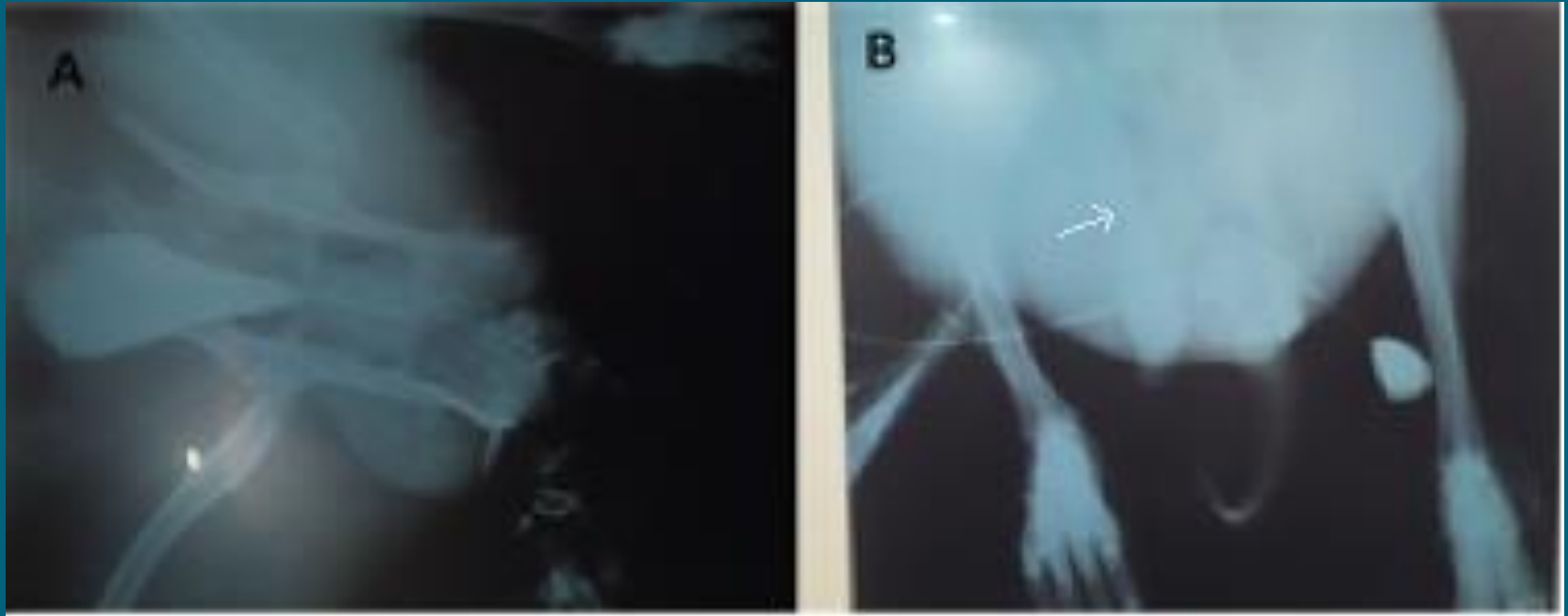
Surgical procedure: Reconstruction of urethra by tissue-engineered prepucal scaffold and application of fibrin glue

Results:

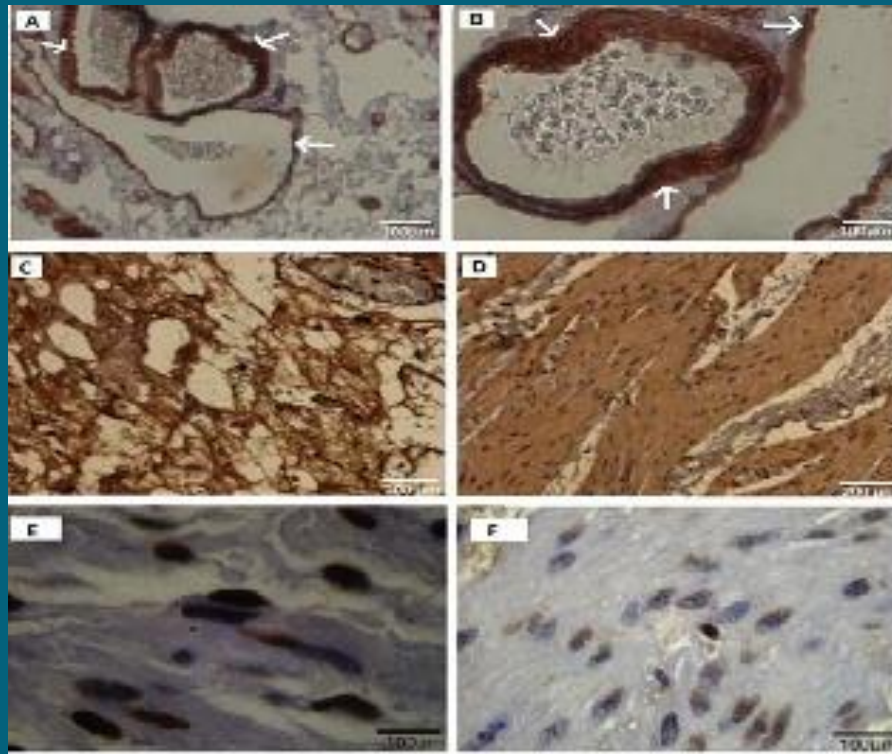
In G1 and G2, the fistula repair failed due to extravasation in the proximal part of urethra. In G3 and G4, serial urethrography confirmed the maintenance of a wide urethral caliber without signs of strictures or extravasations. Satisfactory vascularity was observed in G3 and G4 during the whole study, which was more significant in G4 after 9 months of follow-up. The presence of a complete transitional cell layer was confirmed over the graft in G3 and G4 in all time points. IHC staining confirmed the effectiveness of fistula repair in G3 and G4, 3 months postoperatively.



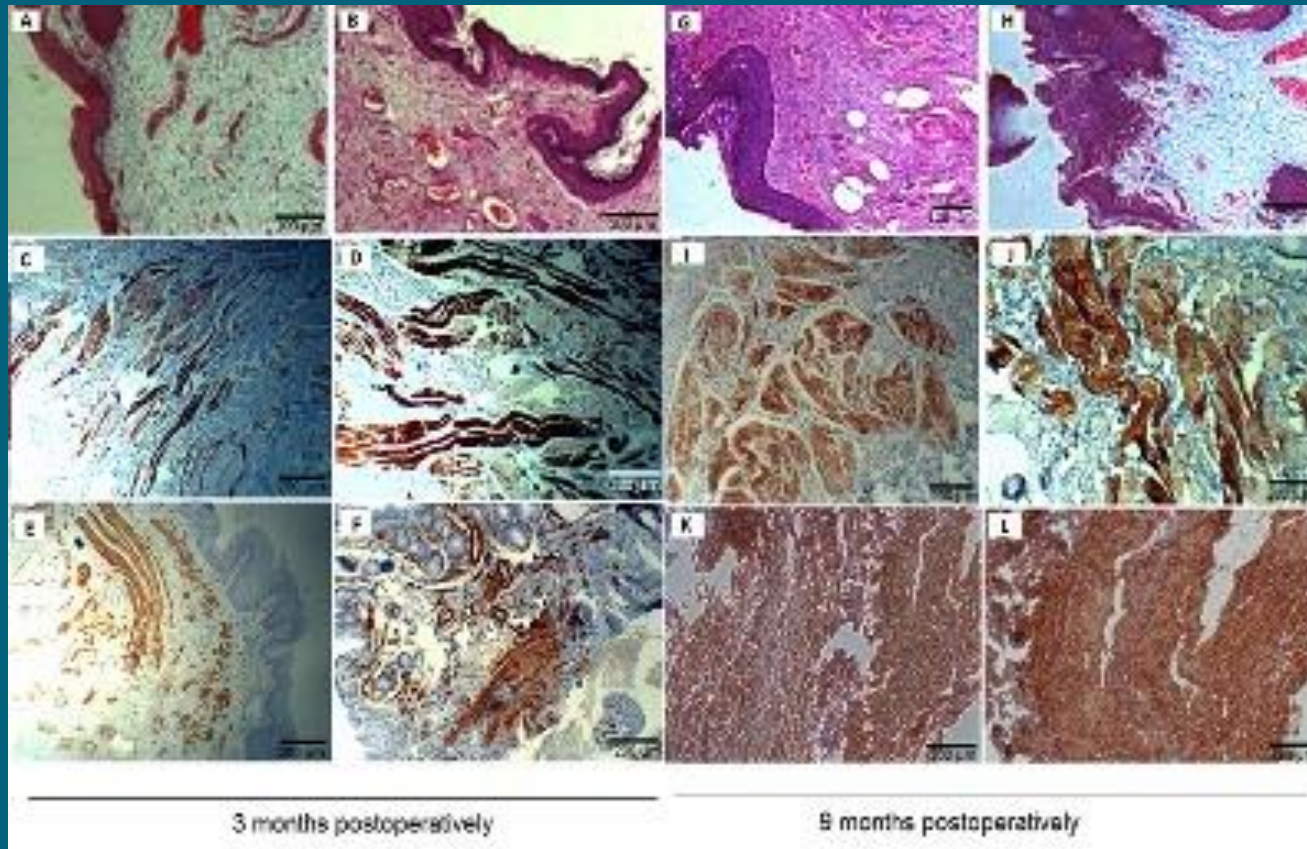
(A) H&E staining of natural preputial tissue and (B) acellular preputial matrix. Trichrome staining of (C) natural and (D) decellularized preputial tissue. Scanning electron microscopy: (E) acellular preputial scaffold (F) Grafted tissue in G3 after 3 months of follow up (G) Grafted tissue in G4 after 3 months of follow up. (H) H&E examination and (I) trichrome staining: No regeneration occurred In G1 and G2 after 3 months.



Retrograde urethrography: (A) urethral repair in G3 and G4 (normally formed tract of urinary stream) (B) urethral repair failure in G1 and G2 (extravasations in the proximal part of urethra).



Vascularization study: (A) CD34+ hematopoietic progenitor cells in G4 after 3 months. (B) CD31+ microvessels in G4, 9 months after grafting. α -Actin staining in (C) G3 & (D) G4, 9 months postoperatively. Apoptotic nuclei in tissue sections in (E) G2 and (F) G4, 3 months postoperatively.



Histopathological evaluations in G3 and G4, 3 months postoperatively: (A-B) H&E staining (normal tissue appearance) (C-D) Immunostaining for Desmin (E-F) SMA staining. Histopathological evaluations in G3 and G4, 9 months postoperatively: (G-H) H&E staining (thick urothelial and muscle layer) (I-J) Immunostaining for Desmin (K-L) SMA staining.

Conclusion:

This rabbit model showed that PAM combined with fibrin sealant may herald a reliable option for repairing segmental urethral defects.

↶ Go to old article view

🔑 Get access


A
Text size

🔗
Share

INTERNATIONAL JOURNAL OF **Experimental Pathology** 
[Explore this journal >](#)

Original Article

A novel technique for simultaneous whole-body and multi-organ decellularization: umbilical artery catheterization as a perfusion-based method in a sheep fetus model

Abdol-Mohammad Kajbafzadeh , Reza Khorramirouz, Aram Akbarzadeh, Shabnam Sabetkish, Nastaran Sabetkish, Paria Saadat, Mona Tehrani

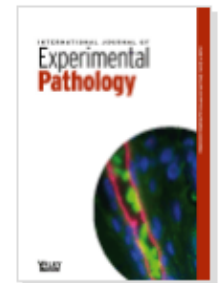
First published: April 2015 [Full publication history](#)

DOI: 10.1111/iep.12124 [View/save citation](#)

Cited by: 0 articles  [Citation tools](#)

 2

[Funding Information](#)



[View issue TOC](#)
Volume 96, Issue 2
April 2015
Pages 116–132

Objectives:

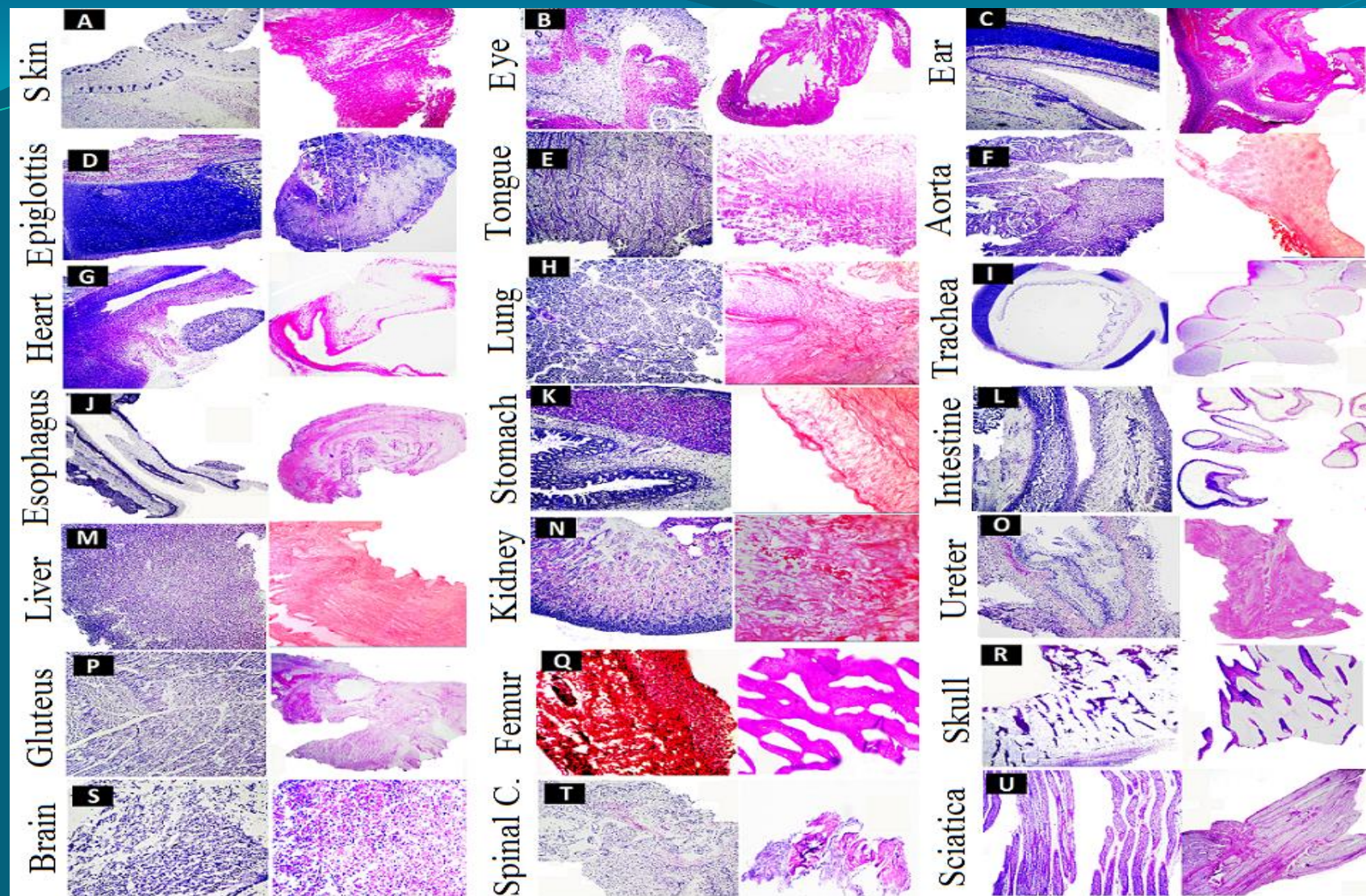
We created multiorgan acellular matrices by using perfusion-based whole-body decellularization via the umbilical artery and used systemic pulsatile perfusion for simultaneous multiorgan decellularization in a fetal sheep model.

Material and Methods:

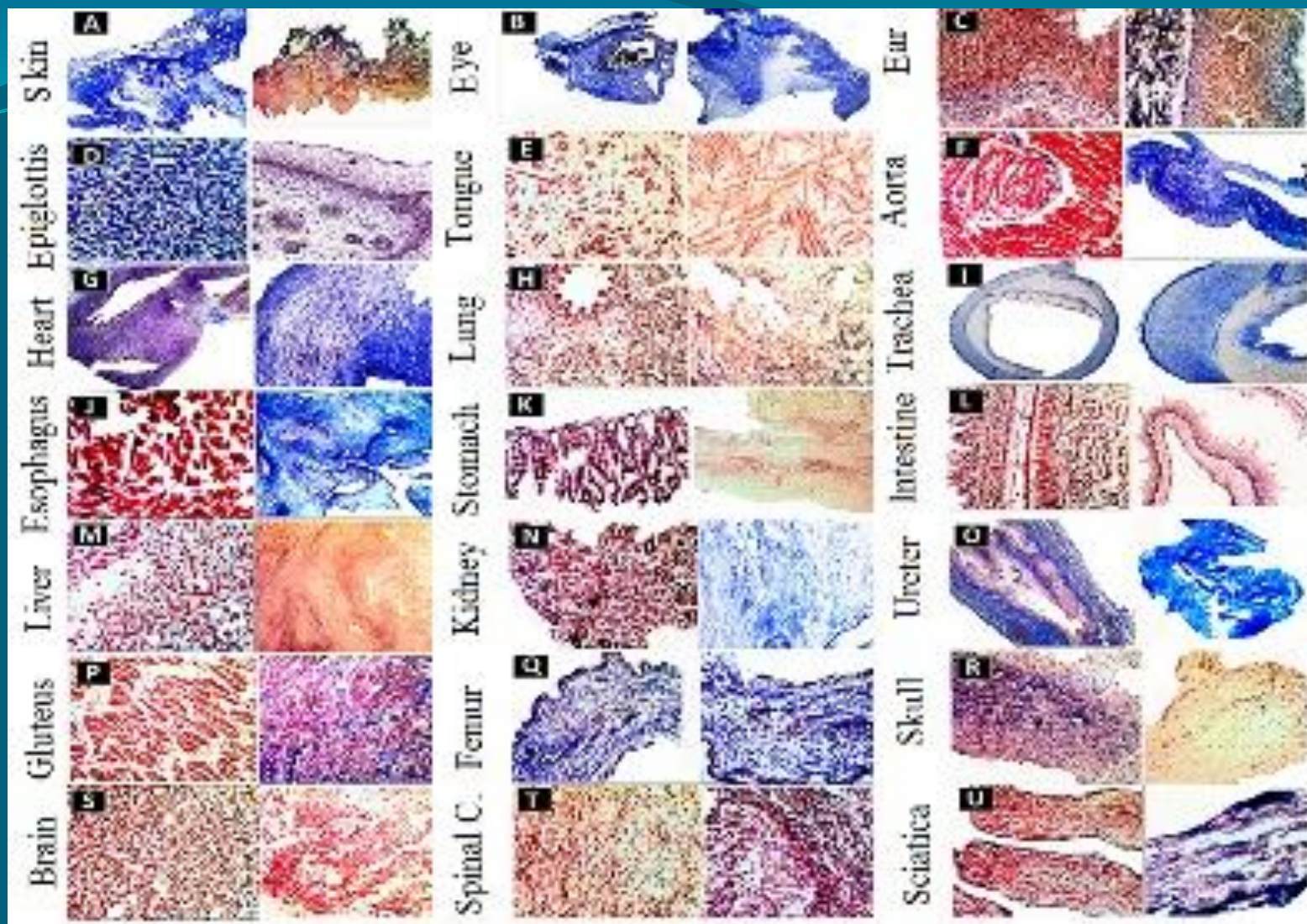
Twenty sheep fetuses were systemically perfused with Triton X-100 and sodium dodecyl sulfate. Following completion of the whole-body decellularization, biopsy samples were taken from different parts of 21 organs to ascertain complete cell component removal in the preserved extracellular matrices. Both the natural and decellularized organs were subjected to several examinations.



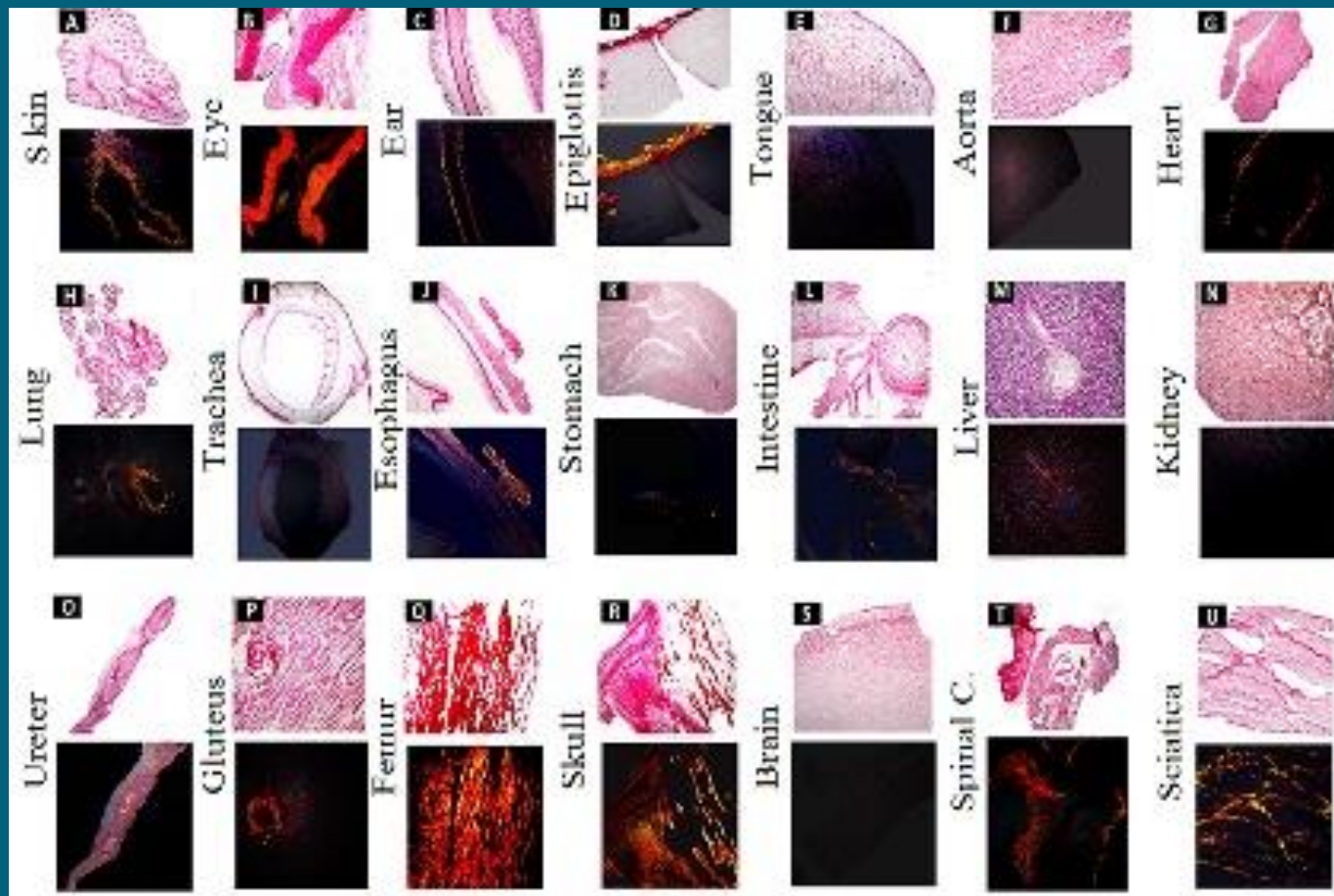
(A) A sheep fetus after whole-body decellularization. (B) Magnetic Resonance Imaging of a whole-body decellularized sheep fetus. (C) Computed Tomography angiogram of a decellularized sheep fetus.



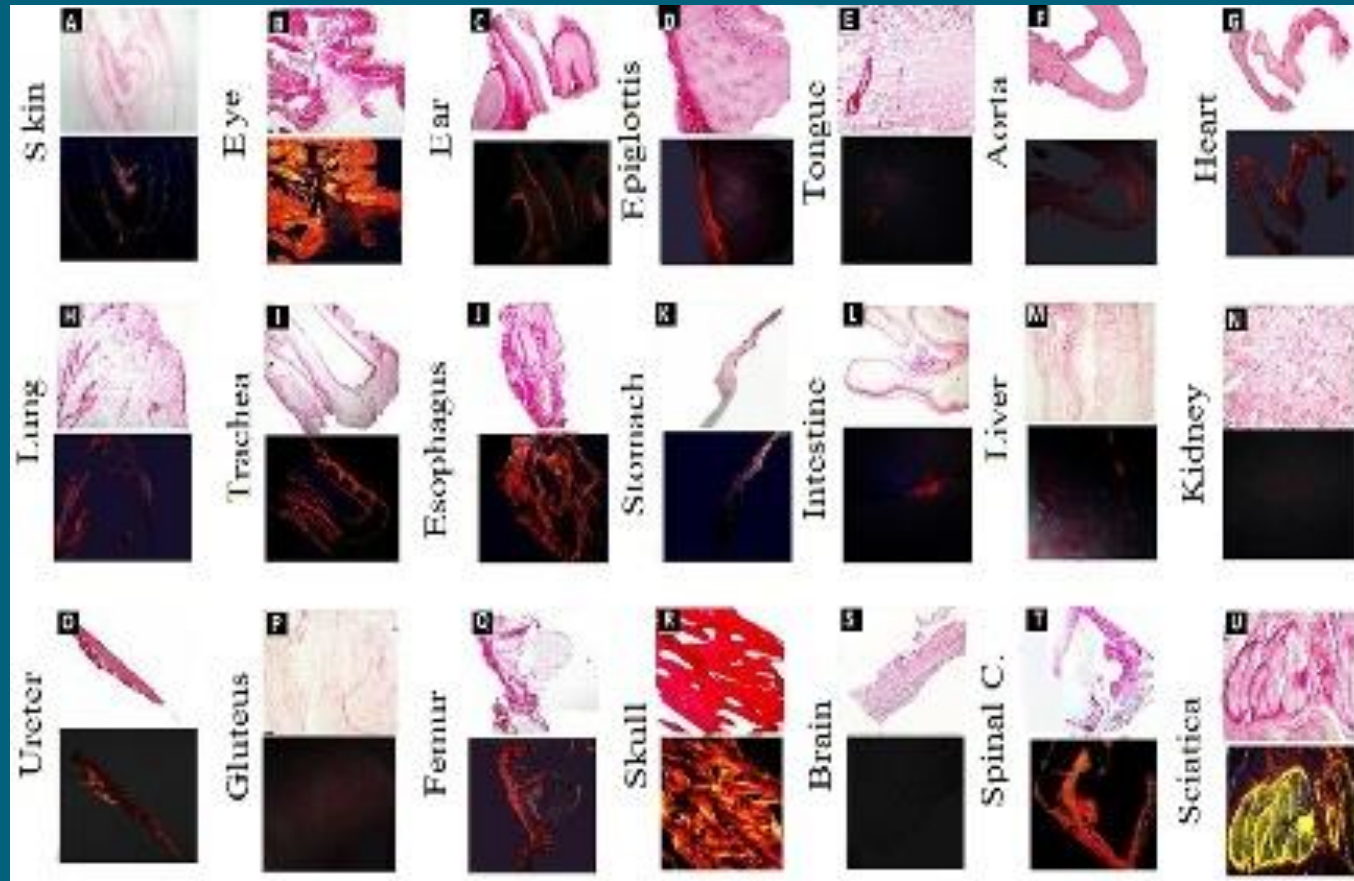
H&E staining of natural (left) and decellularized (right) scaffolds: (A) skin, (B) eye, (C) ear, (D) epiglottis, (E) tongue, (F) aorta, (G) heart, (H) lung, (I) trachea, (J) esophagus, (K) stomach, (L) intestine, (M) liver, (N) kidney, (O) ureter, (P) gluteal muscle, (Q) femur, (R) skull, (S) brain, (T) spinal cord, (U) sciatica.



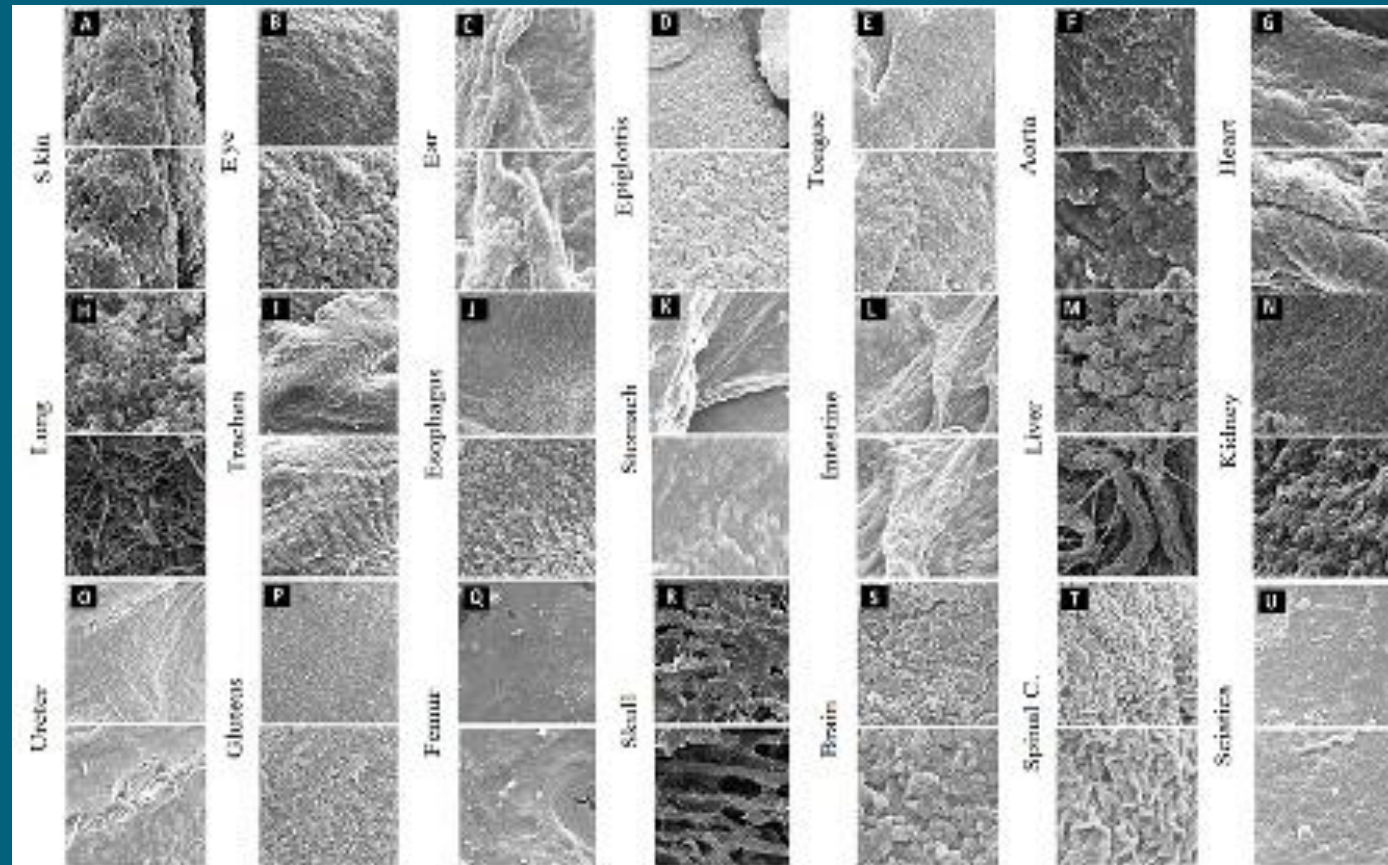
Masson's trichrome staining of normal(left) and decellularized (right) organs: (A) skin, (B) eye, (C) ear, (D) epiglottis, (E) tongue, (F) aorta, (G) heart, (H) lung, (I) trachea, (J) esophagus, (K) stomach, (L) intestine, (M) liver, (N) kidney, (O) ureter, (P) gluteal muscle, (Q) femur, (R) skull, (S) brain, (T) spinal cord, (U) sciatica.



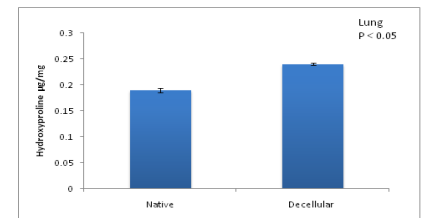
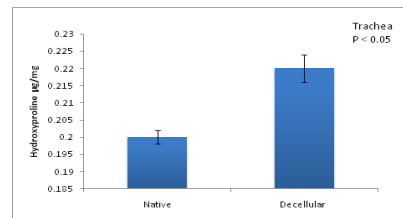
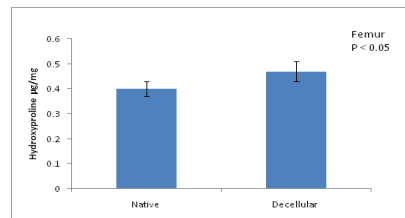
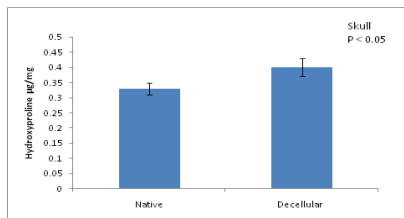
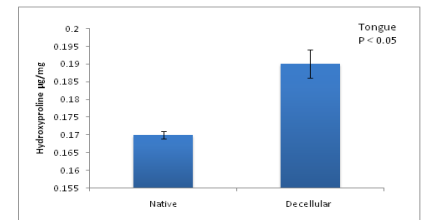
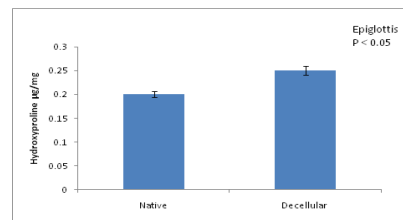
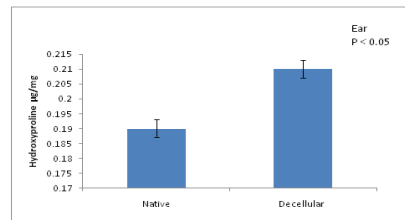
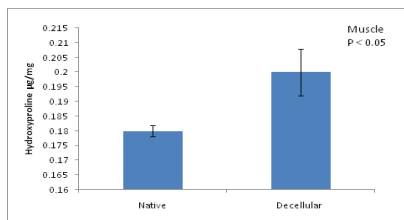
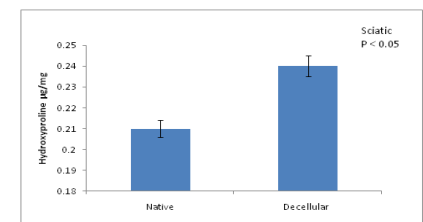
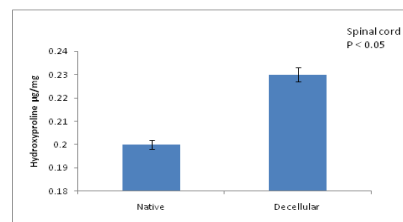
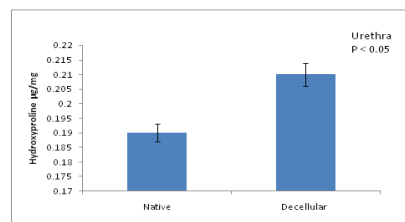
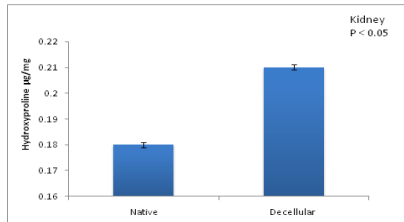
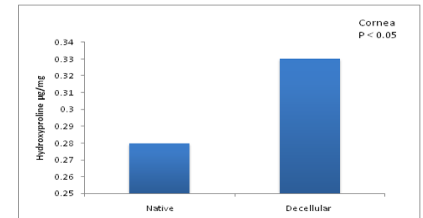
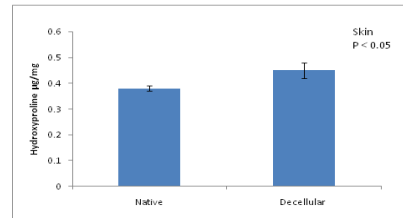
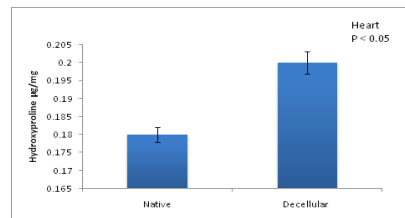
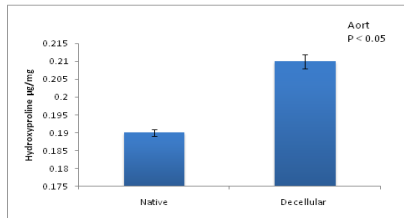
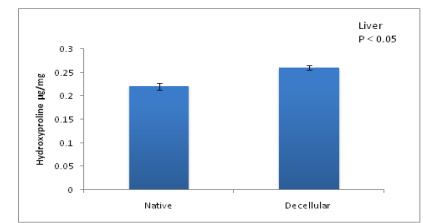
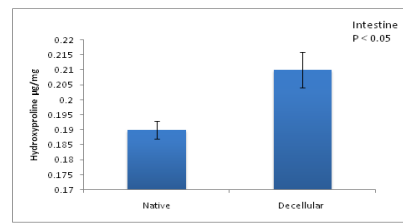
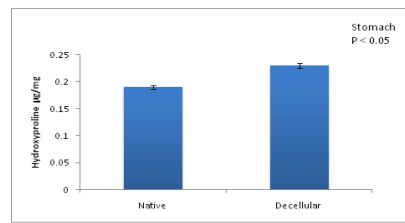
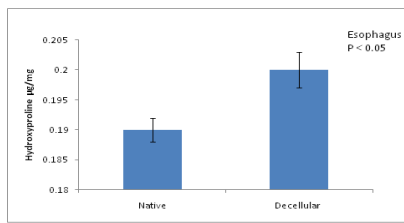
Pentachrome and picrosirius red staining of natural organs: (A) skin, (B) eye, (C) ear, (D) epiglottis, (E) tongue, (F) aorta, (G) heart, (H) lung, (I) trachea, (J) esophagus, (K) stomach, (L) intestine, (M) liver, (N) kidney, (O) ureter, (P) gluteal muscle, (Q) femur, (R) skull, (S) brain, (T) spinal cord, (U) sciatica.



Pentachrome and picrosirius red staining of decellularized scaffolds: (A) skin, (B) eye, (C) ear, (D) epiglottis, (E) tongue, (F) aorta, (G) heart, (H) lung, (I) trachea, (J) esophagus, (K) stomach, (L) intestine, (M) liver, (N) kidney, (O) ureter, (P) gluteal muscle, (Q) femur, (R) skull, (S) brain, (T) spinal cord, (U) sciatica.



Comparison of the architecture of natural and decellularized scaffolds by SEM analysis: (A) skin, (B) eye, (C) ear, (D) epiglottis, (E) tongue, (F) aorta, (G) heart, (H) lung, (I) trachea, (J) esophagus, (K) stomach, (L) intestine, (M) liver, (N) kidney, (O) ureter, (P) gluteal muscle, (Q) femur, (R) skull, (S) brain, (T) spinal cord, (U) sciatica.



Comparison of the hydroxyproline contents of native and decellularized organs. Data were not statistically different

Results:

The samples were obtained from the skin, eye, ear, nose, throat, cardiovascular, respiratory, gastrointestinal, urinary, musculoskeletal, central nervous, and peripheral nervous systems. The histological results depicted well-preserved extracellular matrix (ECM) integrity and intact vascular structures, without any evidence of residual cellular materials, in all decellularized bioscaffolds. The SEM and biochemical properties remained intact, similar to their age-matched native counterparts. Preservation of the collagen structure was also evaluated by hydroxyproline assay. Dense organs such as bone and muscle were also completely decellularized, with a preserved ECM structure.

Conclusion:

In the present study, several organs and different tissues were decellularized by a perfusion-based method, which has not been previously accomplished. Given the technical challenges that exist for the efficient generation of biological scaffolds, the current results may pave the way for obtaining a variety of decellularized scaffolds from a single donor. In this study, there have been unique responses to the single acellularization protocol in fetuses, which may reflect the homogeneousness of tissues and organs in the developing fetal body.



Tissue-Engineered External Anal Sphincter Using Autologous Myogenic Satellite Cells and Extracellular Matrix: Functional and Histological Studies

ABDOL-MOHAMMAD KAJBAFZADEH,¹ MAJID KAJBAFZADEH,² SHABNAM SABETKISH,¹ NASTARAN SABETKISH,¹
and SEYYED MOHAMMAD TAVANGAR³

¹Pediatric Urology Research Center, Section of Tissue Engineering and Stem Cells Therapy, Children's Hospital Medical Center, Tehran University of Medical Sciences, No. 62, Dr. Qarib's Street, Keshavarz Boulevard, Tehran 1419433151, Islamic Republic of Iran; ²Sydney Medical School, The University of Sydney, Sydney, NSW 2006, Australia; and ³Department of Pathology, Shariati Hospital, Tehran University of Medical Sciences, Tehran, Islamic Republic of Iran

(Received 14 November 2014; accepted 22 September 2015; published online 30 September 2015)

Associate Editor Smadar Cohen oversaw the review of this article.

Objectives:

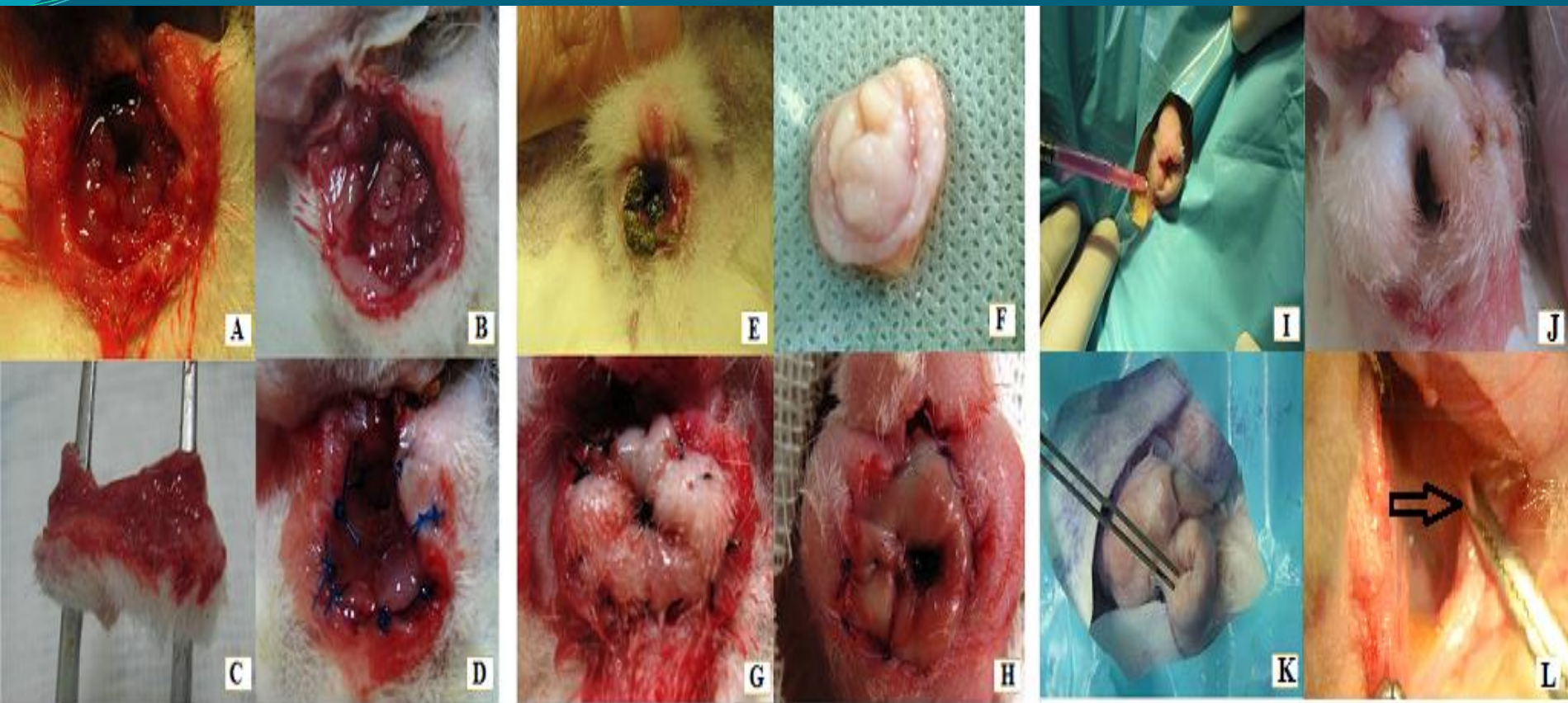
To demonstrate the regaining histological characteristics of bioengineered External Anal Sphincters (EAS) in rabbit Fecal Incontinence (FI) model.

Materials and methods:

EAS of 16 rabbits were resected and decellularized. They were then transplanted to the terminal rectum. The rabbits were divided into two groups: in group 1 (n=8), myogenic satellite cells were injected into the transplanted sphincters. In group 2 (n=8), the transplanted scaffolds remained in situ without cellular injection. The histological evaluation was performed on biopsies stained with Desmin, Myosin, Smooth Muscle Actin (SMA), CD31, and CD34. The rabbits were followed up for 2 continuous years at 3-month intervals.

Results:

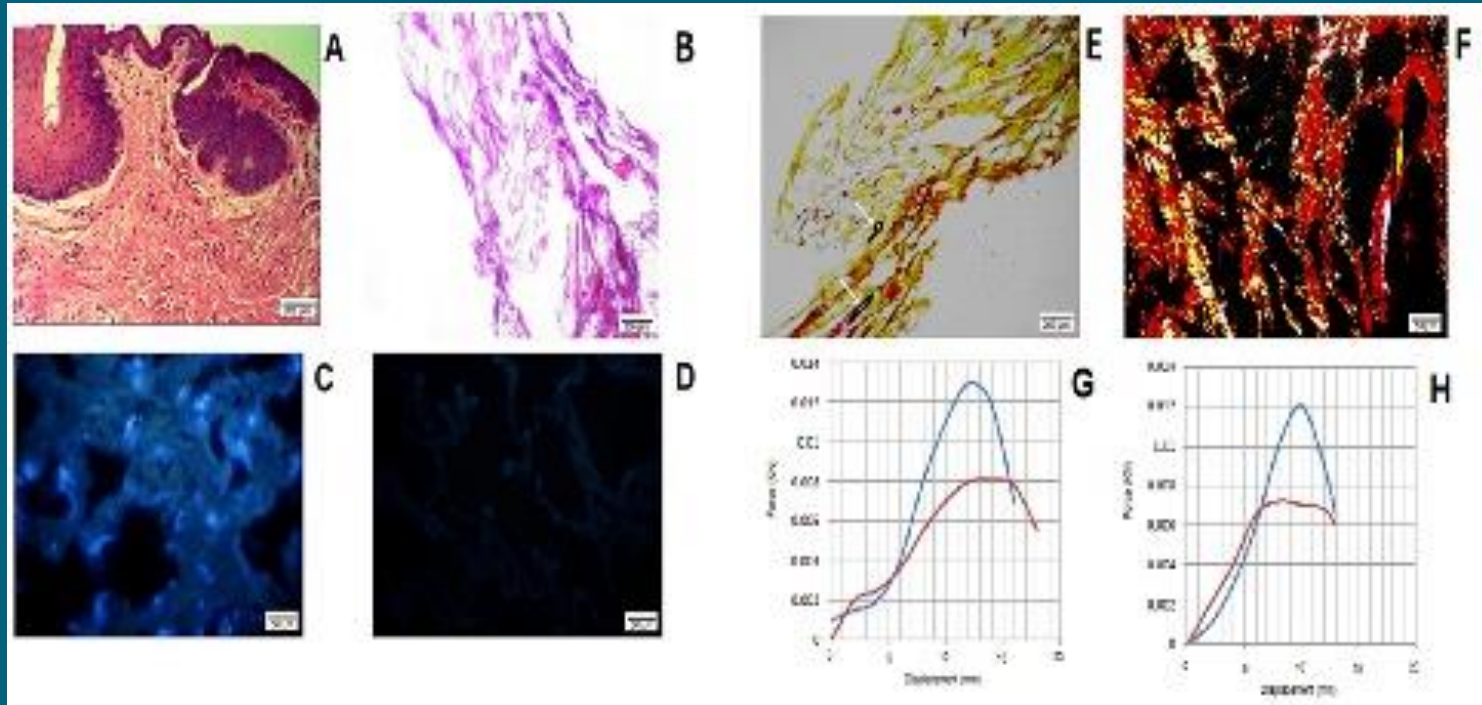
The immunohistochemistry staining validated that both groups were successful in regaining the histological features of EAS. The rabbits with autologous myogenic satellite cells injection into the bioengineered sphincter achieved a more satisfactory histological outcome in short-term follow-up. After 2 years follow-up, no evidence of inflammation, rejection or any major complication was observed and the transplanted EAS appeared histologically and anatomically normal.



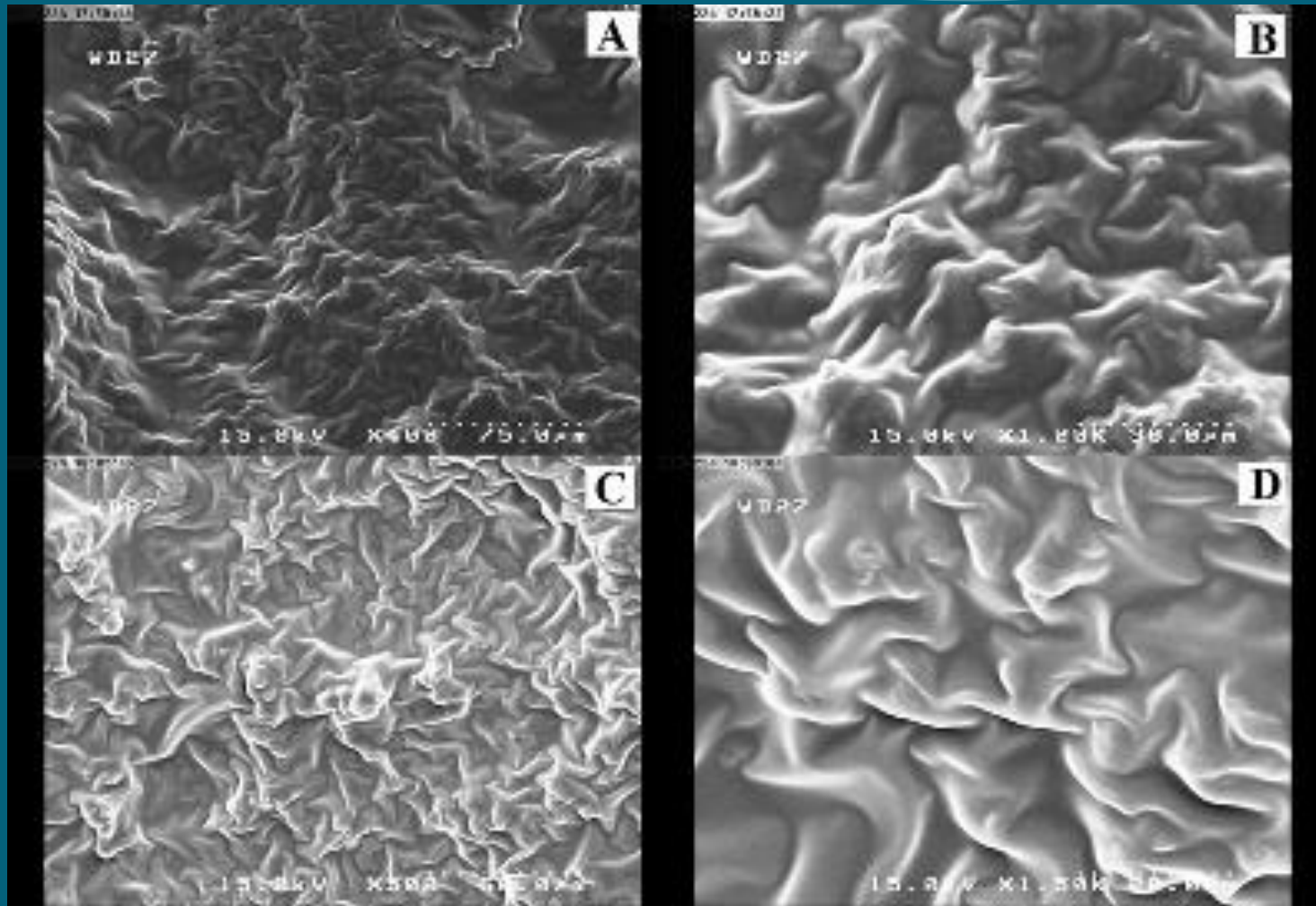
Sphincterotomy

Acellular sphincter transplantation

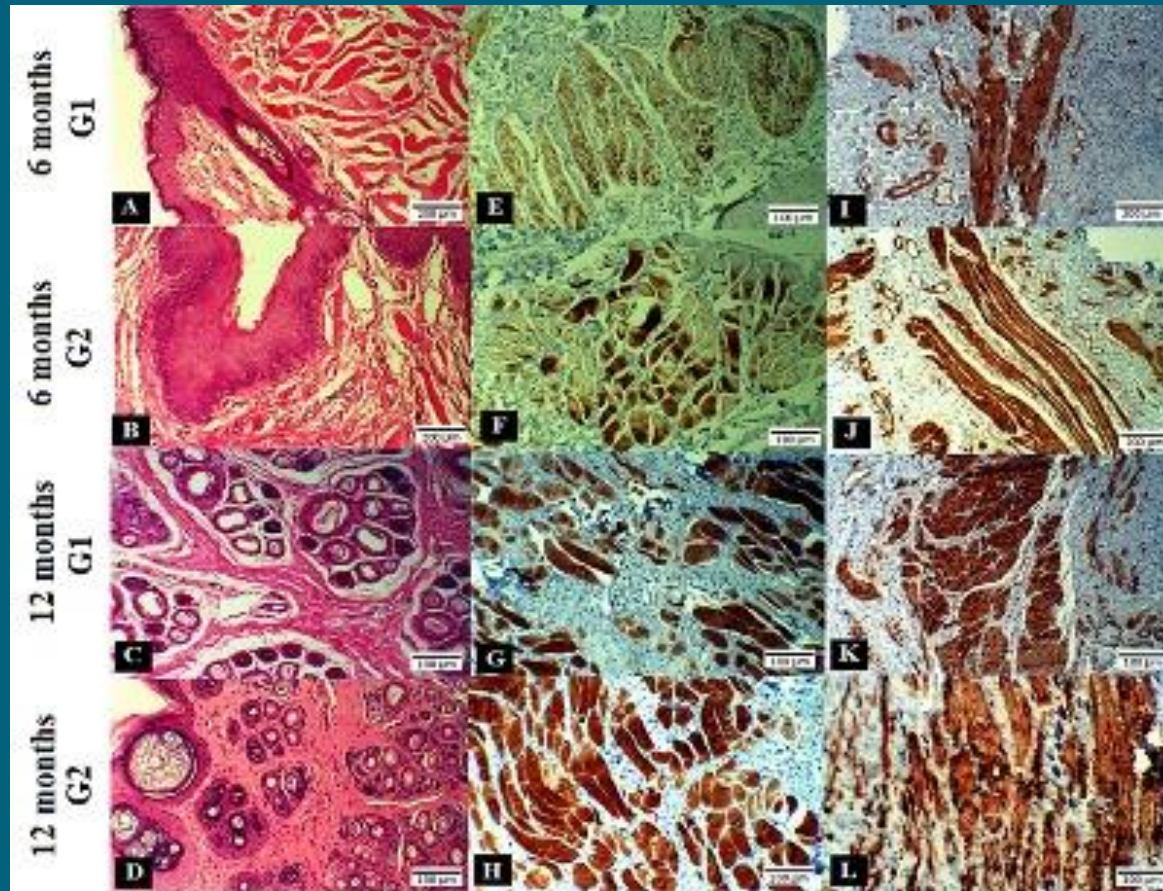
**Autologous myogenic satellite cells
injection & electrostimulation**



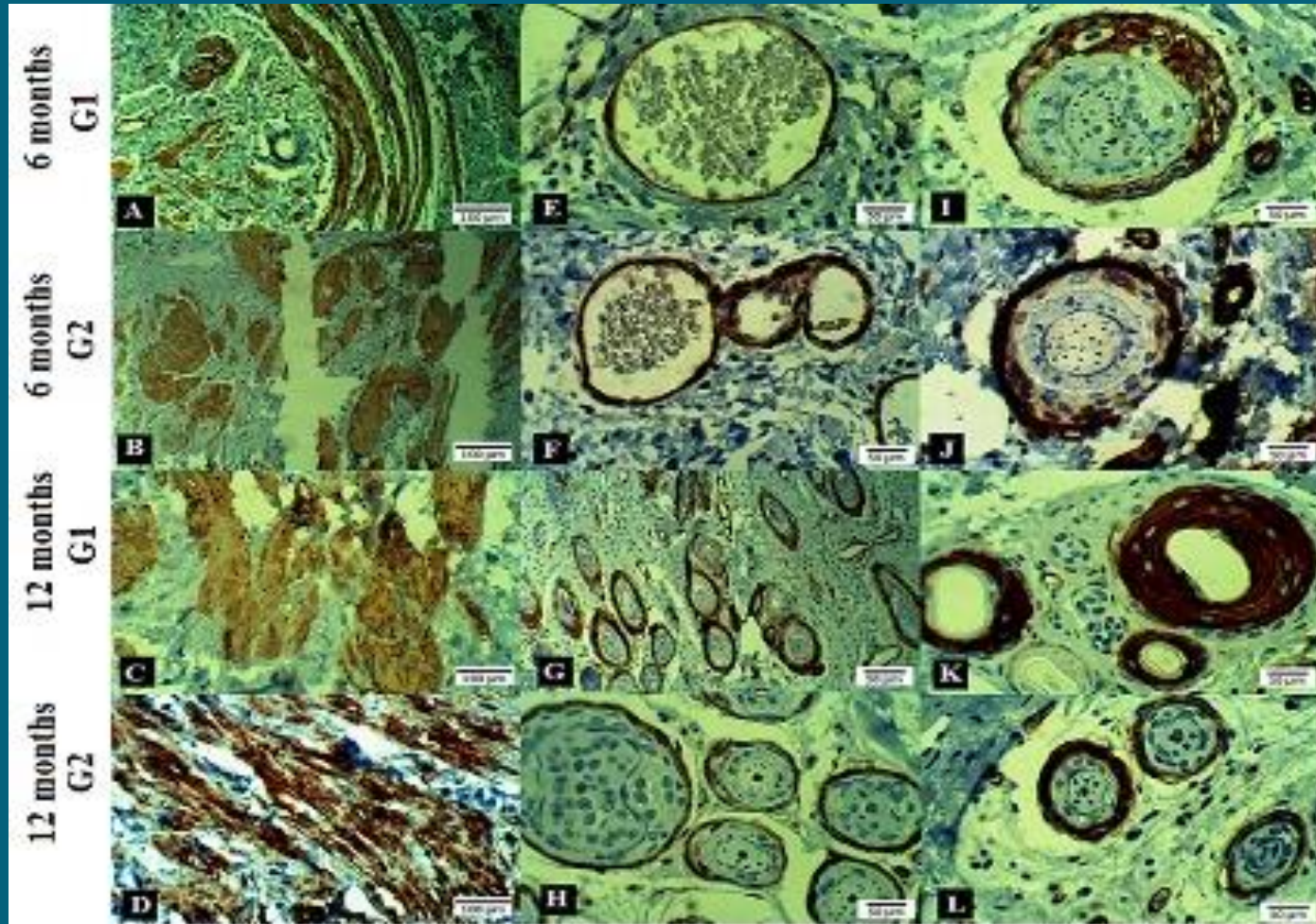
(A&B) H&E staining of natural and decellularized sphincters, (C&D) DAPI staining of normal EAS and DEAS, (E) Pentachrome staining of DEAS. **Arrows:** vessel edge stained in black (elastin fibers) **C:** collagen fibers stained in yellow. **M:** muscle fibers stained in red, (F) Picrosirius Red staining of decellularized EAS (G&H) Force/displacement curve comparing the maximum annular (blue curve) and longitudinal (red curve) force tolerated by intact and decellularized sphincters.



Scanning electron microscope: (A&B) Natural tissue (C&D) decellularized scaffolds.



(A-D) H&E staining of the biopsies (E-H) Immunohistochemical staining for Desmin (I-L) Immunohistochemical staining for SMA.



(A-D) Immunohistochemical staining for Myosin (E-H) Immunohistochemical staining for CD34 (I-L) Immunohistochemical staining for CD31.

Conclusion:

This experimental study was designed in attempt to enhance the histological characteristics of EAS using injection of myogenic satellite cells into DEASM. The presented technique illustrated the potential of bioengineered scaffolds in EAS reconstruction with the best histological compatibility. The results of the current study must be taken as very encouraging in the light of further conducted clinical trial.



Download PDF

Export ▾

Search ScienceDirect



Advanced



ELSEVIER

Journal of Pediatric Surgery

Volume 49, Issue 3, March 2014, Pages 477-483



Recommended articles

Citing articles

Original Article

Augmentation cystoplasty using decellularized vermiform appendix in rabbit model

Nastaran Sabetkish ^a, Abdol-Mohammad Kajbafzadeh ^a✉, Shabnam Sabetkish ^a, Seyyed Mohammad Tavangar ^b

✉ [Show more](#)

<https://doi.org/10.1016/j.jpedsurg.2013.07.016>

[Get rights and content](#)

Purpose:

The aim of this study is to produce a decellularized rabbit vermiform ***appendix*** (sacculus rotundus) scaffold and investigate the feasibility of its application in bladder augmentation or appendicovesicostomy. The superiority of sacculus rotundus over other tissues is its unique mechanical properties as well as its abundant collagens.

Material and Methods:

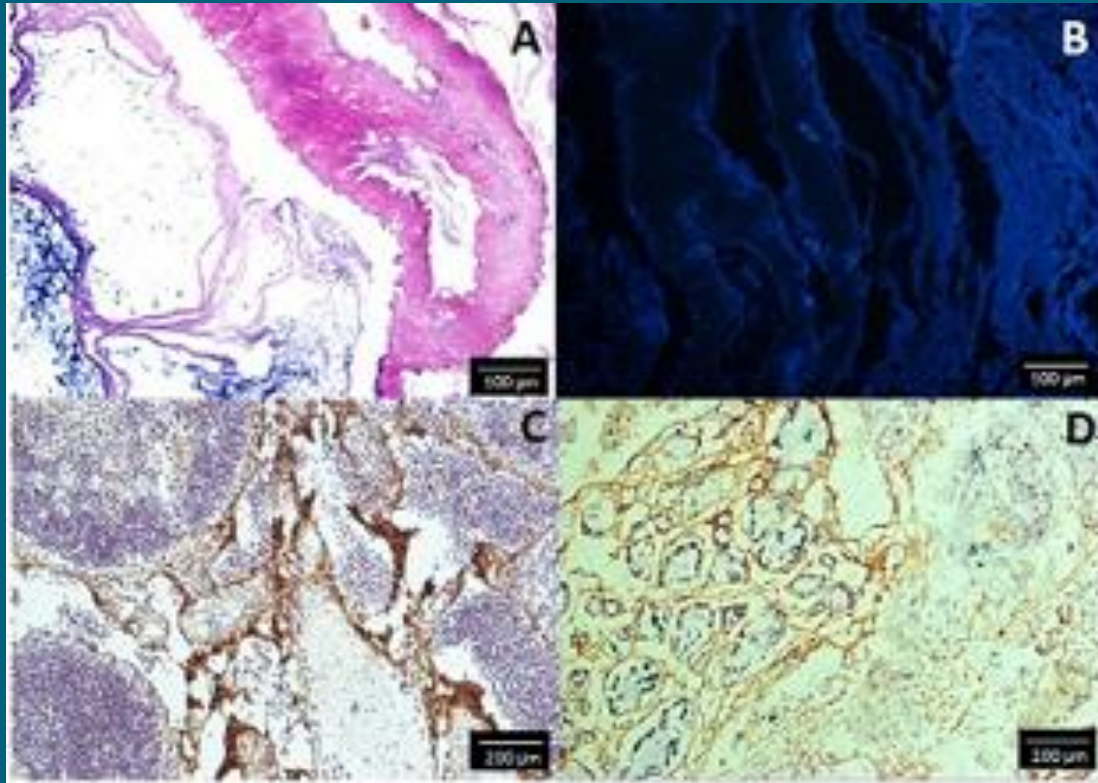
The acellular matrix of vermiform appendix underwent different laboratory investigations prior to transplantation. We divided 12 rabbits in 3 groups: group I underwent bladder augmentation cystoplasty by detubularized acellular matrix. Group II underwent implantation of the tapered (tubularized) acellular matrix just beneath the seromuscular part of the bladder without connection to the bladder urothelium. Group III underwent the same procedure as group II plus reimplantation of tapered and tubularized acellular matrix (actually simulating an appendicovesicostomy). The distal end of the transplanted graft was connected to the bladder mucosal opening and was intubated by a 5 Fr double blind ended feeding tube catheter. Graft biopsies were taken 3, 12, and 36 months post-operatively.

Results:

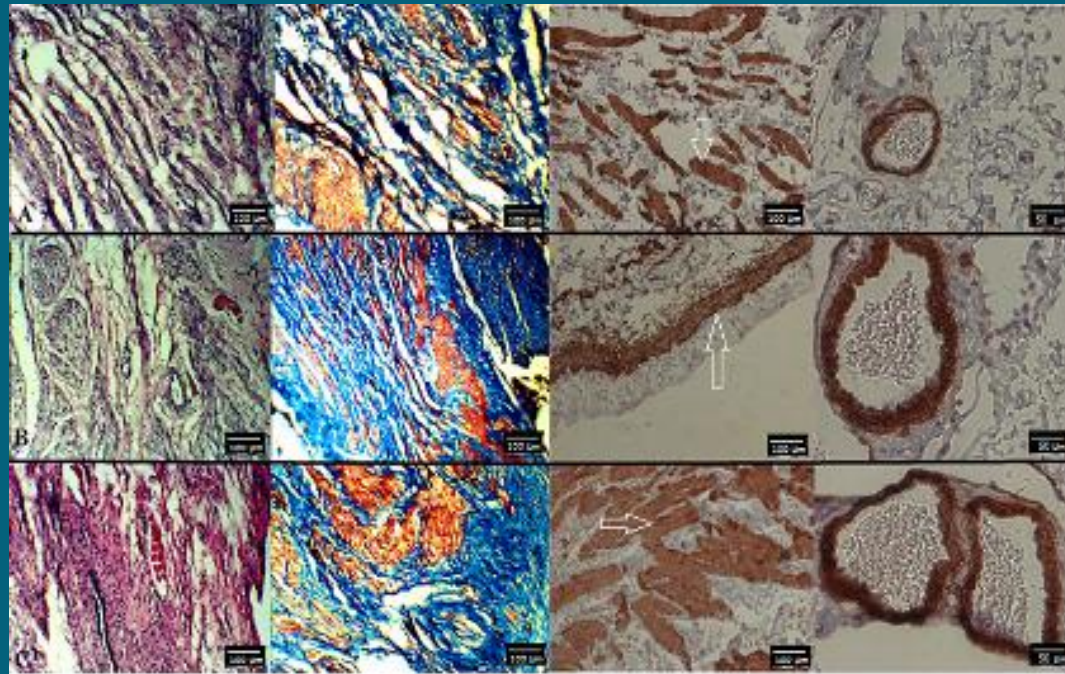
The results of the examinations performed prior to transplantation, revealed a decellularized structure resembling to the native tissue with intact intercellular matrix, normal pits and appropriate gaps that will be suitable for cell seeding. Histopathology examination of the biopsies after transplantations confirmed successful cell seeding with urothelial lining in groups I and III, while the inner lumen in group II showed no urothelial lining.



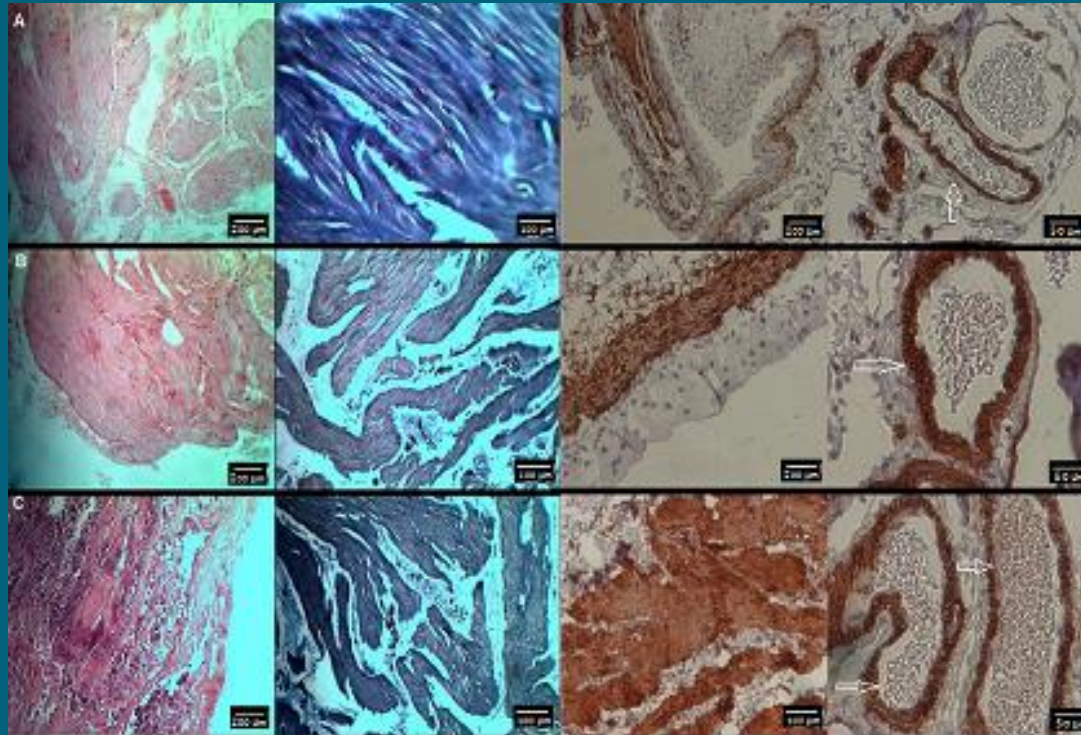
(A) natural vermiform appendix **(B)** decellularized scaffold for further augmentation cystoplasty **(C)** detubularized acellular matrix



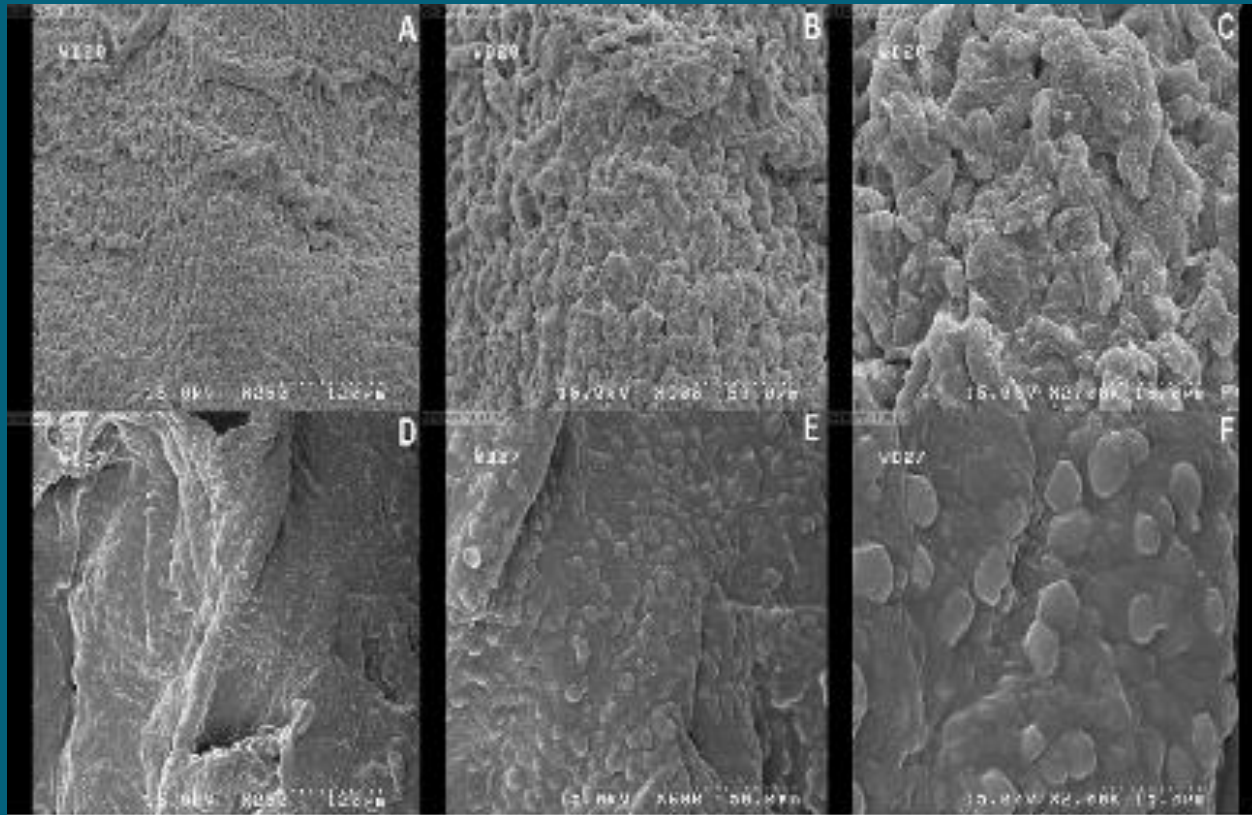
(A & B) Anti-Laminin staining of both natural and decellularized ileocecal tonsils determining the existence of Laminin in ECM that verifies the persistence of elasticity in tissues after decellularization procedure (C) H&E staining of decellularized ileocecal tonsils (D) DAPI staining in decellularized ileocecal tonsils



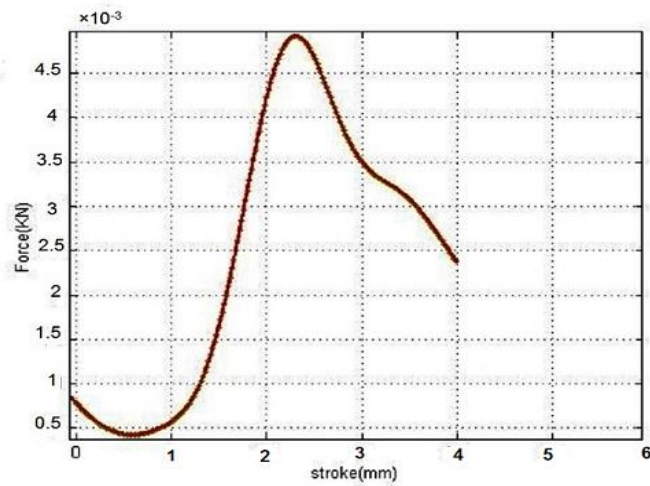
H&E, trichrome, and immunohistochemical staining for SMC and CD34 in group I: (A) 3 months post-operatively (B) 12 months after surgery (C) 36 months after bladder augmentation. The arrows show the muscular layer (Detrusor muscle) of newly formed bladder which is seen under the transitional epithelium.



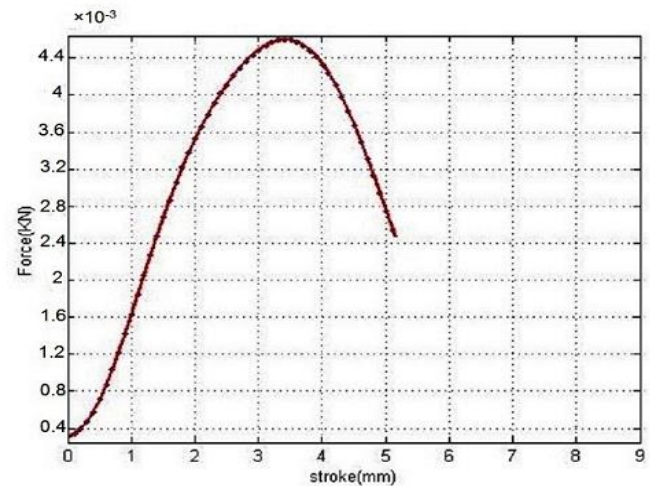
H&E, trichrome, and immunohistochemical staining for SMC and CD34 in group III: (A) 3 months post-operatively (B) 12 months after surgery (C) 36 months after bladder augmentation. The arrows show the new vessels in the decellularized ileocecal tonsils



Scanning electron microscope: (A-C) Natural tissue (D-F) decellularized ileocecal tonsils



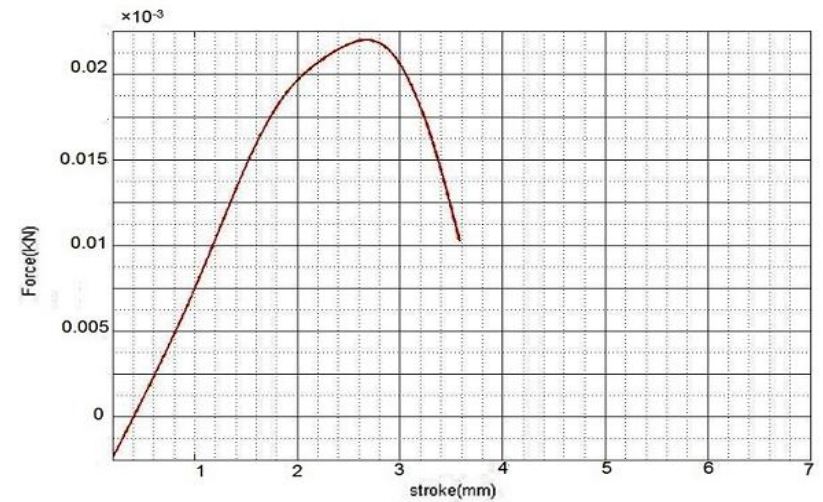
A



B



C



D

Force/displacement curve comparing the maximum force: (A) assessment of annular fibers in natural ileocecal tonsils by the application of a hook (B) hook application in decellularized saccus rotundus for estimating annular fibers properties (C) decellularized ileocecal tonsils for assessment of longitudinal fibers (D) natural bladder for estimation of mechanical properties in fibers

Conclusion:

The results suggest that we can prospect to perform bladder reconstruction by the application of this method without complications of previously reported augmentation cystoplasty by using the bladder as a natural bioreactor that can pave the road for clinical application in acellular matrix augmentation cystoplasty.



Paediatrics

Bladder reconstruction using scaffold-less autologous smooth muscle cell sheet engineering: early histological outcomes for autoaugmentation cystoplasty

Saman S. Talab, Abdol-Mohammad Kajbafzadeh , Azadeh Elmi, Ali Tournchi, Shabnam Sabetkish, Nastaran Sabetkish, Maryam Monajemzadeh

First published: 16 August 2014 [Full publication history](#)

DOI: 10.1111/bju.12685 [View/save citation](#)

Cited by (CrossRef): 6 articles  [Check for updates](#) |  [Citation tools](#) ▼

[Funding Information](#)



[View issue TOC](#)
Volume 114, Issue 6
December 2014
Pages 937-945

Objectives:

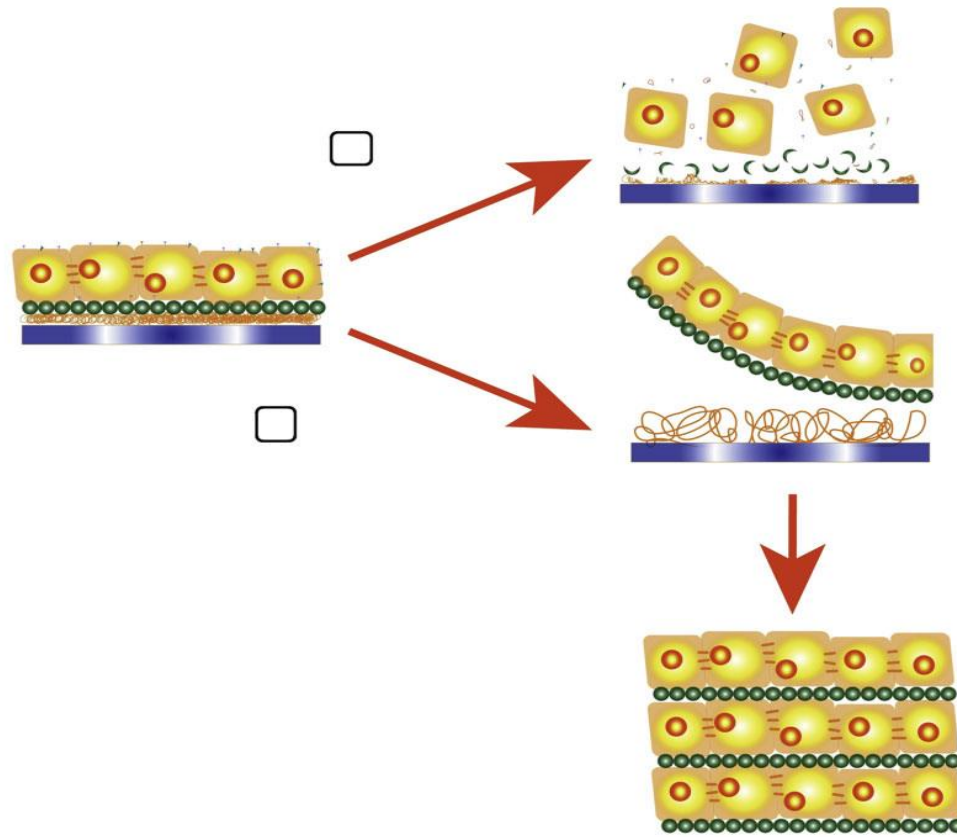
To investigate the feasibility of a new approach for cystoplasty using autologous smooth muscle cell (SMC) sheet and scaffold-less bladder tissue engineering with the main focus on histological outcomes in a rabbit model.

Material and Methods:

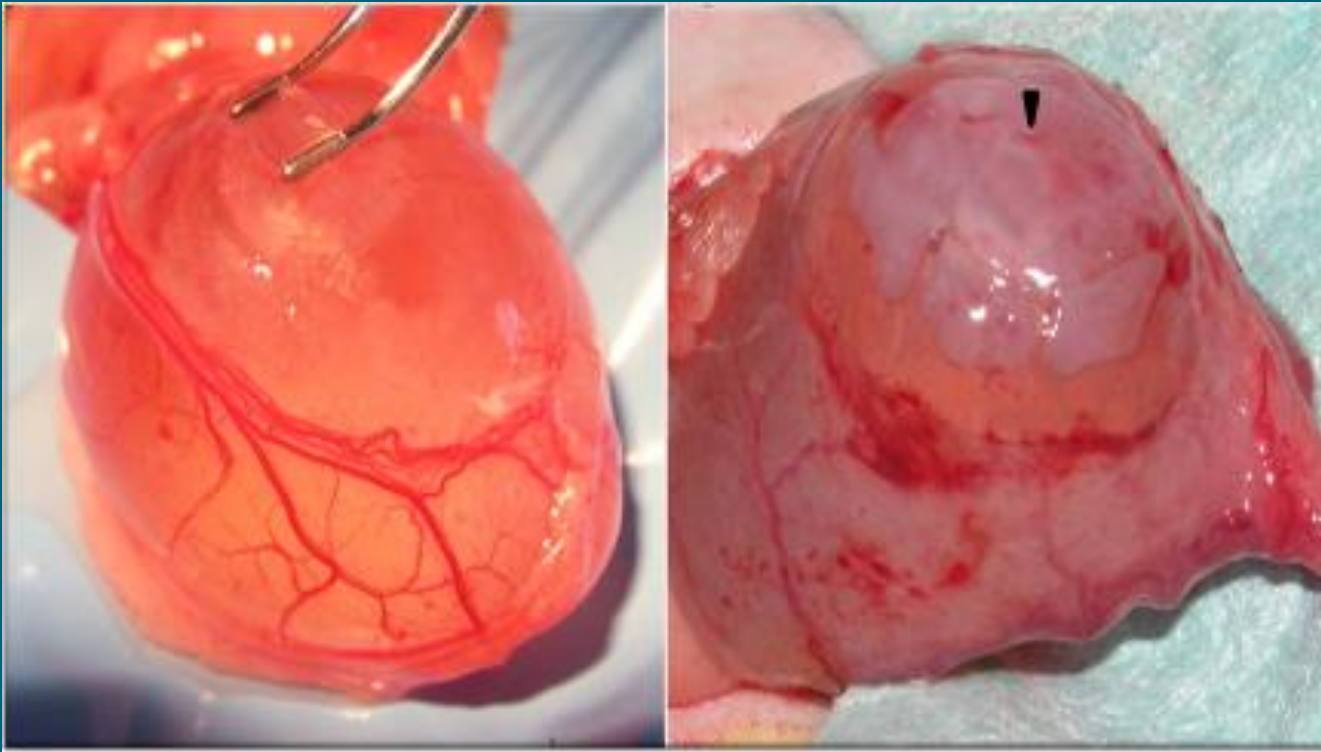
Twenty-four rabbits were randomly divided into two groups. In experimental group, SMCs were obtained from bladder muscular layer, labeled with PKH-26, and seeded on temperature-responsive culture dishes. Contiguous cell sheets were noninvasively harvested by reducing temperature and triple layer cell-dense tissues were constructed. Following partial detrusorectomy, transplantation of engineered tissue onto the urothelial diverticulum was performed. The control group underwent partial detrusorectomy followed by peritoneal fat coverage. At 2, 4, and 12 weeks, animals were sacrificed and Masson trichrome, CD34, CD31, CD3, CD68, α -SMA, Picrosirius red staining, and Pentachrome staining were performed to evaluate bladder reconstruction.

Results:

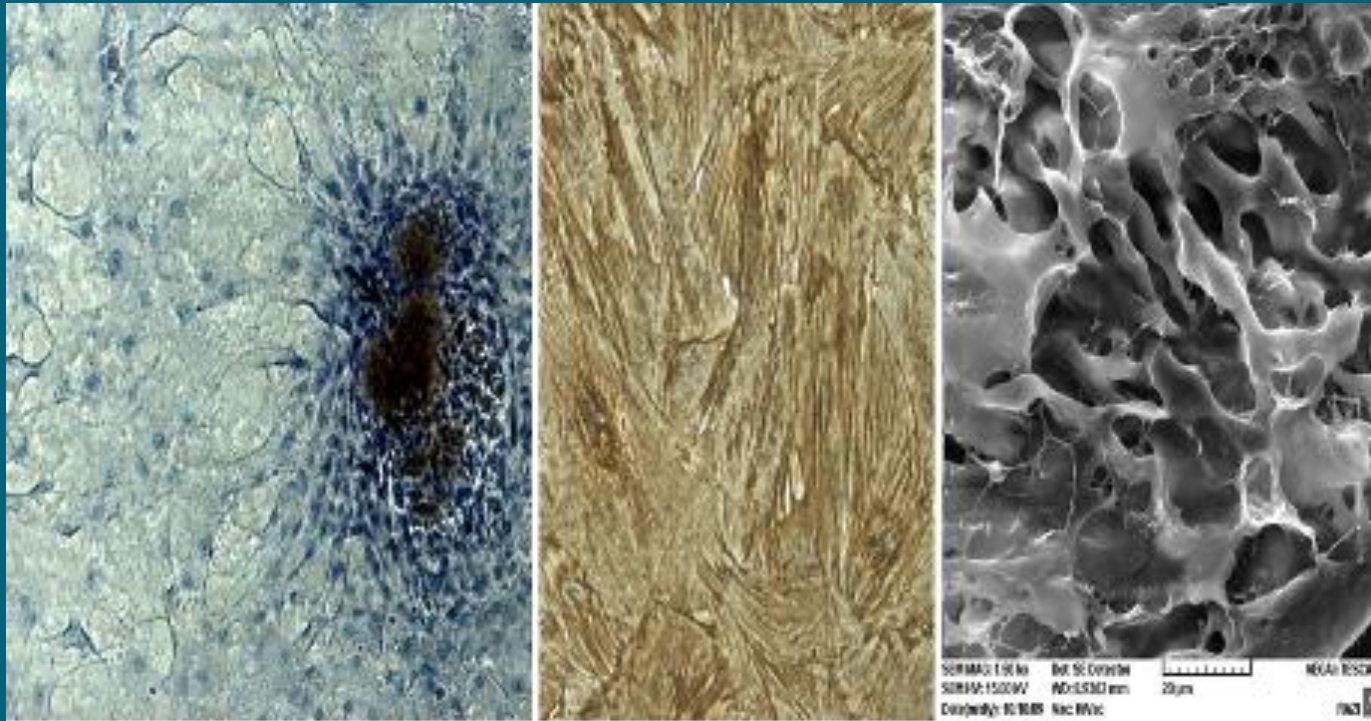
Two weeks after SMC sheets grafting, PKH-26 labeled SMCs were evident in the muscular layer. At 4 weeks 79.1% of the cells in the muscular layer were PKH-positive cells. The portion of the muscular layer increased in the experimental group during the follow-up and was similar to normal bladder tissue after 12 weeks. α -SMA staining showed well organized muscle at 4 and 12 weeks. CD34⁺ endothelial progenitor cells and CD31⁺ microvessels increased continuously and peaked 1 and 3 months after grafting, respectively.



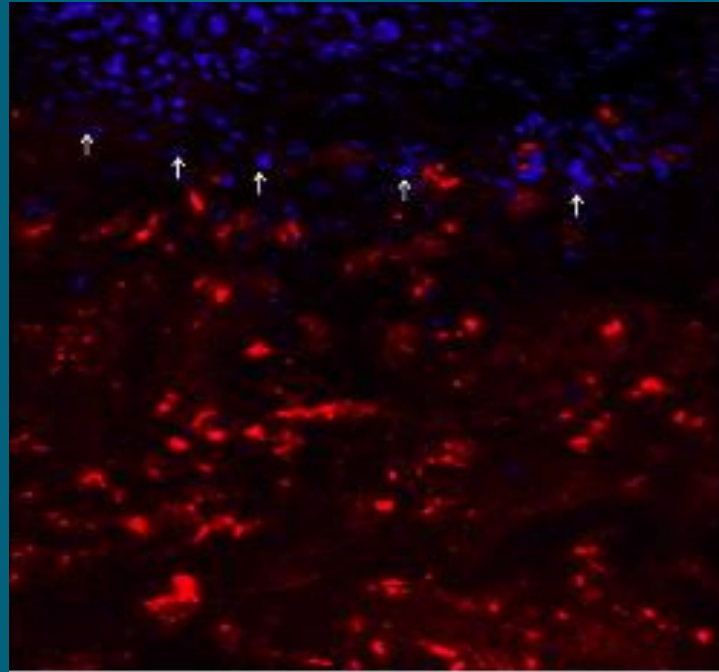
Schematic comparison of cell sheet engineering technique and conventional enzyme based cell harvest system: A. Trypsin disrupts cell-cell connections resulting in single cell suspension, B. Cell sheet engineering technique: the cultured cells spontaneously detach from the temperature-responsive culture dishes surface as an intact sheet when the culture temperature is reduced to below the critical solution temperature.



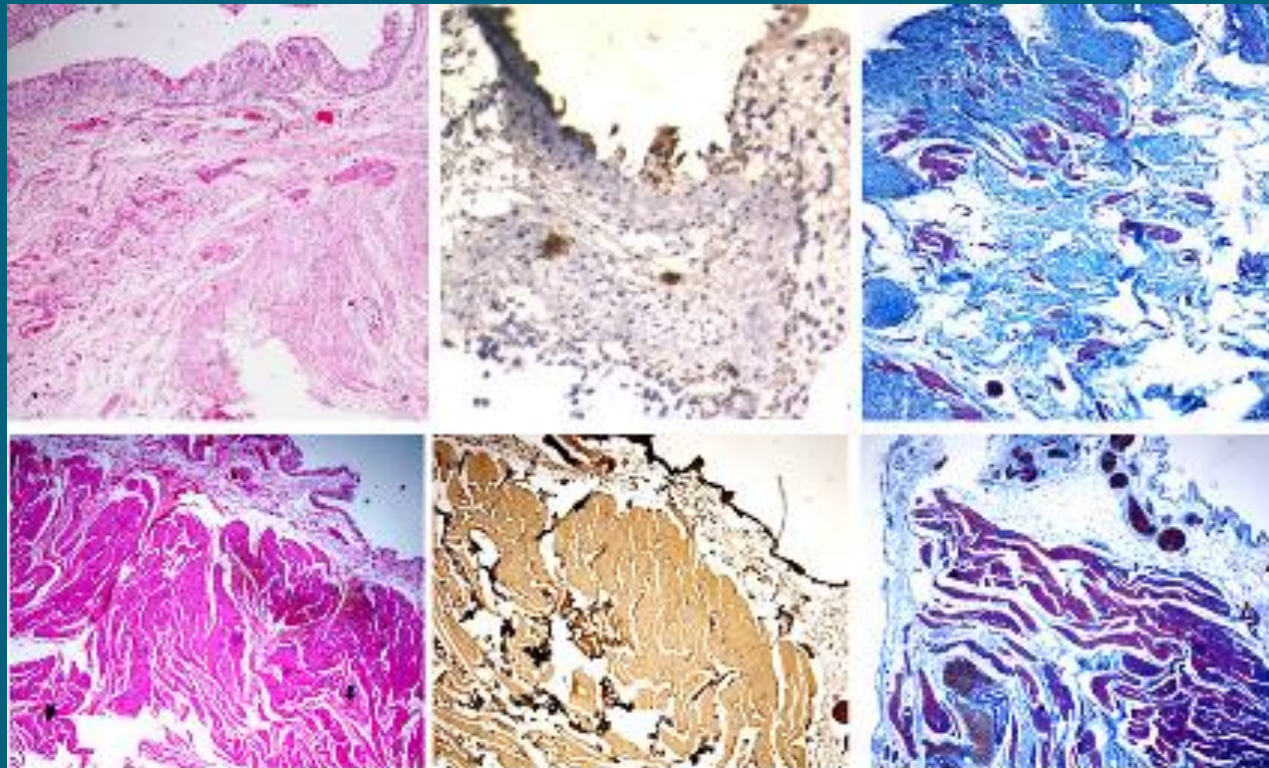
Surgical technique: A. Partial detrusorectomy, B. Grafting of the cell sheet construct (the arrowheads) on the urothelial layer.



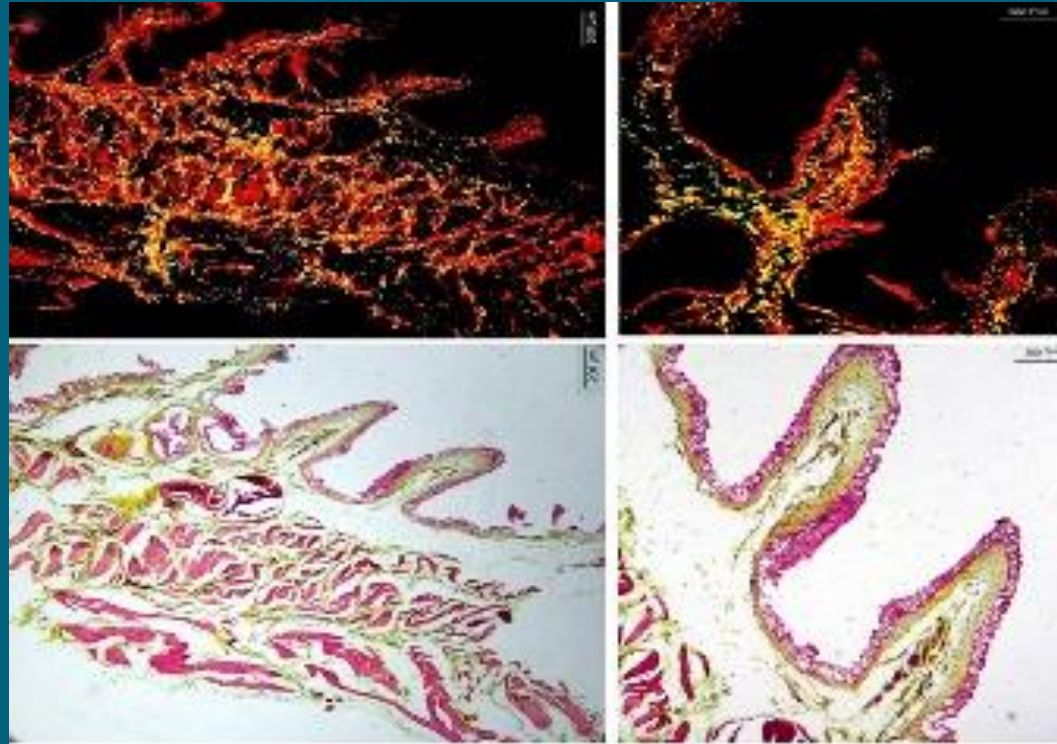
Characterization of the Smooth Muscle Cell sheet: A. The outgrowing cells are visible from the fragment of muscular layer of the bladder (arrow) B. Desmin staining, demonstrating homogenous pattern of spindle-shaped cells that are desmin positive, C. Scanning electron microscopy demonstrates the cellular extensions with continual cell-to-cell contact.



PKH-26 red fluorescent cell linker showing the prestained SMCs as a sheet.



Contribution of SMC sheet in bladder regeneration during three time points: A & B. H&E staining 1 mo after grafting shows a well developed muscular layer, C. Trichrom staining 1 mo after grafting shows a moderate fibrosis, D & E. 3 months after grafting the reconstructed bladder closely resembled native bladder wall. F. Small amount of fibrosis after 3 months in the experimental group.



Collagen staining: A. Picrosirius red staining under polarizing microscopy for collagen typing demonstrates the existence of well-organized collagen fibers (red and yellow colors) 3 months after cell sheet grafting, B. Type-I collagen fibers appeared thick, strongly birefringent, yellow or red whereas type-III collagen fibers are visualized thin, weak birefringence, green. Type-I collagen fibers are predominant in the reconstructed bladder tissues, C and D. Pentachrome staining shows well organized collagen fibers (in yellow color) as well as muscle bundles in cell sheet group 3 months after grafting (in red color).

Conclusion:

In the present study, we demonstrated that autologous SMC sheet grafting has the potential for reliable bladder reconstruction and is technically feasible with a favorable post-surgical evolution within 12 weeks of operation. Our findings would pave the way toward the future bladder tissue engineering using cell sheet technique.




[Annals of Biomedical Engineering](#)

July 2017, Volume 45, [Issue 7](#), pp 1795–1806 | [Cite as](#)

Future Prospects for Human Tissue Engineered Urethra Transplantation: Decellularization and Recellularization-Based Urethra Regeneration

Authors

[Authors and affiliations](#)

Abdol-Mohammad Kajbafzadeh , Reza Abbasioun, Shabnam Sabetkish, Nastaran Sabetkish, Parvin Rahmani, Kamyar Tavakkolizadeh, Hamid Arshadi

Reproductive Tissue Engineering

First Online: 23 May 2017

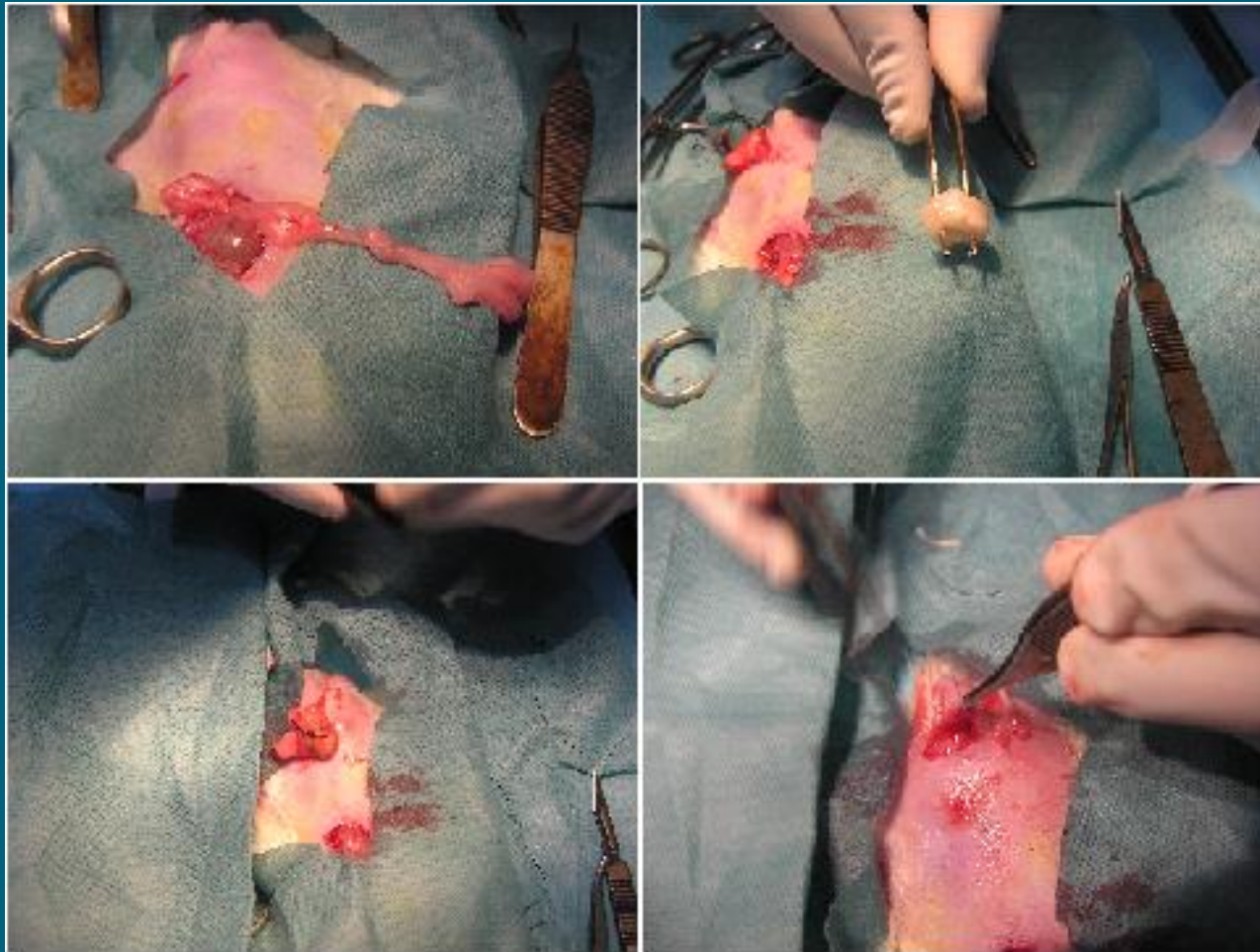


Material and Methods:

Eight adult human male urethras accompanied with the surrounding corpus spongiosum were obtained in sterile condition after obtaining ethical committee approval. Then, the tissues were decellularized with detergent-based method. The efficacy of decellularization and extracellular matrix (ECM) preservation was evaluated by histopathological examinations, DNA quantification, scanning electron microscopy (SEM), and tensile test.

Methods:

Decellularized scaffolds were washed to remove the detergents and transplanted into the omentum of 4 male healthy Sprague Dawley rats and located into the scrotum. Biopsies were taken 1, 3, and 6 months postoperatively to assess the natural recellularization. Histological examination, SEM, DNA quantification, and immunohistochemical (IHC) staining were performed.



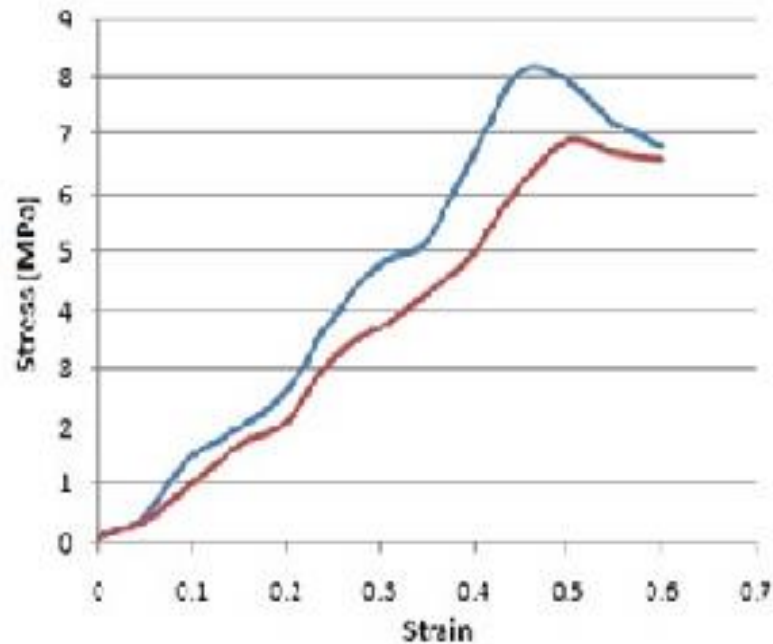
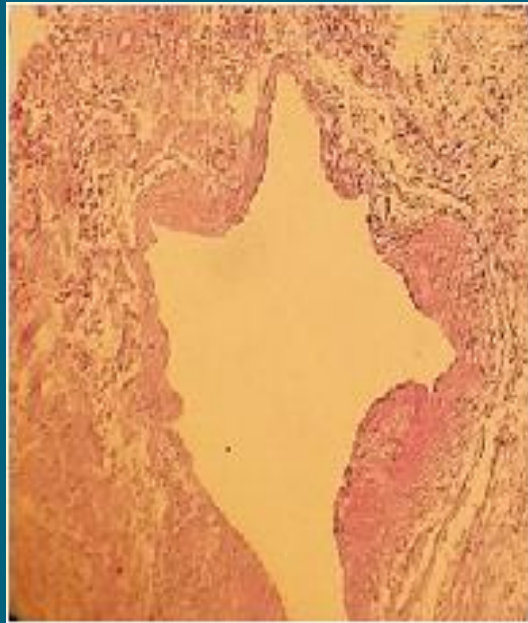
surgical technique for transplanting decellularized human urethra

Results:

DNA quantification and histological evaluations confirmed the removal of all cellular and nuclear components in urethral and surrounded corpus spongiosum scaffolds. Tensile test confirmed that biomechanical properties of the urethral ECM were well preserved.

Results...

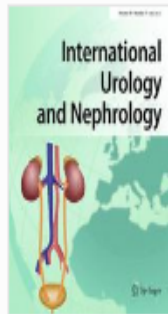
In-vivo recellularization revealed promising results in cell seeding of epithelium-like cells in the lining of the urethra as well as smooth muscle cells in the wall structure. Progressive angiogenesis was also detected in the transplanted scaffolds during the time-points while inflammatory markers were negative.



Histological evaluations and biomechanical properties of decellularized urethral scaffold

Conclusion:

The results suggest that we can prospect to perform urethral reconstruction by using the body as a natural bioreactor that can pave the road for clinical application of acellular matrix in urological reconstructive surgery.




[International Urology and Nephrology](#)

July 2017, Volume 49, [Issue 7](#), pp 1193–1199 | [Cite as](#)

In vivo human corpus cavernosum regeneration: fabrication of tissue-engineered corpus cavernosum in rat using the body as a natural bioreactor

Authors

[Authors and affiliations](#)

Abdol-Mohammad Kajbafzadeh , Reza Abbasioun, Nastaran Sabetkish, Shabnam Sabetkish, Ali Akbar Habibi,

Kamyar Tavakkolizadeh

Urology - Original Paper

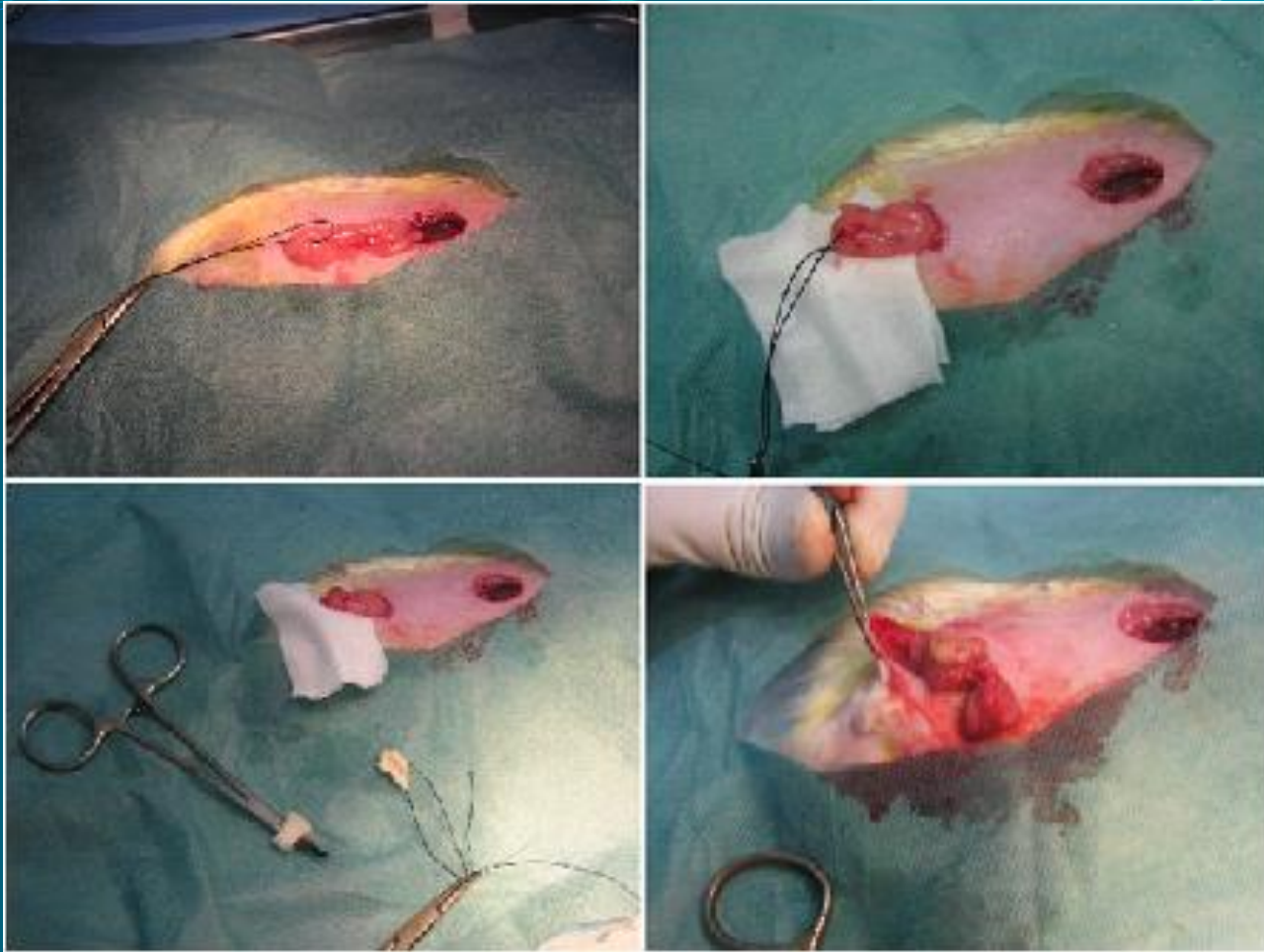
First Online: [05 April 2017](#)

Material and Methods:

Eight adult human male corpus cavernosum were obtained in sterile condition after obtaining ethical committee approval. After dissecting the urethra, corpus cavernosum was decellularized by inserting an 18 gauge needle into the body of the tissue. The gauge was connected to a peristaltic pump to circulate the detergents in the corpus. Histopathological examinations, DNA quantification, scanning electron microscopy (SEM), and tensile test were performed to evaluate the efficacy of decellularization and extracellular matrix (ECM) preservation.

Material and Methods...

A section of decellularized scaffold was washed several times and transplanted into the omentum of 4 male healthy Sprague Dawley rats and located into the scrotum. Biopsies were taken 1, 3 and 6 months after transplantation. Histological examination, SEM, DNA quantification, and immunohistochemical (IHC) staining were performed to assess the efficacy of natural recellularization



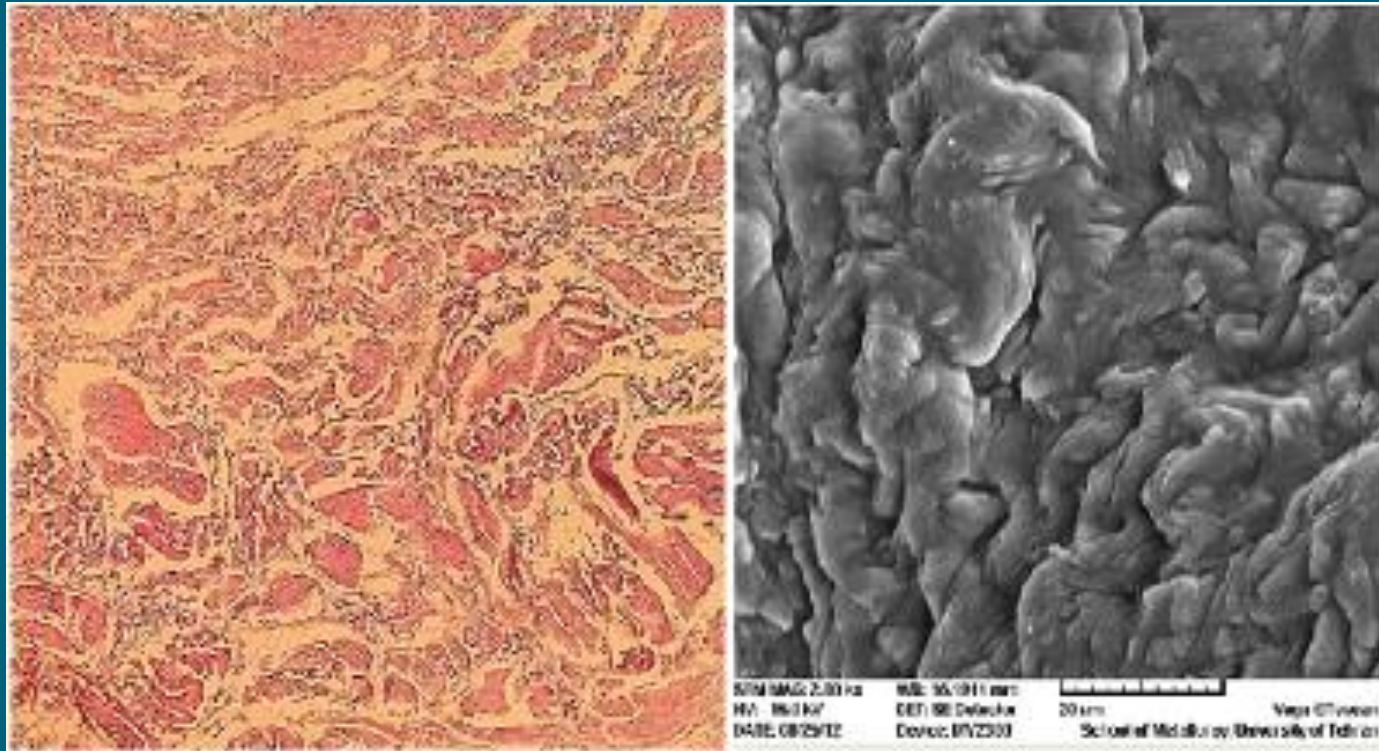
Surgical technique of decellularized human corpus cavernosum transplantation

Results:

The results of the examinations performed prior to transplantation, revealed a decellularized ECM resembling to the native tissue with normal pits that may be appropriate for further in-vivo cell seeding.

Results:

Histopathology examination of the biopsies after transplantations confirmed successful cell seeding with endothelium-like cells in different time-points. CD 34 staining was dominant in the short-time biopsies, while CD31 staining was higher than CD34 in long-term specimens.



Histological evaluations and SEM analysis of decellularized scaffolds

Conclusion:

This study theoretically may pave the road for corpus cavernosum regeneration by transplantation of decellularized scaffolds into the scrotum. The feasibility of natural bioreactor in recellularizing corpus cavernosum was confirmed. This technique may have the potential to facilitate homologous transplantation for repair of corpus defects.



*Thank you for your
attention*